FEASIBILITY OF MICRO-SCALE WIND TURBINES IN ONTARIO

Masaō I. Ashtine

A THESIS SUBMITTED TO THE FACULTY OF GRADUATE STUDIES IN PARTIAL FULFILLMENT OF THE REQUIREMENTS FOR THE DEGREE OF MASTER OF SCIENCE.

Graduate Program in Geography
York University
Toronto, Ontario

July, 2013

Abstract

Wind energy production is constrained by certain environmental factors such as local wind regimes, and by socio-economic variables. Much of the wind energy produced in Ontario comes from utility-scale turbines and micro-scale turbines contribute less than 8 GWh/annum in Ontario with fewer than 3000 units existing across Canada. With plans to increase the small wind turbine industry in Canada, it is important to assess the viability of this technology both spatially and temporally. Using field data collected from two small wind turbines (<30 m) at the Kortright Centre for Conservation, and the integration of turbine data with the North American Regional Reanalysis dataset, an assessment of wind regimes and turbine output was conducted in this study for Ontario. Results indicate that small turbines will be most feasible at the 30 m hub height in regions with proximity to the Great Lakes and northern regions near James Bay.

ACKNOWLEDGEMENTS

I would like to express my sincere gratitude towards my graduate advisor, Dr. Richard Bello for providing me with the opportunity to pursue a Master's degree within the Geography Department at York University. My gratitude is insurmountable to the countless hours and commitment given by Dr. Bello and his dedication to his students and research in climatology will by no means go unnoticed. I would like to thank my co-advisor, Dr. Kaz Higuchi for his time, input, and many contributions to the revision process of this thesis.

Additionally, I would like to thank our industrial partner, the Toronto and Region Conservation Authority, for making the field aspect of this research possible. The provision of wind turbine data and access to facilities at Kortright has proven invaluable to this thesis and its results. Great appreciation is also given to the MITACS Accelerate Program for being a substantial financial resource in acquiring equipment, subsidizing travel costs and allowing for an industry connection. I further extent my gratitude to my external examiner, Dr. Tarmo Remmel.

I would like to sincerely thank my fellow colleagues Monica Vaswani and Kristina Delidjakova my all their guidance, computational assistance and motivation throughout my data analysis and field work. Their support, encouragement and input have truly helped me through difficult times. Lastly, to my friends, family, and everyone else who consoled or celebrated with me during this process, I am forever in your debt.

TABLE OF CONTENTS

LIST OF FIGURES

LIST OF TABLES

NOMENCLATURE

A	Swept area of a wind turbine rotor
C_p	Wind turbine power coefficient
C_p max	Maximum wind turbine power coefficient (Betz limit)
D	Wind turbine rotor diameter
$F(U)$	Rayleigh cumulative wind speed probability distribution function
GCM	Global Climate Model
HAWT	Horizontal Axis Wind Turbine
NARR	North American Regional Reanalysis
NCEP	National Centers for Environmental Prediction
VAWT	Vertical Axis Wind Turbine
P	Wind turbine power output
R	Wind turbine rotor radius
RPM	Rotations Per Minute
u	Instantaneous longitudinal wind speed measurement
U	Moment magnitude wind speed
Uz	Longitudinal component of wind velocity
U^*	Friction velocity, related to the shear stress at ground-level
v	Instantaneous lateral wind speed measurement
zo	Surface roughness
ρ	Air density
σ	Standard deviation

CHAPTER 1

INTRODUCTION; LITERATURE REVIEW; RESEARCH METHODOLOGY

1.1 Introduction

1.1.1 Research Rationale

Signs of increased atmospheric instability and changing weather patterns are evident globally and the province of Ontario is no stranger to the effects of a variable climate. The scientific community is largely in agreement that the global climate is in a state of change, especially at northern latitudes where rates of warming are unprecedented, forcing many countries to revamp their policy around energy and the reliance on hydrocarbons (IPCC-AR4, 2007). It is now widely accepted that the global climate is changing, at least in part as a result of human modification of the atmosphere through greenhouse gas production and emission (Weaver, 2003). Temperatures have increased at an unprecedented rate in the last 100 years, and warming trends are particularly pronounced in the higher latitudes (Griggs*et al.*, 2002). Climate models estimate that future climatic conditions are likely to be without precedent in the last 10,000 years, and it is anticipated that the effects will be felt earliest and strongest in the Arctic (Serreze*et al.*, 2000; Houghton *et al.*, 2001). A significant part of mitigating climate change is to incorporate a more steady reliance on alternative energies such as wind driven turbines, so as to decrease anthropogenic CO_2 emission into the atmosphere. There is considerable interest in the potential impact of climate change on the feasibility and predictability of renewable energy sources including wind energy (Pryor *et al.*, 2005) and very often the implementation of this technology is limited to large wind farms utilizing utility scale

wind turbines (> 80 m hub height) and very little attention is given to the development of smaller aerogenerators which bring the accessibility of wind energy closer to major load centers such as Toronto.

The potential of small turbines is yet to be assessed in Ontario and currently there is extremely limited standardized field testing for their calibration and power output throughout the North American wind energy industry, particularly in Canada (Li and Li, 2005). Much of the research being conducted on micro-scale wind turbines (< 30 m hub height; typically between 300 W to 25 kW) is being done through wind tunnel analysis and is focused heavily on the modeling of electrical components and blade design. Field research involving small wind turbines is highly lacking in the wind turbine industry. There is much debate politically over the cost-effectiveness of small aerogenerators, mainly if the unit cost per kW of wind turbines can compete with that of hydrocarbon energy sources. More focus should be placed on the accuracy of manufacturer testing, especially in the field, but few peer-reviewed studies have empirically analyzed power outputs in relation to differing wind patterns and many have ignored the shift in patterns with a changing climate all together. This research seeks to determine the environmental efficiencies of small wind turbines and how complimentary are these efficiencies of performance with modeled wind regimes for Ontario. As these wind turbines have the potential of supplying electricity to the grid, it is beneficial to determine how well these turbines are performing, when they perform best, which turbine models perform better

than others and how do these wind turbines perform in varying regions around Ontario under varying conditions.

In 2012, global wind energy capacity grew by 19%, with the global wind industry installing approximately 44,711 MW of wind power (CanWEA, 2012) and today there are over 150,000 large wind turbines operating around the world in over 90 countries. While wind energy has been increasing substantially in many new emerging economies, it has been a relatively new provider of clean energy in Canada. In 2012, clean wind energy grew by nearly 20% in Canada, representing over $2.5 billion in investment and Canada's current installed capacity is just over 6,500 MW (CanWEA, 2012). The province of Ontario has 2,043 MW of installed wind capacity (*ca.* 31% of Canadian wind capacity; IESO, 2012).

With the Canadian government and private investors such as CanWEA aiming to have 20% of energy supplied by wind by 2025 across Canada, the wind regimes, patterns and potential across Canada are of substantial importance. However, wind energy supplied just under 3% of electricity supplied in Ontario in 2012 (IESO, 2012), and there exists a push for greater investment in wind energy in the province. Specifically relating to small wind turbines, Canada has an annual sale of $4.2 million in units, roughly 600 to 800 units per annum. However, Canadian manufacturers are exporting 87% of their sales. The Canadian government intends on investing $3 billion for the installation a total of over 140,000 small wind turbine units with a total capacity of 600 MW and an annual energy output of 1 terawatt-hour (CanWEA, 2012). This goal is small in comparison to the

American wind industry's which has already seen an installation of over 150,000 small wind turbines by the end of 2012.

Micro-scale wind turbine manufacturers such as Bergey, claim that their turbines can significantly lower operating costs over a diesel generator and provide sustainable power where the power grid cannot reach. However, there are many factors which must be considered such as hub height, wind regime, site characteristics and location which affect turbine performance and power output and this study seeks to determine the limitations placed on the testing of small wind turbines based on these factors. Small wind turbines, although they produce significantly less energy than utility-scale wind turbines, offer the opportunity for greater accessibility of wind energy to consumers and households.

Wind farms are often in areas far from the grid and are difficult to integrate into more suburban areas due to reasons such as logistics, aesthetics and other minor concerns such as safety or residents (Gipe, 2004). Small wind turbines can help offset community energy demands and this research sought to determine if this technology is currently feasible and with a changing climate based on field performance analysis and modeled NARR (North American Regional Reanalysis) data. Four small wind turbines at Kortright were assessed through this study, a Westwind 5 kW, a Bergey 1kW, a Bergey Excel 10 kW and a Skystream 2.4 kW. Although four turbines were initially to be assessed, two small wind turbines were damaged due to high wind events. The Westwind 5 kW turbine was had its blade snapped during a previous thunderstorm in 2011 and the Bergey 10 kW was uprooted during the passing of Hurricane Sandy in 2012. The two

remaining wind turbines are nonetheless industry standard models and are commonly referred to in the North American industry. Turbine performance in varying months was also considered as the quantification of energy production is important, but the timing of this energy and its usefulness will further add to performance data as energy demands are almost doubled in winter versus summer. Data collected may also prove useful to the Small Wind Certification Council that sets standards on micro-scale wind turbine technology. This research area will be the first of its kind in Ontario and is in close accordance with the current provincial government's drive for Ontario to be a world leader in innovative alternative energy usage and research. Results not only provide a comprehensive analysis of Ontario wind and potential wind power but will couple this information with wind turbine field performance to best determine the feasibility of small wind turbines across the province.

1.1.2 Research objectives

Based on the body of literature reviewed and the need for a detailed assessment of the feasibility of small wind turbines in Ontario, an extensive study of selected small wind turbine performance was carried out, along with the application of the NARR wind data for Ontario, with the following three objectives:

1. Quantify the field performance of select wind turbines at the Kortright field testing site over six months and determine parameters which influence turbine performance and efficiency in the field.

2. Employ the NARR dataset to determine Ontario wind regimes, potential wind power and future wind patterns.
3. Assess the feasibility and performance of select small wind turbines within Ontario based on measured field coefficients of performance and on permutations of certain turbine features such as swept area and hub height.

1.2 Literature review

1.2.1 Testing of Small Wind Turbine Performance

Where the North American wind industry is concerned, much of the standard testing of turbines is limited to utility or large-scale wind turbines (> 1MW). Wind turbines also go through extensive wind tunnel testing during the design, manufacturing and assembly stages but severely lack field testing once they have been erected. Manufacturers often assign rated power quantifications to their wind turbines but they lack rate powers based on field testing and conditions. A literature review on peer-reviewed studies which have done testing on wind turbines are almost always limited to wind tunnel testing, focus primarily on blade design and generator/inverter efficiency and are usually from an engineering perspective (Orlando *et al.*, 2008; Arifujjuman *et al.*, 2008; Mirecki *et al.*, 2007; Wang *et al.* 2007; Arifujjaman *et al.,* 2006; Ozgener, 2006; Bumby and Martin, 2005; Abe *et al.,* 2005; Guo and Chang, 2005; Hirahara *et al.*, 2005; Abe *et al.*, 2004;

Wright and Wood, 2004). Many of these studies have set guidelines for strict quality control and conditions under which wind turbines are assessed. Fewer peer-reviewed studies have looked at small wind turbine performance in the field (Matsushima *et al.*, 2006; Eggers *et al.*, 2000; Bechly *et al.*, 1996; Bose, 1992; Hogstrom *et al.*, 1988) in comparison to studies done in wind tunnels, and within the literature review of this thesis, no studies on small wind turbine testing in the field within Canada were known to exist.

Field testing studies on small wind turbines usually conduct analysis with the goal of further design improvement and thus focus on blocking effects, blade aerodynamics, shear velocities and wind patterns formed by the functioning of the wind turbine. Field testing of small wind turbines with the intention of producing performance curves is very limited to private certificate bodies such as Intertek and NREL in the U.S. or to individual testers that have been contracted by manufacturers wishing to test new turbine designs (Gipe, 2004). Field testing of small wind turbines is essential in developing accurate and real world assessments of turbine performance. Many environmental conditions which do not exist within wind tunnel testing or which have been factored out can highly influence the performance of small wind turbines in the field where they ultimately function (Gipe, 2004). Atmospheric variables such as wind variability, instantaneous wind direction changes and eddies, extreme temperatures, radiation, environmental wear of electrical components and moisture for instance can all affect turbine efficiency (Gipe, 2004). Field testing of wind turbines is usually on the time scale of four to six months to capture a wide wind distribution and environmental

conditions and thus allow the wind turbine to run for a much longer period of time than seen with wind tunnel analysis (usually in the order of a few days to a few weeks).

With field data on small wind turbine performance, this information can be assessed together with observed or modeled wind conditions spatially and temporally allowing for the examinations of these turbines in varying locations. Field testing of wind turbines however is largely limited due to mounting costs, time period needed to collect vast quantities of wind information and the present lack of manufacturer interest in this field of study. Due to stringent certification standards, small wind turbine testing is also inhibited by the lack of resources needed to meet SWCC (Small Wind Certification Council) and IEC (International Electrotechnical Commission) standards. Certification is the formal process through which the SWCC, an independent organization, assesses and issues certificates and consumer labels for the performance and safety of small wind turbines in accordance with criteria established in the AWEA (American Wind Energy Association) Standard. SWCC Certification is based on an evaluation of the wind turbine design (structural Analysis) and field testing (power performance test, acoustic sound test, safety and function test, and duration test) (SWCC, 2012). These requirements prevent many independent testers from establishing field testing sites. While an economic recession in the U.S. has slowed small wind incentives, in Europe, the European Commission funds the Small Wind Industry Strategy (SWIS) with the intention of stimulating growth in the small wind turbine industry and thus research comparable to

this study will provide useful information in decision making when concerning turbine performance over time and the projections of future turbine output.

1.2.2. Small Wind Turbine Efficiency

Modern wind turbines can be categorized into the horizontal-axis wind turbines (otherwise known as HAWTs, Fig. 1.1), and the vertical-axis wind turbine design (VAWTs). Utility-scale turbines range in size from 100 kW to as large as several MW. Larger turbines (*ca.* 80 m in height) are grouped together into wind farms, which provide bulk power to the electrical grid (Shikha *et al.,* 2003). Single small turbines, below 100 kW and 30 m in height, are used for homes, industrial purposes, urban settings and/or mechanized water pumping in agriculture. For HAWTs (Fig. 1.1), the axis of rotation is parallel to the ground and rotors are usually classified according to the rotor orientation (upwind or downwind of the tower), hub design (rigid or teetering), rotor control (pitch versus stall), number of blades (usually two or three blades), and how they are aligned with the wind (Manwell *et al.*, 2009).

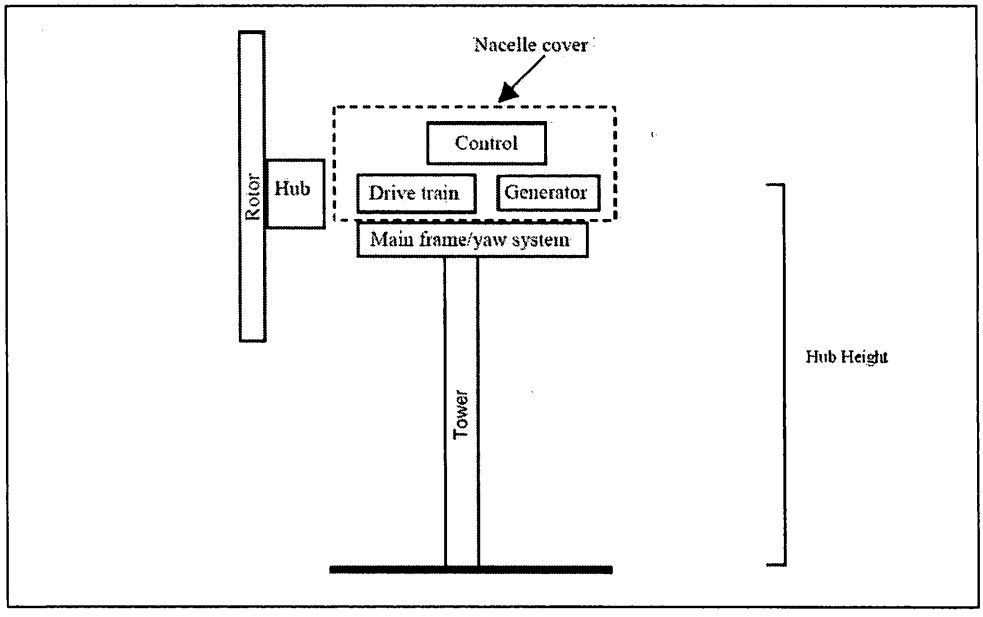

Fig.1.1: Simplistic diagram of standard small wind turbine components and orientation. *Modified from Manwell*et al.*,(2009).

Instead of using electricity to make wind, like a fan, wind turbines use wind to make electricity. The wind turns the blades, which spin a shaft, which connects to a generator and makes electricity through this mechanical motion which rotates a series of magnets (Shikha *et al.*, 2003). Small wind turbines are very similar in design to utility scale wind turbines which have some design modifications to adjust for the faster wind speeds experienced at higher altitudes. The major components to a small horizontal-axis wind turbine include blades, alternator, slip ring and brush assembly, nacelle, yaw head, and tail assembly. Most HAWT wind turbines have three blades, typically made of fibreglass, glass polypropylene, or some other composite material (McGowan *et al.*, 2003). The blades act like aircraft wings (in design, not function) to convert the wind's energy into

rotational energy to turn the alternator. Based on a phenomenon first described by Bernoulli, the rotor blade edge creates lift because of the differential air pressure between the flat side and the rounded side of the blade (Grogg, 2005). As wind travels over the rounded, upper half of the blade, it has to move faster to reach the end of the blade in time to meet the wind travelling over the flat, lower half of the blade. This gives the upper, curved surface with a low-pressure pocket just above it and this low-pressure area sucks the blade in the upper half direction, an effect known as lift. On the lower half of the blade, the wind is moving slower and creating an area of higher pressure that pushes on the blade, trying to slow it down, known as drag (Grogg, 2005).

$$\mathrm{L} = \frac{1}{2}\,\rho v^2 a C_L \tag{1.1}$$

Lift (L) is influenced by a variety of factors including wind speed (v), planform/blade area (a), air density (ρ) and the coefficient of lift (C_L) as expressed in Equation (1.1). Blade aerodynamics largely influences the extraction of wind energy by the wind turbine and the power produced (P) is expressed in Equation (1.2):

$$P = C_p \frac{1}{2}\,\rho A v^3 \tag{1.2}$$

where C_p is the coefficient of performance and A is the swept area of the turbine rotor. Due to wind turbine inefficiencies and technological limitations, wind power is not

extracted at 100% from the wind. This ratio of theoretical/environmental wind power to the actual power produced is defined by the variable C_p (Equation 1.3):

$$C_p = \frac{\text{Rotor Power}}{\text{Power in the wind}} = \frac{\text{P } rotor}{\frac{1}{2}\rho A v^3} \quad (1.3)$$

Wind energy production is further inhibited by what is known as the Betz limit ($C_{p\,\max}$). The ratio of energy hitting the rotor versus the amount remaining after is described by the Betz limit of 59.3%, and above this limit, extracting more energy from the wind causes a reduction in power extraction even though wind speed increases. The Betz limit can be simply explained by considering that if all of the energy coming from wind movement into the turbine were converted into useful energy then the wind speed afterwards (in the leeward side of the turbine) would be zero. However, if the wind stopped moving at the exit of the turbine, then no more wind can pass (it would be inhibited in movement). In order to keep the wind moving through the turbine, to keep getting energy, there has to be some wind movement on the outside with energy left in it (Grogg, 2005). Ideally we want a wind turbine that operates at a C_p as close to the Betz limit of 0.59 as possible and this turbine will operate at maximum C_p until the wind speed corresponds to the rated power, then, with increasing wind speed, it operates at a reducing C_p, so that the power output remains constant at its rated value. However a common misconception is that faster wind speeds lead to greater power outputs, and this is true to an extent, but at higher wind

events, the power has to be limited in order to protect the mechanical and electrical components of the machine from overloading and vibration stresses (Hansen, 2002).

The alternator, most of which use permanent magnets, converts the rotational energy into electricity. The nacelle provides housing for the alternator and wiring. The electricity produced by the alternator is transferred to the fixed cables running down the turbine tower by a slip ring and brush assembly (Grogg, 2005). An inverter takes the direct current produced by the generator of a wind turbine and converts it to alternating current which can be directly exported to the electrical grid. Thus, power output efficiency is finally influenced by the efficiencies of the turbine alternator and the corresponding inverter. This study focuses on the efficiency of the energy transfer at the rotor and the quantification of energy loss from the alternator and inverter are not considered. Wind energy efficiency is also affected by cut in and out speeds (the speed at which the rotor begins or stops rotation), wind variance, surface roughness, mechanical wear and hub heights. As wind speeds tend to increase with height as seen with logarithmic wind profiles, higher hub heights will allow wind turbines to capture energy from faster winds aloft (Grogg, 2005).

1.2.3. Wind Resource Analysis

In essence, the importance of the wind resource in a particular area is dependent on the available wind turbine technology to extract the energy of the wind. In recent times,

many areas with more moderate wind regimes are now being regarded as potential sites for the placement of wind turbines as current wind turbine technology is more efficient in capturing wind power at lower speeds. Nonetheless, a crucial aspect of any site assessment for wind turbine placement is that of wind resource analysis. One of the earliest global wind energy resource assessments was carried out by Gustavson (1979). Gustavson based his resource estimate on the input of the solar energy reaching the Earth and how much of this energy was transformed into useful wind energy. Wind resource management has come a long way but these wind energy resource atlases remain important in establishing regions of strong wind patterns, quantitative estimates of available 'windy' land area and potential electrical outputs from land development (Elliott *et al.*, 1987). Complete assessments of potential wind energy sites also consider terrain characteristics, population statistics, distance from urban centers and other variables that influence the efficiency of wind energy production and distribution.

In order to obtain an accurate assessment of the wind regime of an area, ideal wind data measurements over a 10-year period are required (Nfaoui *et al.*, 1998). As this observational data is very often not available for many areas, especially in less developed nations, such long-term data is not used and some studies make comparative short-term estimates based on long-term data available from nearby sites (Bechrakis *et al.*, 2004; Frandsen and Christensen, 1992). This is especially seen in the wind industry where data is unavailable but potential wind energy data is required quickly (Bechrakis *et al.*, 2004). Relying on data from the nearest measuring station and on a wind flow analysis which

takes into account the topography and surface roughness of the surrounding land may result in substantial errors in estimating the wind speed and thus even greater errors in energy estimation especially in complex terrains (Ayotte *et al.*, 2001; Suarez *et al.*, 1999; Bowen and Mortensen, 1996). Other methods for measuring wind resource estimation include the measure-correlate-predict methods and assessments which rely upon global meteorological data or models such as the NARR dataset. The former is used whereby the wind potential is determined using a short measuring time period at a particular site and then correlating these measurements with an overlapping time series of another site using simple statistical models (Bechrakis *et al.*, 2004). Although computationally intensive, using global models, datasets or reanalysis data can provide a wide spatial area of wind resource data and can be modified to include an extensive temporal resolution, providing both short and long-term estimates.

For this study, the NARR data were used to establish wind resource estimates at 10 and 30 m heights, the common range for small wind turbines. This regional reanalysis dataset provides a temporal resolution of 3-hr intervals and a high spatial resolution of 32 km, providing significantly more detailed meteorological information than those provided by general circulation models (GCMs). Although an ideal assessment of wind energy potential in Ontario will incorporate a widespread system of meteorological stations coupled with detailed terrain characteristics, the NARR data have been validated against observed station data across North America, confirming wind average estimates to be an acceptable for wind resource assessment (Mesinger *et al.*, 2006). Not only is NARR

available for 33 years at a highly-resolved 32-km resolution, wind data are also assessed alongside other atmospheric parameters such as air temperature and pressure, providing wind power estimates and distribution.

1.2.4. NCEP-NARR Data (National Centre for Environmental Prediction – North American Regional Reanalysis)

The NCEP-NARR is a long-term, dynamically consistent, high-resolution, high-frequency, atmospheric and land surface hydrology dataset for the North American domain (Mesinger *et al.*, 2006). At present this dataset comprises of reanalysis data for the time period of 1979–present and within this study, data from 1980-2012 were used. The NARR model uses the very high resolution NCEP Eta Model (32 km, 45 layer) together with the Regional Data Assimilation System (RDAS) which, substantially assimilates precipitation along with other variables (Mesinger *et al.*, 2006; Mesinger *et al.*, 1988; Black, 1988; Janjić, 1994;).NARR is widely known for its successful assimilation of high-quality and detailed precipitation observations into the atmospheric analysis which was previously lacking from many global models. The forcing to the land-surface model component of the system allows for a more accurate analysis than in previous reanalysis. Thus, NARR is regarded as a much improved analysis of land hydrology and land-atmosphere interaction in particular (the overall atmospheric circulation throughout the troposphere has been substantially improved as well).

While previous spatial resolutions prevent a detailed analysis of wind regimes, the reanalysis wind data from NARR have a spatial resolution of 32 km with wind output on a 3-hour basis (Mesinger *et al.*, 2006) for the time period of 1980-2012 (reanalysis data comprise of previously observed climate data for wind speed which have been interpolated onto a system of grids, allowing for the initialization of a 3-D forecasting model). This 33-year dataset gives NARR an enhanced estimation of historical wind patterns with an improved spatial and temporal component, allowing for dynamically consistent meteorological information away from station point data. Atmospheric parameters such as temperature, humidity, pressure and wind speed are collected and assimilated into NARR from rawinsondes (wind speed and direction measuring unit in weather balloons) and surface meteorological stations. Rawinsondes are launched twice daily from a network of sites and the data are evaluated to create a vertical profile of the atmosphere. These data are then organized and reanalyzed to provide a complete spatial replication of the atmosphere (Oort, 1977). The North American rawinsonde network is comprised of approximately 120 launch sites (Fuller, 2012).

NARR is widely used in precipitation modeling and many scientists place confidence in its ability to predict atmospheric parameters, including wind, based on its comparison with observed data (Fall *et al.,* 2010; Li *et al.*, 2010; Pryor *et al.,* 2009; Markovic *et al.,* 2009; Dominguez *et al.,* 2008; Trapp *et al.,* 2007; Luu *et al.,* 2007; Yashimura and Kanamitsu, 2007; West *et al.,* 2006; Bukousky and Karoly, 2006; Mesinger *et al.,* 2006; Ruiz-Barradas and Nigam, 2005; Mesinger *et al.,* 2004; Geng and Sugi, 2001; Felzer and

Heard, 1999; Higgins *et al.,* 1997).Within this study, the NARR wind speeds at 10 and 30 m were of main focus as they represented important tropospheric layers in modeling wind parameters for small wind turbines which have average hub heights below 30 m. Both 10 and 30 m wind speeds are extrapolated on the basis of mid-layer winds at the four neighboring mass points at the lowest of 45 model layers following a procedure originally developed by Lobocki (1993) and described in detail by Chuang et al. (2001).

Recent research in wind resource forecasting, trend analysis and wind power analysis is largely dependent on data from lower spatial resolution climate models than NARR (Yao *et al.*, 2012; Frossard Pereira de Lucena *et al.*, 2010; Pryor *et al.*, 2005; Breslow and Sailor, 2002). In efforts to improve the spatial resolution of many GCM's, many studies have approached wind resource estimation through downscaling. Downscaling is a technique that bridges the gap of GCM prediction skills over different scales but has been recognized for its limitations in providing accurate estimates when compared to observational data (Sailor *et al.*, 2008). On the other hand, nested modeling uses a higher resolution dynamic climate model to account for mesoscale forcing and this approach of dynamic downscaling is attractive for wind resource studies as it produces a continuous representation of wind statistics over the entire region of study (Sailor *et al.* 2008). Many studies have used the NARR wind data and other environmental parameters such as atmospheric pressure and air temperature in wind resource analysis over North America and have shown wind estimates at 32 km to be reliable and consistent with observation estimates (Mesinger *et al.*, 2006). Daily average 10-m wind speeds from about 450

stations across the continental United States for 2 months (January and July 1988) indicate daily average biases mostly underestimate but are below 1 ms^{-1} and the typical daily average RMSE (Root Mean Square Error) is below 4 ms^{-1} (Pryor *et al.*, 2009; Mesinger *et al.*, 2006;).

Limitations do exist with the NARR data however. Surface roughness length does not vary with time and has been incorporated into the model with a fixed value of 0.1 m plus a correction for orographic effects (Pryor *et al.*, 2009) but very little definition is given to the role of this parameter in low level wind speed estimation.

1.3 Site description

1.3.1 Kortright Field Testing Site

The Toronto and Region Conservation Authority (TRCA) has proposed the Kortright Centre for Conservation as the prototype site for the testing and standardization of micro-scale wind turbines. The proposed small wind turbine testing site is a grassy field site within the Kortright Centre for Conservation (43°49'54"N and 79°35'16"W) and has a very wide and open fetch (Fig.1.2). The dominant vegetation within this area is low lying grass (max. 0.2 m) and shrubs along with trees (average height of ?? m) which border the

field. The area below the wind turbine in regularly maintained and vegetation height is very close to the surface. It is assumed that nearby tree boundaries do not obscure the dominant wind direction nor wind profile and the field testing site is fairly uninhibited from surface roughness influences.

Fig.1.2:Satellite image of the test site at the Kortright Centre for Conservation. Red markers represent locations of small wind turbines (S marker: Skystream 2.4 kW Turbine; B marker: Bergey 1 kW Turbine; D markers: Damaged Wind Turbines).

Surface roughness influence for the Bergey wind turbine will be greatest during period of southwestern winds which blow over a narrow ridge of trees. This influence is greatest for the Skystream wind turbine during periods of wind blowing from the west over the

'Archetype' house (model show house on site, Fig. 1.2) and from the south as wind blow over a patch of birch trees (genus *Betula*). Kortright is currently being used for evaporation measurements which also require large open spaces and thus I am confident that data collected from this site can be used in supplementing modeling of larger areas of Ontario.

The Kortright field testing site (elevation, 188 m) is situated approximately 25 km from the Toronto city center and thus shares similar annual weather patterns. Lake Ontario serves to moderate Toronto's weather to the point that its climate is one of the mildest in Canada. Spring and summer temperatures range from 15 to 25°C and during winter months, the average daytime temperature, with the exception of January, the coldest month, hovers just slightly below freezing. Wind speeds vary from an average of 3.5 ms^{-1} in the summer months to 5 ms^{-1} in winter.

1.3.2 Wind Turbines

The Skystream wind turbine, located on the north western side (292° and 117 m away) of the meteorological tower, is a HAWT manufactured by Southwest Windpower and has a hub height of 15.24m with a rated power of 2.4 kW. The Bergey wind turbine is located much closer to the meteorological tower at a distance of 18 m and bearing of 32 degrees. The latter wind turbine is a HAWT with a hub height of 16.76 m with a rated power of 1

kW. Both wind turbines have specific designs that influence performance and power output (Table 1.1).

Table 1.1: Wind turbine specifications for Skystream and Bergey turbine at the Kortright field testing site. Information obtained from manufacturer description.

		Bergey	**Skystream**
Structural	Hub Height	17.37 m	15.24 m
	Turbine type	HAWT, upwind	HAWT, downwind rotor with stall regulation control
Manufacturer rating	Rated Power	1 kW	2.4 kW
	Rated Wind Speed	11 ms^{-1}	13 ms^{-1}
Rotor specifics	Rotor Diameter	2.5 m	3.72 m
	Swept Area	4.91 m^2	10.87 m^2
	Rotor Speed (RPM)	490 (rated rotor speed, no range applied)	50 – 330
	Blade Material	Pultruded fiberglass	Fibreglass reinforced composite
Wind	Cut-in Wind Speed	2.5 ms^{-1}	3.5 ms^{-1}
	Cut-out Wind Speed	None	25 ms^{-1}
	Max Design Wind Speed	54 ms^{-1}	63 ms^{-1}
Protection	Furling Wind Speed	13 ms^{-1}	No furling
	Overspeed protection	Auto tail furl, electrical breaking system	Electronic stall regulation

Each wind turbine design accounts for protection of the rotor during extreme wind events (Fig.1.3). The Bergey can perform furling of its blades (blade edges face into wind) during high speeds (> 13 ms^{-1}) with a breaking system to slow or stop rotor rotation. The Skystream is incapable of furling but does possess an electronic stall regulation system to stop rotor rotation in high wind speed events (at or above 25 ms^{-1}).

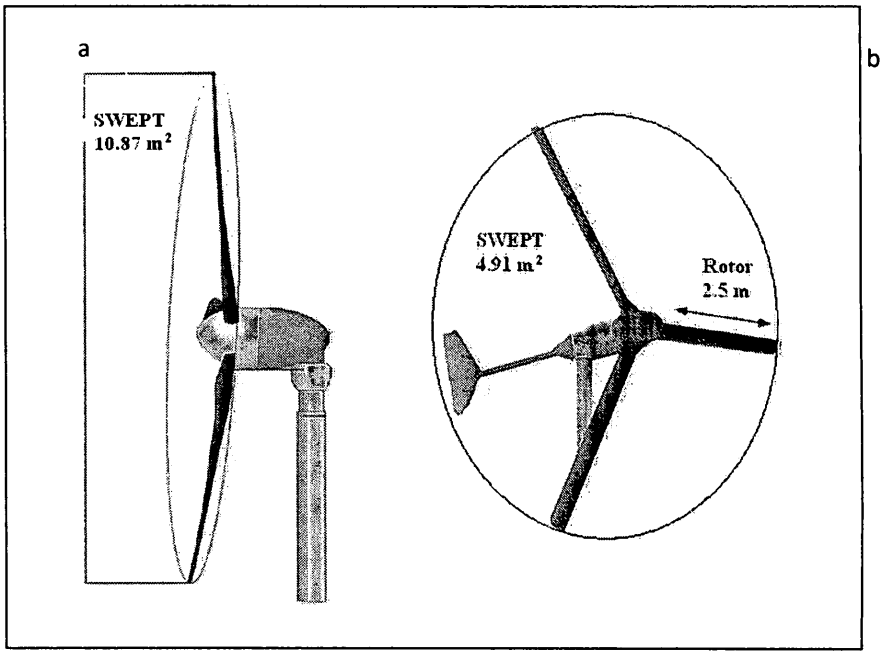

Fig.1.3: Sketch diagrams of each small wind turbine design; a) Skystream 2.4 kW b) Bergey 1 kW.

1.4 NARR Dataset

The NARR reanalysis data were obtained from http://nomads.ncdc.noaa.gov/#narr_. Running the reanalysis data in MatLab™ allowed for statistical analysis of the wind data from 1980 –2012, spanning 33 years. Owing to an uneven spacing of projected grid cells

(Fig. 1.4), MatLab™ also provides a framework for the interpolation of data to account for this grid cell layout. The scope of this dataset fully encompasses the province of Ontario and has a scope of 3,364 32 km^2 grid cells capturing the Great Lakes, Ontario, southern Hudson Bay and other regions of Canada and the U.S. owing its rectangular outline.

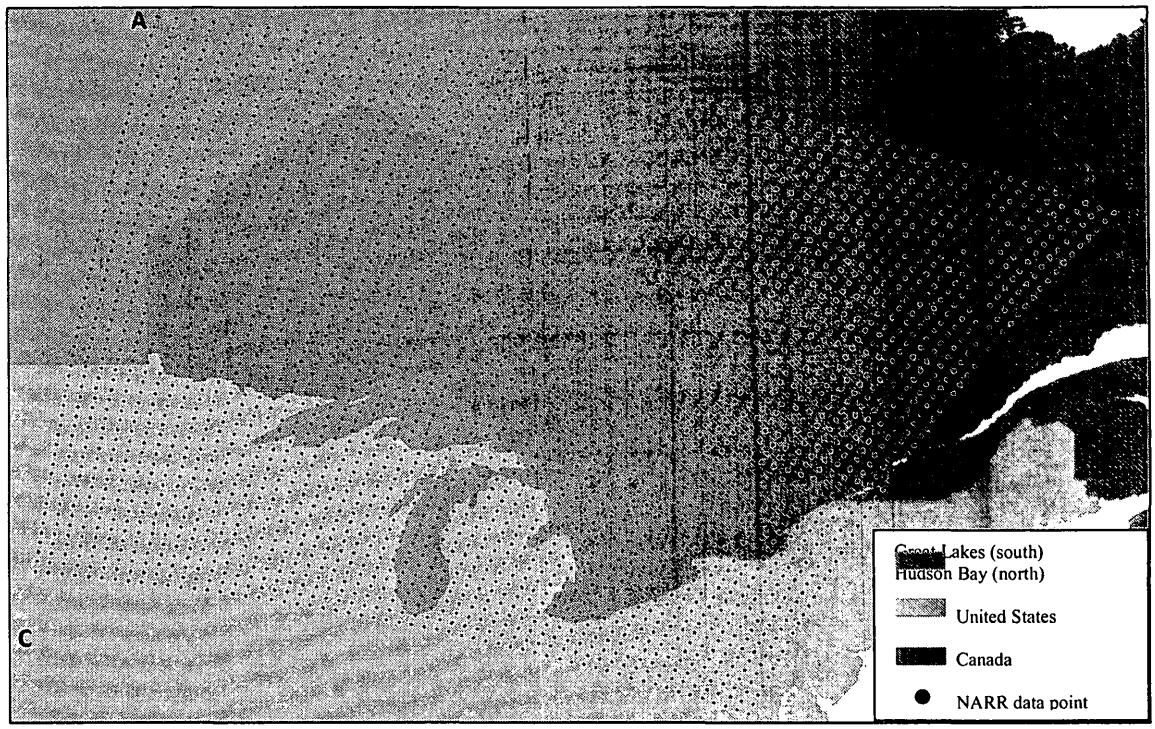

Fig.1.4: Boundary layer subsection of Hudson Bay lowlands with a North American Regional Reanalysis (NARR) products domain overlay showing projected points. Each grid cell represents a 32km spatial resolution with 3-hr temporal resolution. *i*-coordinates (196-253) run east-west and *j*-Coordinates (120-177) run north-south. Border latitude and longitude coordinates are represented by A (59.34503 N, 94.81555 W), B (53.54945 N, 66.56531 W), C (42.92014 N, 98.47565 W) and D (38.73314 N, 77.38446 W).

Data were of the spatial resolution of 32 km and a temporal resolution of 3-hrs. This gave eight 3-hr readings for each day. The atmospheric parameters of u and v (east-west and north-south horizontal wind components respectively, ms^{-1}), ambient air temperature (K) and atmospheric pressure (Pa) were captured for the aforementioned scope at tropospheric heights of 10 and 30 m.

1.5 Research methodology

1.5.1 Experimental Setup

A 30 m tall meteorological tower was erected in early July, 2012 in the test field containing the small wind turbines (Fig. 1.5). The main instrumentation on the tower mast is that of the eight calibrated anemometers at the heights of 6.10 m, 10 m, 12.19 m, 15.24 m (Skystream hub height), 17.37 m (Bergey hub height), 18.29 m, 24.38 m and 30.48 m. Four anemometers were attached to the mast at the hub height corresponding to each of the turbines (two no longer operational) and one anemometer was mounted at the 10 m environmental standard. These anemometers are strategically placed to capture vertical variations in wind and will be used to describe wind distribution and profiles at the Kortright testing site.

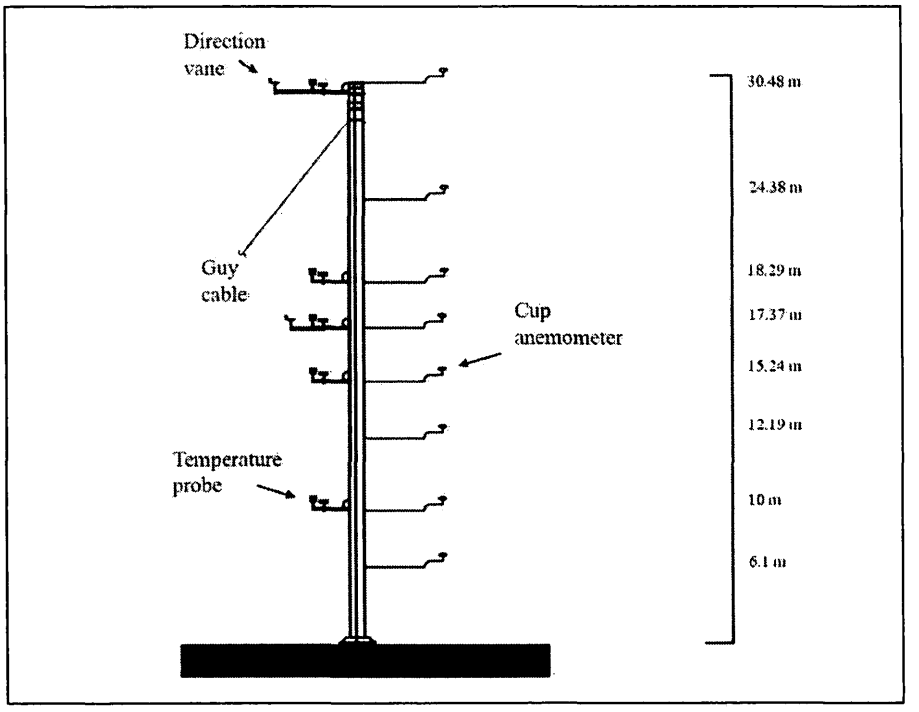

Fig.1.5: Simplified diagram of mounted instruments on the test site Meteorological tower.

Ambient air temperature is measured at five heights of 10 m (environmental standard), 15.24 m (Skystream hub height), 17.37 m (Bergey hub height), 18.29 m and 30.48 m. A nearby weather station records hourly air temperature and humidity at screen height (1.5 m) and environmental standard of 10 m if further refinements in air density are required. As the directionality of wind is important role in establishing site characteristics and wind patterns, two wind vanes were mounted on the tower mast at heights of 15.24 m and 30.48 m. Further specifics of the mounted instrumentation are provided in Table 1.2.

Table 1.2: Specifications for mounted sensors on meteorological tower at Kortright testing site.

	Mounted Height	Model	Operational Range	Data Capture
Anemometers	6.10 m, 10 m, 12.19 m, 15.24 m, 17.37 m, 18.29 m, 24.38 m, 30.48 m	8 NRG #40c 3-cup anemometers,	1 ms^{-1} to 96 ms^{-1}	5-second recording, 0.1 ms^{-1} accuracy (5 ms^{-1} to 25 ms^{-1})
Temperature Sensors	10 m, 15.24 m, 17.37 m, 18.29 m, 30.48 m	5 NRG #110s RTD sensor with radiation shield	-40 °C to 52.5 °C	5-second recording, +/- 0.8 °C accuracy maximum
Wind Vanes	15.24 m, 30.48 m	2 NRG #200p Wind Vane	360° mechanical, continuous rotation	5-second recording

Electrical power is measured with transducers mounted in the power supply lines downstream of turbine inverters used to convert power to 110V AC 60 Hz compatible with the electrical grid. Data from transducers are routed through conductors to the basement of Archetype House where data is stored on the main computer.

1.5.2 Deviation from IEC61400 Standards

Research costs and resource constraints have prevented the Kortright testing site from adapting all of the IEC standards as per the IEC 61400 standards which are defined for

the design and testing of wind turbines (61400-2 is specifically for small wind turbines, Appendix A). The TRCA (Toronto and Region Conservation Authority) has proposed the Kortright site to become the first small wind turbine testing site in Ontario and the first in Canada outside of Prince Edward Island, PEI. Results from this study will help advise this motion and further progress in becoming SWCC certified. Variations in data sampling, instrumentation setup and data analysis do not vary widely from certification standards and many variations will not have concerning effects on the creditability of the analysis. The largest deviation from IEC 61400 standards lies in the absence of a meteorological tower for each wind turbine and this is owing to the large costs involved in testing more than one turbine at a time.

1.5.3 Field Data Acquisition

The data acquisition unit for the meteorological tower is a National Instruments CFP-1804 which is housed in a nearby instrumentation house. This is a slave unit for the controllers based in the Archetype house, and is access from the main computer with a wireless bridge. The individual modules of the CFP (Compact Field Point) system accept different signal parameters and three modules on the CFP were used for the anemometer, RTD (temperature) and wind vane sensors and the wind turbine inverters. Data were recorded at 5 second intervals and the parameters recorded were date stamp, wind speed (ms^{-1}), wind direction (degrees), ambient air temperature (°C), and Bergey inverter voltage (Volts) and current (Amps) readings for the turbine, battery and battery-dump.

The Skystream wind turbine was not connected to the main meteorological tower wiring owing to its position within the field test site. Data from the Skystream wind turbine were acquired wirelessly using a Southwest Windpower USB radio receiver which was mounted on the east facing wall of the Archetype house with a direct line of sight to the Skystream wind turbine nacelle. This data were then instantaneously processed with the Skyview 2.0 software on the main computer. Data were also recorded on a 5 second interval and were also further extracted from SQL format for analysis.

Data acquisition for the Skystream 2.4 kW wind turbine started as of 25 September 2012 and the Bergey 1 kW wind turbine data began recording as of 7 November 2013 owing to unforeseen delays in mounting of the meteorological tower and instrument setup.

1.5.4 Wind speed data

As the NARR data gave u and v, moment magnitude wind speeds, U (ms^{-1}) were calculated using the standard magnitude formula as represented by Equation 1.4.

$$U = \sqrt{u^2 + v^2} \tag{1.4}$$

Wind speeds at 10 and 30 m heights were derived for every 3 hrs from the corresponding NARR wind data from 1980 to 2012. Monthly mean wind speeds for years 1980 to 2012 were computed and 33-yr monthly averages were also computed. Trend analysis using a

simple linear regression was also performed (Equation 1.5) to establish monthly trends in wind speeds over the entire 33 years for both tropospheric heights:

$$U_t = a + R_t \tag{1.5}$$

Where t represents the time (in unit of years in this study), R_t and a are the slope and intercept, respectively. Plots of p-values < 0.05 show areas with significant trends and standard deviations for wind data at 10 and 30 m from 1980 to 2012 was also computed for each grid cell. Since a minor error is found in the code for the calculation of 30-m wind speed, which results in zero values in high terrain and coastal regions (http://www.emc.ncep.noaa.gov/mmb/rreanl/faq.html#zero-30m-winds), 30 m wind speed for gird cells outlined in Appendix A, Table A1 are disregarded in the analysis of this study. The coding was affected by regions which have altitude very close to sea level and thus many grid cells outlining James Bay and southern Hudson Bay lowlands are affected.

1.5.5 Wind power estimates

The power in the wind (P) can be computed with the knowledge of wind speeds and air density (kgm^{-3}) based on the following Equation 1.6:

$$P = C_p \frac{1}{2} \rho A v^3 \tag{1.6}$$

where the coefficient of performance of the wind turbine (C_p) is considered to be 100% or 1.0 and the swept area (A) is considered to be 1 m^2. Air density (ρ) was computed for every 3 hrs from the corresponding NARR pressure and temperature data from 1980 to 2012 at 10 and 30 m using Equation 1.7:

$$\rho = \frac{p}{R_{spec}T} \tag{1.7}$$

Where p is the absolute atmospheric pressure (Pa), R_{spec} is the specific gas constant for dry air, 287.04 $Jkg^{-1}K^{-1}$, and T is the absolute temperature (K). Air density values were coupled with wind speed data to estimate wind power across the study scope. As with wind speed, monthly means for wind power were computed for each year and over the 33-yr timespan. Regression analysis and interannual variability of wind power was also assessed. Furthermore, the difference in wind power between the 10 and 30 m levels ($P_{30m} - P_{10m}$) was computed.

1.5.6 Turbine electrical output

Meteorological and electrical output data was captured for both turbines between 7 November 2012, and 30 April 2013. This data provided 5 second readings of wind speed at 8 levels above ground (Table 1.2), temperature, wind direction and electrical output readings (Bergey and Skystream) for approximately 6 months. Analysis of this data was

used to produce performance data through power curves which demonstrated how the Bergey and Skystream wind turbines performed at differing wind speeds. Applying a best fit curve, quadratic equations were produced for each turbine that best described the ability of the turbine to convert wind energy into electrical power in Watts (Equations 1.8, Bergey and 1.9, Skystream):

$$y = -0.1007x^4 + 2.02x^3 - 2.8783x^2 - 2.1873x + 2.7317 \quad (1.8)$$

$$y = -0.1442x^4 + 2.9853x^3 - 8.2462x^2 + 9.3011x - 3.9783 \quad (1.9)$$

where y is the power produced by the respective turbine in Watts and x is the hourly wind speed in ms^{-1}. These power curve equations were then applied to the analyzed wind speed data from NARR. Using the hourly (3 hour) wind speeds for each month over the period of 1980 – 2012, the power curves, the electrical output for each 3 hour reading from NARR was calculated in megajoules (MJ) and the summed electrical output for each month was averaged based on 33 years on wind speed data. Thus, the resultant output showed the mean, summed electrical output in MJ for each grid cell within the NARR study scope (3364 cells) with particular interest in Ontario and the Great Lakes. This method was repeated at the 30m hub height as well and thus electrical output was given at two atmospheric heights for each wind turbine. Trend analysis was also performed for electrical output over 33 years and corresponding slope and *p*-values were mapped to show areas with statistically significant trends in electrical output.

CHAPTER 2

POTENTIAL FOR ELECTRICAL GENERATION OVER ONTARIO AND THE GREAT LAKES: AN ASSESSMENT OF NARR WIND TRENDS.

Potential for Electrical Generation over Ontario and the Great Lakes: An Assessment of NARR Wind Trends.

Masaō Ashtine[a]

a Department of Geography, York University, 4700 Keele Street, Toronto, Ontario, Canada.

*Corresponding authors: mashtine@yorku.ca, bello@yorku.ca

2.1 Abstract

Current climatic changes have driven research in adapting to predicted weather patterns. Renewable energy for wind is greatly impacted by climatic changes and its potential in Ontario is yet to be fully understood. Understanding this potential involves the estimation of present and future wind regimes. The North American Regional Reanalysis (NARR) dataset has been widely used in wide data analysis and many studies have attested to its validity and agreement with measured wind patterns. Trends in wind speed and wind power over Ontario and the Great Lakes for small wind turbine hub heights (10 and 30m) were analyzed using the NARR dataset for 1980 to 2012. Air density, atmospheric pressure, temperature, and the instantaneous wind speeds u and v, at 10 and 30m wereused for estimating wind speed and power. Statistically significant and positive annual trends in wind speed and powerwere predominant over the Great Lakes and eastern James Bay, with more substantial trends occurring in the fall and winter months. Significant trends of decreasing albedo and increasing stability in the fall and winter months were also noted over the Great Lakes, particularly over Lake Superior. The former suggests changing thermal dynamics that encourage increasing wind speeds which ultimately manifest in increasing wind power potential in these regions.

2.2 Introduction

The demand for wind energy is rapidly growling around the world and has become a major contributor of new electricity in many wind resource rich countries. In 2012, global wind energy capacity grew by 19%, with the global wind industry installing approximately 44,711 MW of wind power (CanWEA, 2012) and today there are over 150,000 wind turbines operating around the world in over 90 countries. While wind energy has been increasing substantially in many new emerging economies, it has been a relatively new provider of clean energy in Canada. In 2012, clean wind energy grew by nearly 20% in Canada, representing over $2.5 billion in investment and Canada's current installed capacity is just over 6,500 MW (CanWEA, 2012).The province of Ontario has 2,043 MW of installed wind capacity (*ca.* 31% of Canadian wind capacity; IESO, 2012).

With the Canadian government and private investors such as CanWEA aiming to have 20% of energy supplied by wind by 2025 across Canada, the wind regimes, patterns and potential across Canada are of substantial importance. Sub-arctic and northern regimes are experiencing the greatest trends in warming as outlined but IPCC reports and these trends can result in energy used to drive winds. It is important to understand these trends in wind owing to climate change and their future projections in order to fully comprehend the potential for wind energy in Ontario. Wind energy supplied just over 3% of electricity supplied in Ontario in 2012 (IESO, 2012), and there exists a push for greater investment in wind energy in the province.

As the atmosphere warms up and climate change progresses, it is expected that this will be translated in wind patterns of many regions. Previous studies analyzing wind trends over North American have shown strong trends in winds with both model-based and measured estimations (Holt and Wang, 2012; Pryor *et al.*, 2011; Pryor *et al.*, 2010; Hundecha *et al.*, 2008; Lorenz and DeWeaver, 2007; Archer and Jacobson, 2003; Klink, 1999; Lambert, 1995). Canada has been shown to have a substantial potential for wind energy, both offshore and onshore but very little research has been done on trend analysis of wind regimes. If the top ten CO_2 emitting countries were ordered in terms of wind power potential, Russia would rank number 1, followed by Canada with the United States in the third position (Lu *et al.*, 2011). Li et al. (?) show the Great Lakes as having a large wind resource with the areas over Lake Superior, Michigan, and Ontario appearing to be rich in wind potential and have an interannual variability correlated with changing sea ice over the lakes.

Ground-based observations have proven inefficient and inadequate for the analysis of wind trends of an expansive region. Their spatial and temporal discontinuities are well noted as limiting estimations due to the heterogeneous interpolation of wind speeds. Furthermore, like modeled data, weather station measurements can have substantial error associated with their estimates owing to *in situ* environmental conditions and reading methodologies which are further compounded by spatial limitations. Modelled data presents many challenges in the assessment of wind resources and are dependent on our understanding of the physics involved. Global climate models have each been rigorously

tested and compared amongst other models and observational data in their ability to accurately estimate wind speeds. Reanalysis data have been used in many recent studies as these data allow for a more complete integration of both modeled and observed wind speeds (Fall *et al.*, 2010; Markovic *et al.*, 2009; Pryor *et al.*, 2009; Dominguez *et al.*, 2008; Bukousky and Karoly, 2006; Ruiz-Barradas and Nigam, 2005).

2.2.1 NARR dataset

The NCEP-NARR is a long-term, dynamically consistent, high-resolution, high-frequency, atmospheric and land surface hydrology dataset for the North American domain (Mesinger *et al.*, 2006). At present this dataset comprises of reanalysis data for the time period of 1979–present and within this study, data from 1980-2012 were used. The NARR procedure uses the very high resolution NCEP Eta Model (32 km, 45 layer) together with the Regional Data Assimilation System (RDAS) which, substantially assimilates precipitation along with other variables (Mesinger *et al.*, 2006; Janjić, 1994; Mesinger *et al.*, 1988; Black, 1988). NARR is widely known for its successful assimilation of high-quality and detailed precipitation observations into the atmospheric analysis which was previously lacking from many global models. This study focuses around the electrical output potential over Ontario through investment in small wind turbines (< 300 kW rated power or < 30m hub height) and wind data from the tropospheric heights of 10m and 30m were assessed. Both wind speeds are extrapolated

on the basis of mid-layer winds at the four neighboring mass points at the lowest of 45 model layers following a procedure originally developed by Lobocki (1993) and described in detail by Chuang *et al.*, (2001). However, owing to preliminary coding error at the 30m level, grid cells along the lower Hudson Bay shoreline have been erroneous in their wind speed estimation due to their low lying elevation (marginally above sea level; http://www.emc.ncep.noaa.gov/mmb/rreanl/faq. html#zero-30m-winds). These 43 grid cells were irrefutably defined, non-influential on neighboring cells, and represented less than 0.01% of the study scope (Appendix A).

The question concerning the link between wind speed trends and estimated wind power potential over Ontario and the Great Lakes is highly understudied and reflect a research void in wind speed analysis within Canada. With this NARR research, wind regimes across Ontario can be defined at a more precise and refined estimates.

2.3 Materials and Methods

2.3.1 Wind speed estimates at 10 and 30m

As the NARR data gave u and v, directional wind speeds, the moment magnitude wind speed U (ms^{-1}) for each grid cell and both tropospheric levels was calculated using the standard magnitude formula as represented by the following Equation 2.1:

$$U = \sqrt{u^2 + v^2} \quad (2.1)$$

Wind speeds at 10 and 30 m heights were derived for every 3 hrs from the corresponding NARR wind data from 1980 to 2012. Monthly mean wind speeds for years 1980 to 2012 were computed and 33-yr monthly averages were also computed. Grid cells along the lower Hudson Bay shoreline have been erroneous in their wind speed estimation due to their low lying elevation (marginally above sea level; http://www.emc.ncep.noaa.gov/mmb/rreanl/faq.html#zero-30m-winds).

2.3.2 Method for wind trend

Trends for each grid point of the study were computed from 1980-2012 using the Ordinary Least Squares (OLS) linear regression method. Wind trends at the 95% confidence level were considered highly significant using a two-tailed *t*-test for each grid point. Trend analysis established monthly trends in wind speeds over 33 years for both tropospheric heights (Equation 2.2):

$$U_t = a + R_t \quad (2.2)$$

Where t represents the time in years R_t and a are the slope and intercept, respectively. Plots of wind trends are of those with of p-values < 0.05 (95% confidence) and show

areas with significant trends and interannual variations for wind data at 10 and 30 m from 1980 to 2012 were also computed for each grid cell. As a minor error was found in the code for the calculation of 30m wind speed, which results in zero values in coastal regions near sea level, 30 m wind speed for gird cells outlined in Appendix A, Table A1 are disregarded in the analysis of this study. Depending on geographical location, significant temporal autocorrelation of wind can occur over a period of 30 years and should be filtered out of the time series before applying OLS in effort to prevent statistical exaggeration of wind trends.

Wind trends in this study were not treated for temporal autocorrelation for it was found in Holt and Wang (2012) after using the Cochrane-Orcutt method to remedy the effect of the temporal autocorrelation, the significance of wind speed trends slightly lowered(below 5% in difference). Holt and Wang compare their findings with that of Pryor and Ledolter (2010), who showed that ''treatment of temporal autocorrelation slightly reduces the number of stations for which the linear trends in 10 m wind speed are deemed significant (at the 90% confidence level)''.Furthermore, Pryor and Ledolter (2010) showed that the magnitudes of the wind speed trends estimated through linear regression may also be relatively negligible to trends analyzed with data treated for temporal autocorrelation. Plot of wind speeds show no apparent temporal autocorrelation.

2.3.3 Method for wind power estimates and trends

The power in the wind (P)can be computed with the knowledge of wind speeds and air density (kgm^{-3}) based on the following Equation 2.3:

$$P = C_p \frac{1}{2} \rho A v^3 \quad (2.3)$$

where the coefficient of performance (the ratio at which a turbine can convert wind energy into electrical power) of the wind turbine (C_p) is considered to be 100% or 1.0 and the swept area (A) is considered to be 1 m^2. Air density (ρ) was computed for every 3 hrs from the corresponding NARR pressure and temperature data from 1980 to 2012 at 10 and 30 m using the following Equation 2.4:

$$\rho = \frac{p}{R_{spec}T} \quad (2.4)$$

where p is the absolute atmospheric pressure (Pa), R_{spec} is the specific gas constant for dry air, 287.04 J kg^{-1} K^{-1}, and T is the absolute temperature (K). Air density values were coupled with wind speed data to estimate wind power across the study scope. As with wind speed, monthly means for wind power were computed for each year and over the 33 year timespan. These monthly averages represented the summed wind energy available based on the criteria mentioned and include a summed average for each month in MJ.

Trend analysis in wind power over Ontario and the Great Lakes was computed through the OLS method and interannual variability of wind power was also assessed through the standard deviation of 33 year monthly averages. Furthermore, the difference in wind power between the 10 and 30 m levels ($P_{30m} - P_{10m}$) was computed to illustrate the change in power output with height.

Further analysis was done on the methods used to estimate total wind power through summation versus binning for select NARR grid cells representing regions of Toronto (43.6681° N, 79.2902° W), Sudbury (46.28981° N, 80.9729° W) and Central Ontario (51.28542° N, 84.01013° W) at both the 10 m and 30 m hub height. The former analysis established a sense of the sensitivity of varying bin size (0.5, 1 and 2 ms^{-1}) on the estimation of wind power as the binning method is frequently used to estimate wind power potential in wind site assessments. Wind power data from the NARR data at 3-hr recording were used to determine a 'true' estimation of monthly wind power which was compared to wind power estimates derived from the binning method where the frequency of wind speeds is used to calculate total wind power potential.

2.3.4Stability estimates

In order to assess stability changes in the atmosphere over the study area, the Richardson number (Ri) was calculated using temperature, atmospheric pressure and wind speed data from the two hub heights of 10 and 30 m using the following Equation 2.5:

$$Ri = \frac{g}{\bar{T}} \cdot \frac{\Delta\bar{T}/\Delta z}{(\Delta\bar{u}/\Delta z)^2} \qquad (2.5)$$

Where g is the acceleration due to gravity (ms^{-2}), $\bar{T}$ is the mean temperature in Kelvin in the atmospheric layer Δz (10 m–30m), and $\bar{u}$ is the mean wind speeds at each hub height (ms^{-1}). This was calculated for each month for 33years over the study area and seasonal means and trends are also reported.

2.4 Results

2.4.1 Trends in wind speed

When considering winds at the 10 m hub height, seasonal trends in wind speeds show a common occurrence of higher mean wind speeds over the Great Lakes, particularly over Lake Superior (Fig. 2.1). Higher mean wind speeds are also persistent over southern James Bay, but these patterns are seasonally limited. During the winter (derived as the

months of December, January and February), mean wind speeds over the Great Lakes vary in the range of 5.5 ms^{-1}- 7.5 ms^{-1}, values which are substantially higher than seen across central and northern Ontario (4.5 ms^{-1}) and are more frequent over the larger Great Lakes than with Lake Erie or Ontario. Wind speed means are reduced during spring in most, if not all regions, with central and northern Ontario experiencing a lesser change. Hudson Bay, and lower James Bay wind speeds in particular, decrease from winter means. Spring winds are reduced over the Great Lakes, with Lake Michigan still experiencing higher means at its southern extent. While wind speeds over central and northern Ontario stay consistent from the previous seasons, the winds over the Great Lakes have largely died down with wind speeds over Lake Superior being the highest of the Lakes but still lower than spring means. The Great Lakes have become much less distinct in wind speed means in comparison to the surrounding land, particularly for Lake Erie and Ontario, and south of Ontario experiences lower wind speeds, *ca.* 3 ms^{-1}. Patterns are much different in the fall where wind speed means in increase substantially over Hudson Bay and the majority of the Great Lakes have mean of approx. 6 - 6.5 ms^{-1} which are larger than those of summer but not as high as winter means.

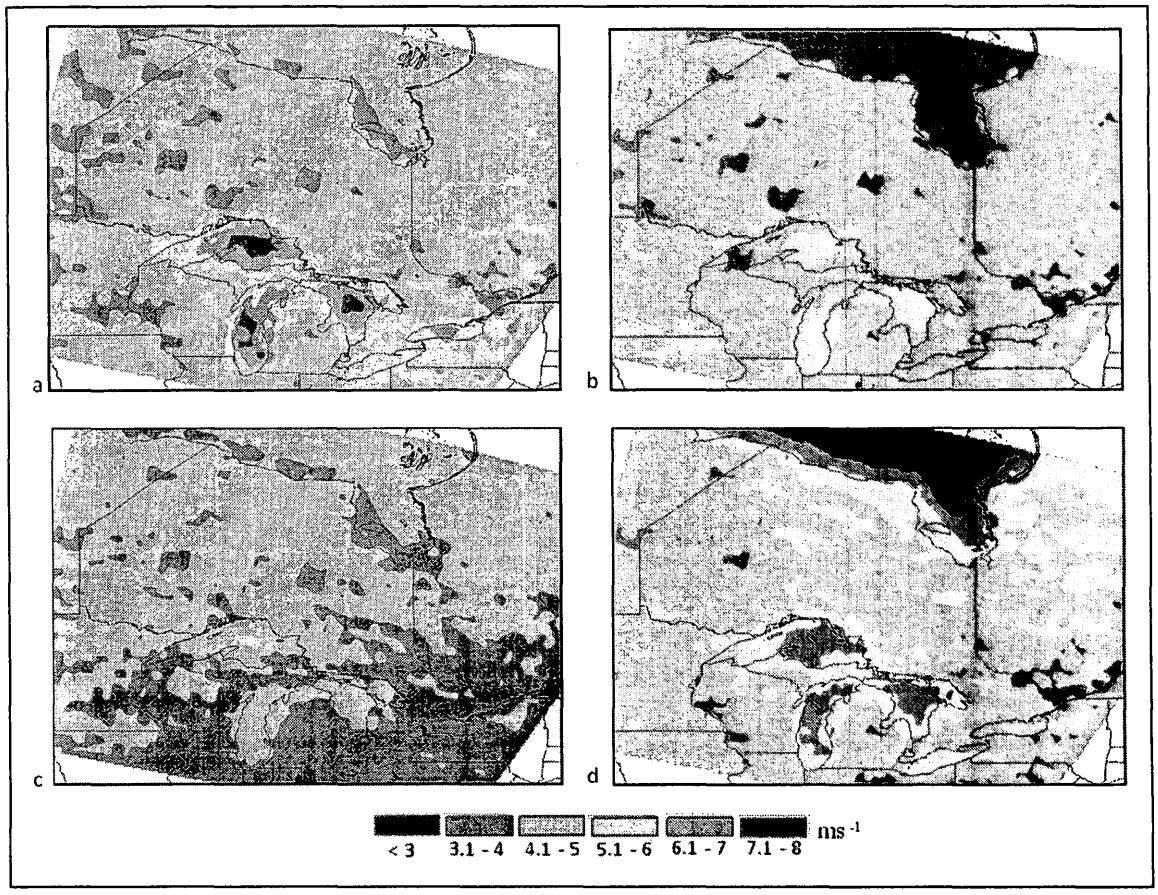

Fig. 2.1: Seasonal mean wind speeds for study area at 10 m for a) Winter (December, January, February), b) Spring (March, April, May), c) Summer (June, July, August), d) Fall (September, October, November).

These wind regimes persist at the 30 m hub height (Fig. 2.2) with slight spatial and temporal variations. Winter means show wind speeds over central and northern Ontario blowing at roughly $2ms^{-1}$ higher at 30 m and the same occurs over the Lakes where the latter appear more even in wind speed distribution. During spring the wind speeds are higher over Ontario than at 10 m but the Great Lakes are not distinctive in wind speed patterns except for small regions in central Lake Superior and southern Lake Michigan.

Lake Superior dominates the landscape with higher wind regimes but most of the lake has lower means than during winter.

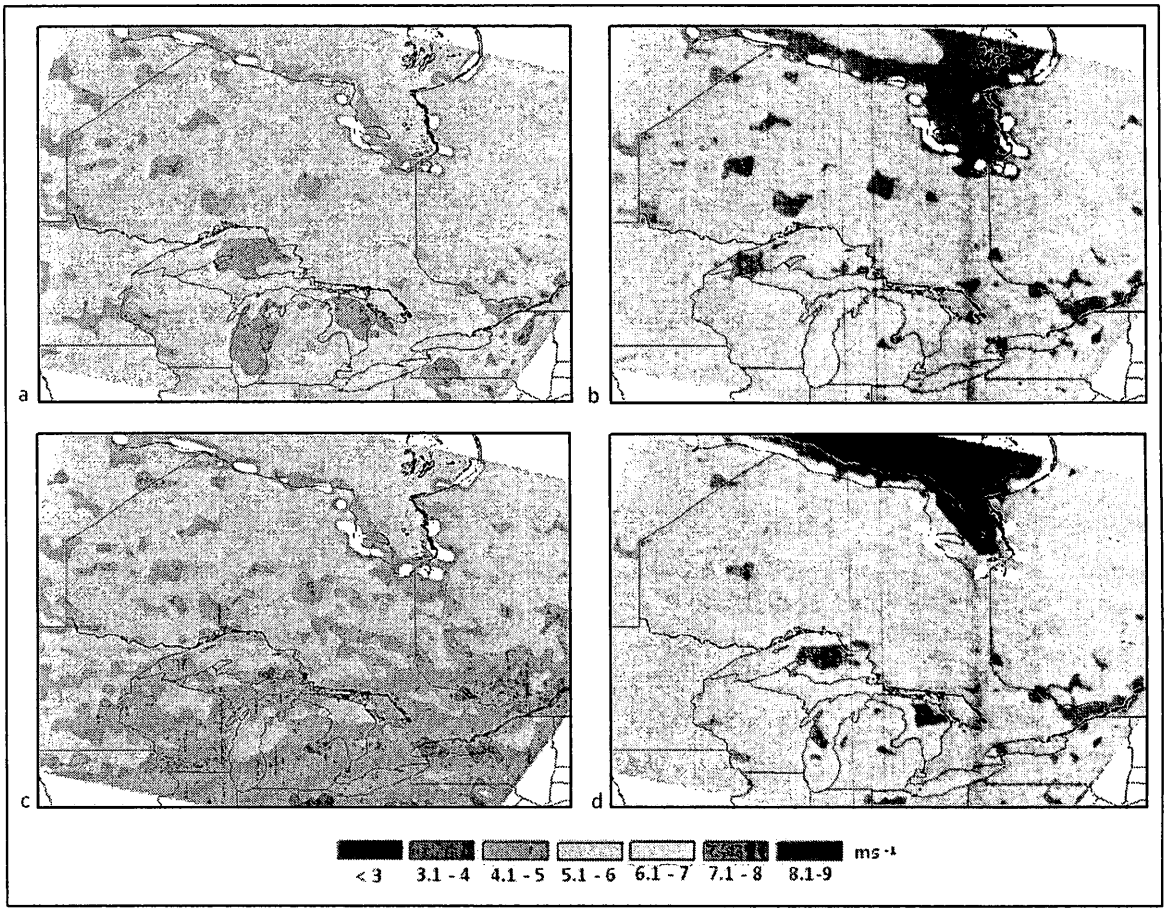

Fig. 2.2: Seasonal mean wind speeds for study area at 30 m for a) Winter (December, January, February), b) Spring (March, April, May), c) Summer (June, July, August), d) Fall (September, October, November). *Coastal regions in white have been omitted due to coding error at the 30 m hub height.*

Throughout each season, the wind speed boundaries between the Great lakes and land become less defined at the 30 m height and wind patterns become more uniform over land. The largest variation in wind speeds means with hub height exist during the winter

months with an approximate increase in wind speeds by 30% but this increase is not much greater than that experienced in other seasons as wind speeds over much of Ontario increase by roughly 1 ms^{-1} at the 30 m hub height. It must be noted again that coding errors at the 30m hub height has distorted estimates in specified cells along the Hudson Bay shoreline (A.1).

Wind speed trends (Fig. 2.3) computed through OLS were first analyzed for temporal autocorrelation where it was realized that no apparent autocorrelation in wind speed means over 33 years existed. James Bay demonstrated areas with the highest wind speed trends at the 10 m hub height (maximum of *ca.* 0.1 $ms^{-1}yr^{-1}$, particularly over eastern James Bay) during winter. Trends over the Great Lakes are also strong (*ca.* 0.05 $ms^{-1}yr^{-1}$ with some areas experiencing around 0.07 $ms^{-1}yr^{-1}$) and trends over Lake Erie and Ontario are not as strong as the larger Lakes. This trend over the Lakes changes in spring where Lake Superior has higher wind trends, but most of the lake has lower trends than during winter and Lake Erie and Ontario appear to have slightly negative trends but at means very close to 0 $ms^{-1}yr^{-1}$. Increases in wind speed appear to be greatest over James Bay in the fall where trends indicate wind speed rates between 0.1 and 0.12 $ms^{-1}yr^{-1}$ in some regions. That represents an approximate 55% increase in wind speeds versus the mean over 33 years or *ca.* 17% increase per decade. The opposite is true for the Lakes during the summer where trends over the lakes appear no different from the surrounding land with very low rates of change.

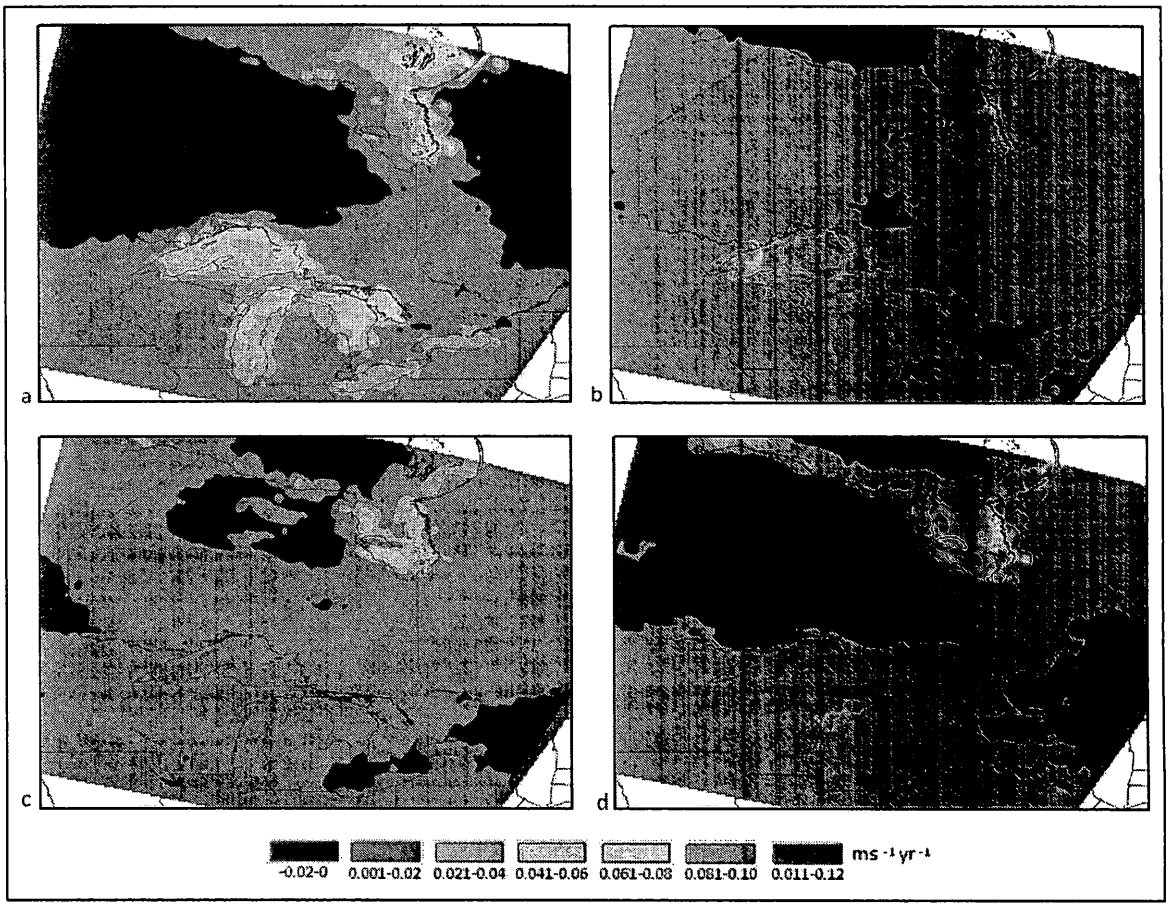

Fig. 2.3: Multi-year trends in seasonal wind speeds for study area at 10 m for a) Winter (December, January, February), b) Spring (March, April, May), c) Summer (June, July, August), d) Fall (September, October, November).

The wind speed trends are also experienced at the 30 m hub height (Fig. 2.4) with no distinct increase or decrease in trends. For most seasons, many of the trends experienced were highly significant ($p< 0.005$) over the Great Lakes and James Bay at both hub heights (Fig. 2.5). Spring does not experience significant trends ($p< 0.05$) over all the Great Lakes but these are limited to regions over Lake Superior and southern Lake

Michigan, and during the summer, this statistical significance is localized mainly to James Bay and some of the Great Lakes (Huron, Erie and Ontario).

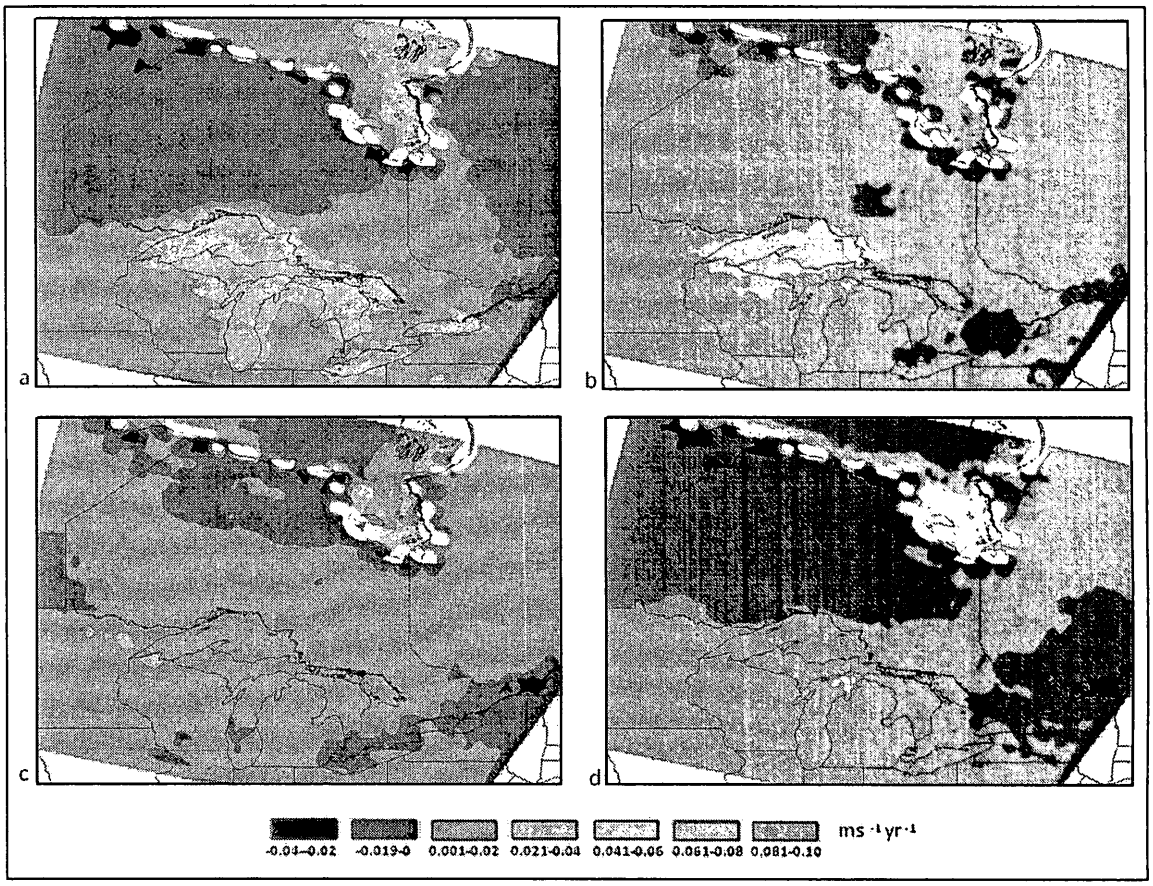

Fig. 2.4: Multi-year trends in seasonal wind speeds for study area at 30 m for a) Winter (December, January, February), b) Spring (March, April, May), c) Summer (June, July, August), d) Fall (September, October, November). *Coastal regions in white have been omitted due to coding error at the 30 m hub height.*

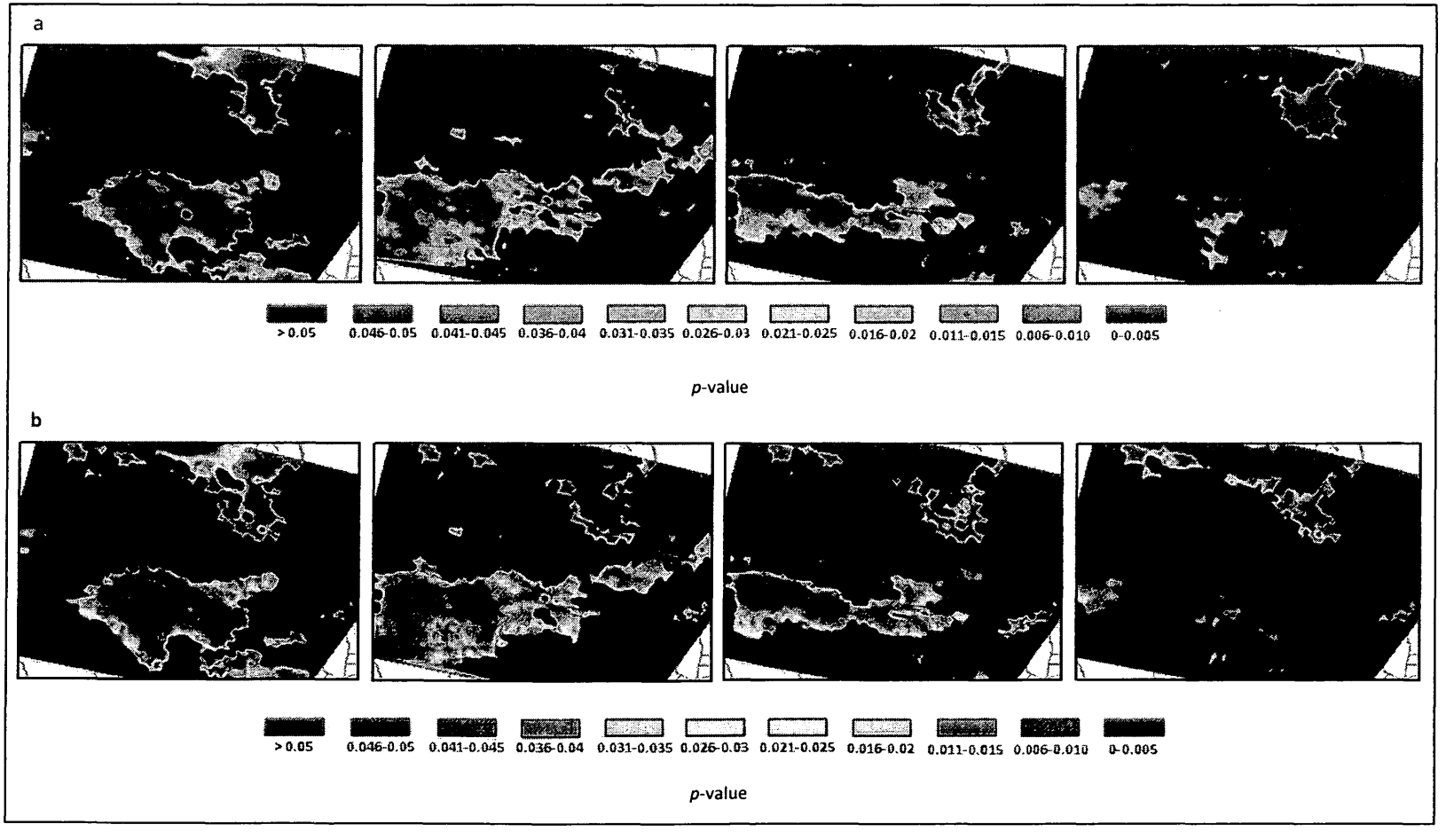

Fig. 2.5: Statistical significance (*p*-values) of multi-year trends in seasonal wind speed for the study area at a) 10 m and b) 30 m for Winter (December, January, February), Spring (March, April, May), Summer (June, July, August), Fall (September, October, November) from left to right respectively.

2.4.2 Wind energy patterns

The described wind speed trends manifest into very similar patterns of potential wind energy across Ontario and over the Great Lakes and James Bay (Fig. 2.6). Winter mean wind energy values are distinctively higher over the Great Lakes with Lakes Superior, Michigan and Huron showing the highest mean wind energy available. Much of central and northern Ontario have generally low wind energy means of approximately 500-1000 MJ whereas over the lakes can experience means of 3 GJ and more and areas surrounding the Lakes can see means of 1.5 GJ and greater.

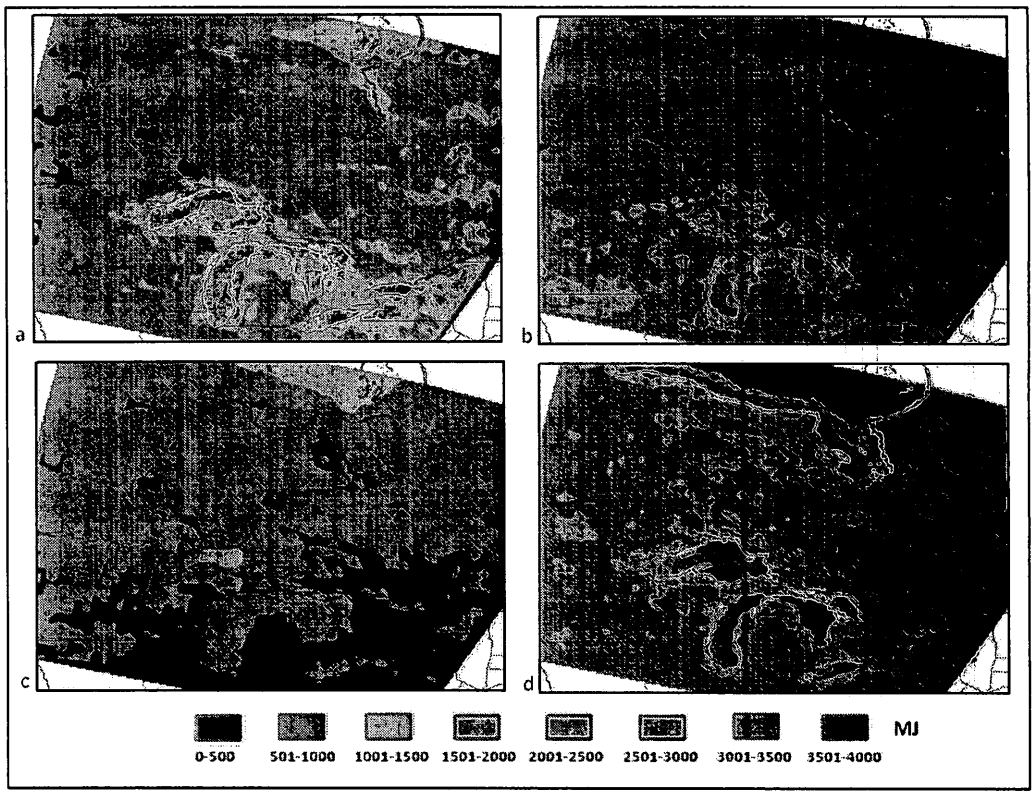

Fig. 2.6: Seasonal mean wind energy potential for study area at 10 m for a) Winter (December, January, February), b) Spring (March, April, May), c) Summer (June, July, August), d) Fall (September, October, November).

In the spring it is clear that the Hudson Bay has the lowest wind energy values whereas the lakes are still higher than the surrounding land and northern and central Ontario have similar means as in winter. In southern Ontario, except for areas surrounding the Lakes, lower means in wind energy persist. Wind energy values in the summer have decreased across the board with central Ontario having a mean energy of 600 MJ and patterns becoming more irregular. In the fall however, the Great Lakes and Hudson Bay possess much higher wind energy than the surrounding land with regions in central Hudson Bay having up to 4 GJ of wind energy and shoreline areas having around 2 GJ of wind energy available. The Lakes appear to be evenly distributed in wind energy along with central and northern Ontario.

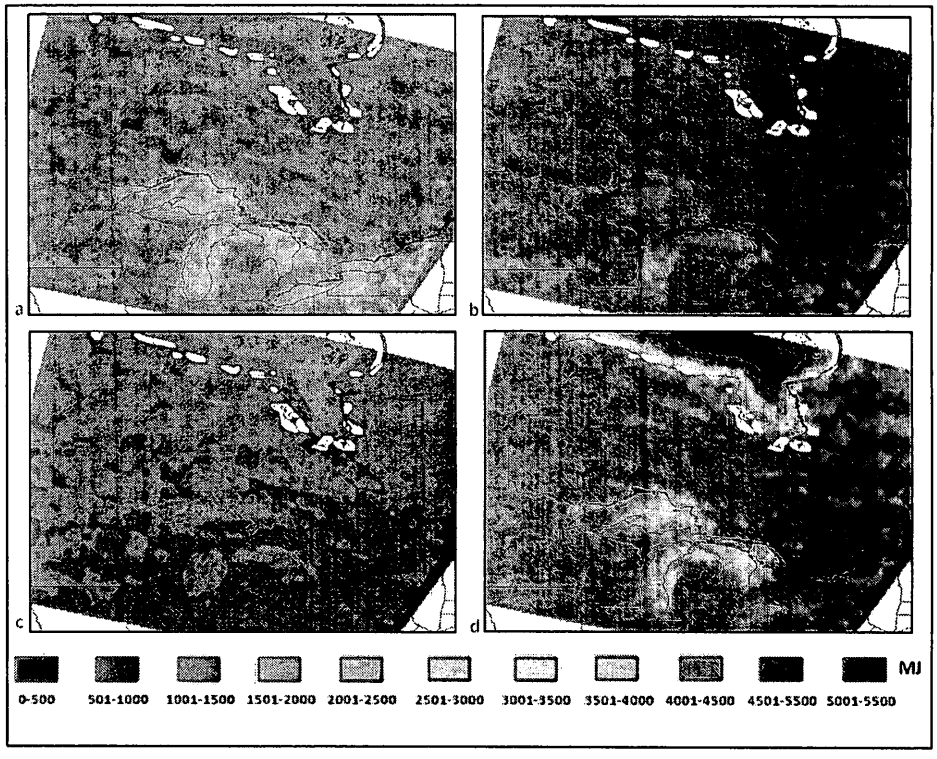

Fig. 2.7: Seasonal mean wind energy potential for study area at 30 m for a) Winter (December, January, February), b) Spring (March, April, May), c) Summer (June, July, August), d) Fall (September, October, November). *Coastal regions in white have been omitted due to coding error at the 30 m hub height.*

These patterns are once again seen at the 30 m hub height (Fig. 2.7) with increased wind energy potential with stronger winds aloft. The Hudson Bay shoreline and regions due south of James Bay (excluding error cells) shows pockets of slight negative trends in the spring, summer and fall seasons at both hub heights (Fig. 2.8 and 2.9). Going up to 30 m, these patterns are consistent and wind energy trends over the Lakes and James Bay are generally statistically significant ($p < 0.05$) in each season with few exceptions over individual Lakes (Fig. 2.10).

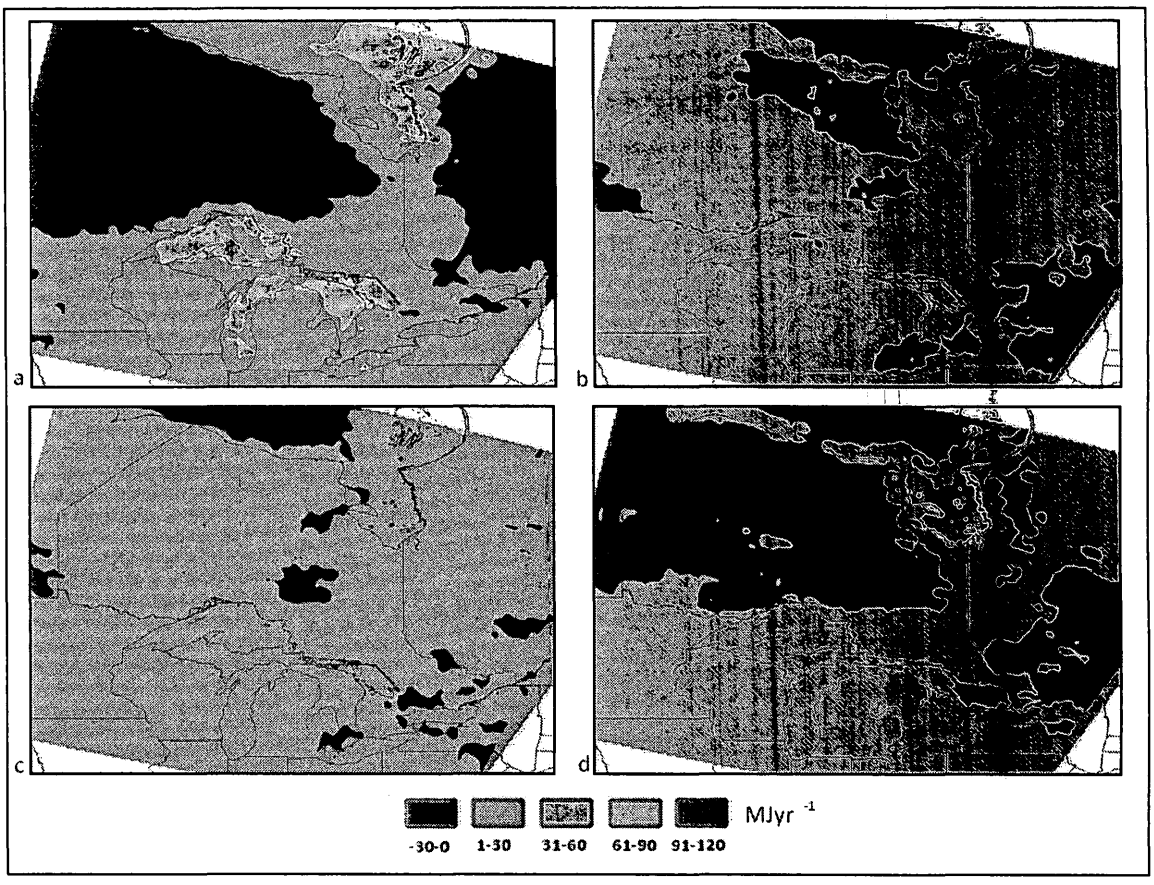

Fig. 2.8: Multi-year trends in seasonal wind energy for study area at 10 m for a) Winter (December, January, February), b) Spring (March, April, May), c) Summer (June, July, August), d) Fall (September, October, November).

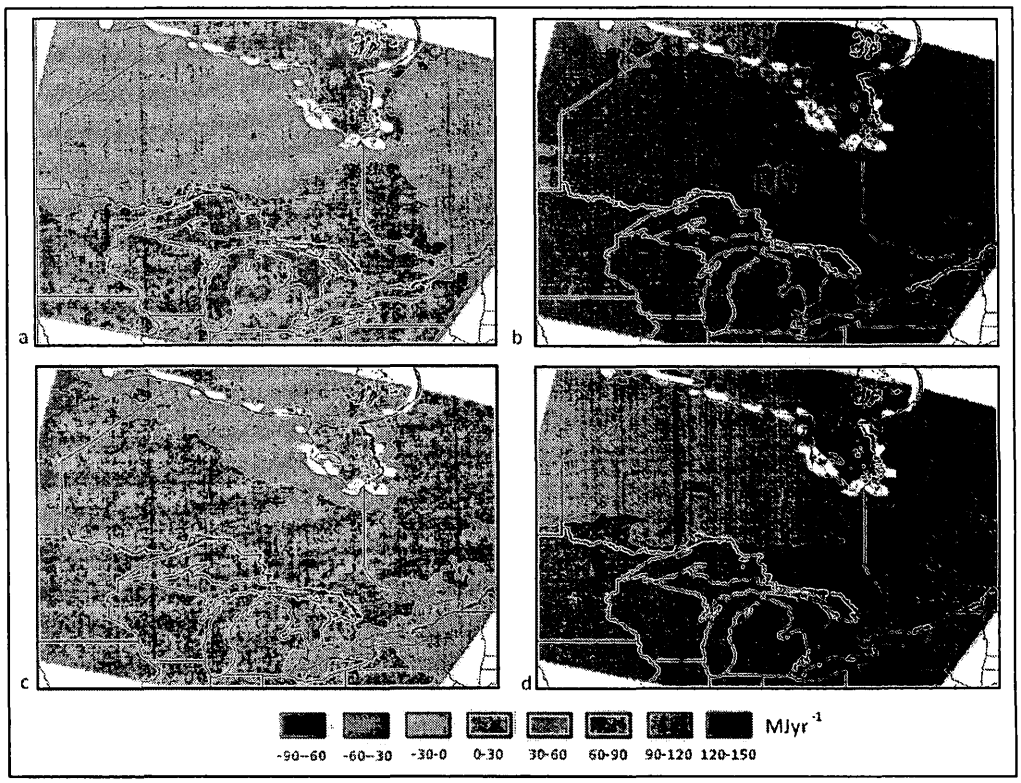

Fig. 2.9: Multi-year trends in seasonal wind energy for study area at 30 m for a) Winter (December, January, February), b) Spring (March, April, May), c) Summer (June, July, August), d) Fall (September, October, November). *Coastalregions in white have been omitted due to coding error at the 30 m hub height.*

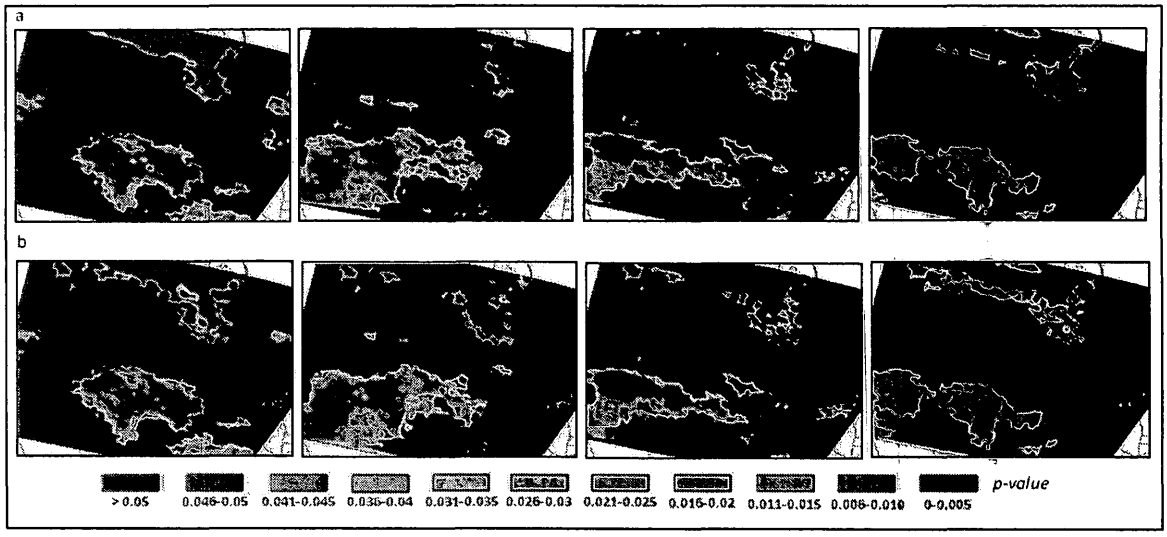

Fig. 2.5: Statistical significance (*p*-values) of multi-year trends in seasonal wind energy for the study area at a) 10 m and b) 30 m for Winter (December, January, February), Spring (March, April, May), Summer (June, July, August), Fall (September, October, November) from left to right respectively.

It is important to understand the sensitivity and measure of error involved in estimating wind power and it was found that wind power estimated not only varying with the size of the wind bins used but vary temporally and spatially as well. Data from the analyzed NARR grid cells at the 10 m hub height show that wind power estimates can vary among months in geographic locations such as Toronto (Fig. 2.11) where using 2 ms^{-1} wind speed bins can induce up to 5% overestimation error in estimations for summer months whereas this value is lowest in November at 1.5% overestimation. For all analyzed regions and months, reducing the wind speed bin size allowed for a reduced error in wind energy estimation but this difference varied monthly with some months giving very similar values of wind energy for both the 0.5 and 1 ms^{-1} wind speed bins. Toronto data showed overestimation was greatest in the summer whereas data from Sudbury (Fig. 2.12) and Central Ontario (Fig. 2.13) showed that error in wind energy estimation was more uniform temporally, however, the later had slightly higher overestimation errors. These patterns were similar at the 30 m hub height but show that error estimates are slightly smaller at each wind speed bin.

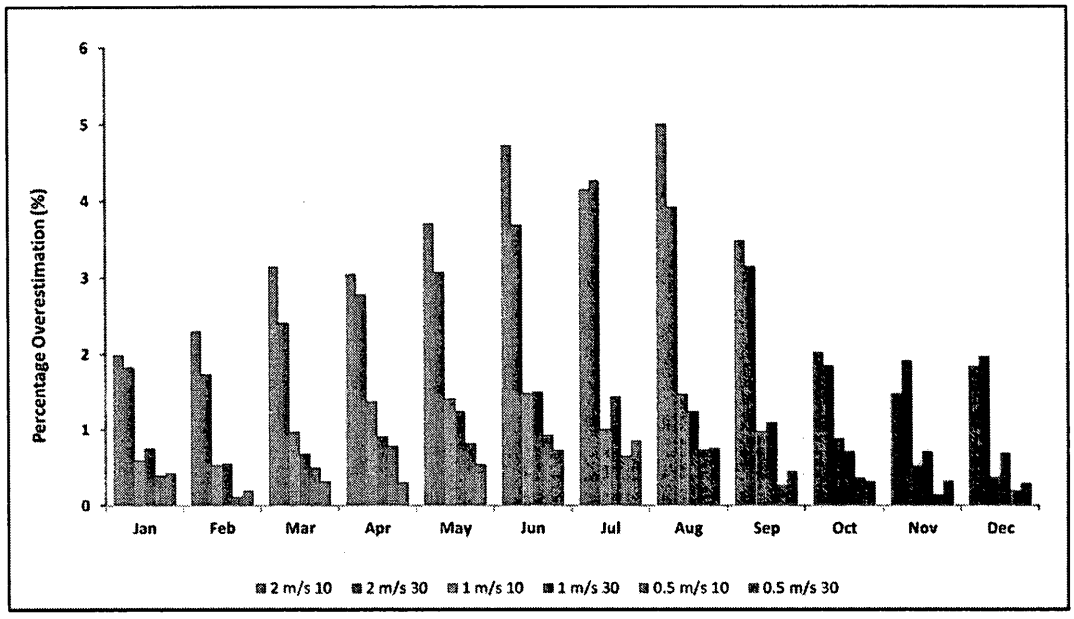

Fig. 2.11: Comparison of varying wind speed bin size (2, 1, 0.5 ms^{-1}) on the monthly estimation of wind energy estimations for Toronto NARR grid cell based on the use of summation estimates of wind energy from 3-hr NARR recordings as 'true' estimates.

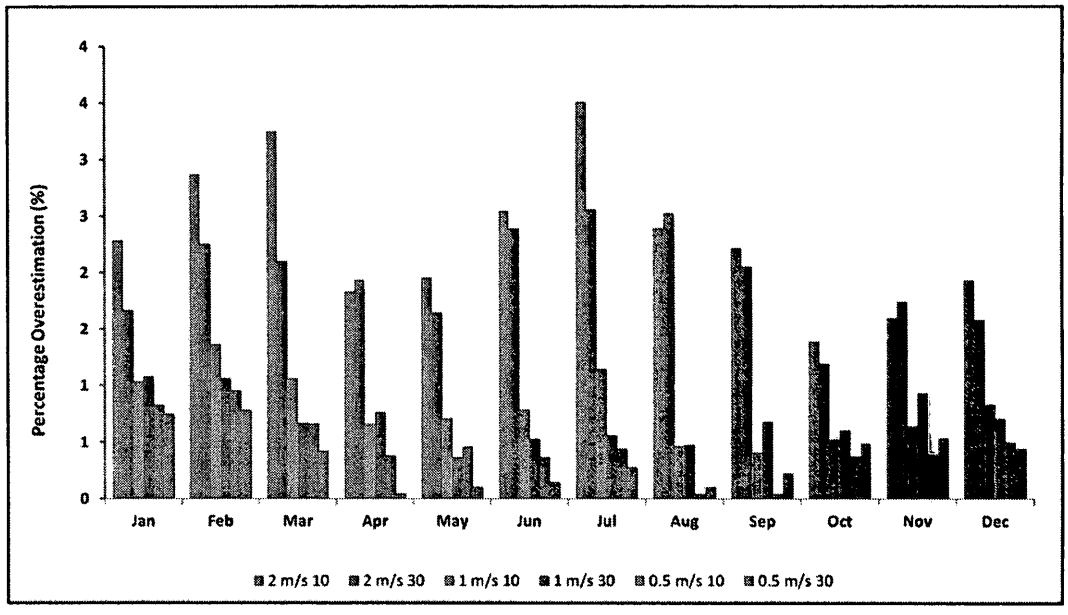

Fig. 2.12: Comparison of varying wind speed bin size (2, 1, 0.5 ms^{-1}) on the monthly estimation of wind energy estimations for Sudbury NARR grid cell based on the use of summation estimates of wind energy from 3-hr NARR recordings as 'true' estimates.

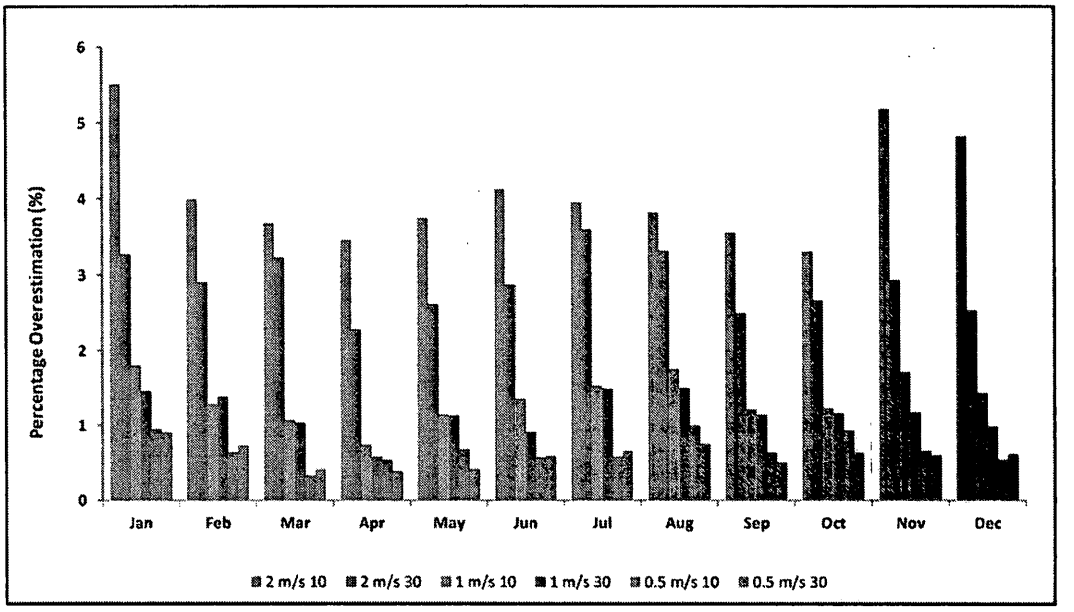

Fig. 2.13: Comparison of varying wind speed bin size (2, 1, 0.5 ms^{-1}) on the monthly estimation of wind energy estimations for Central Ontario NARR grid cell based on the use of summation estimates of wind energy from 3-hr NARR recordings as 'true' estimates.

2.4.3 Atmospheric Stability

Much of Ontario that is not in close proximity to the Great Lakes and Hudson Bay has very neutral conditions (Ri ~ 0) and is temporally consistent (Fig. 2.14). The Great Lakes and James Bay show differences in atmospheric stability in comparison to stability over land with negative Ri values persisting in winter and fall with more stable conditions occurring in the spring and summer seasons. Stability values in the winter are estimated around -1 over the Great Lakes, with particular instability over northern Lake Superior, where Ri values fall between -1.7 and -3.5. Transitioning into spring, stability increases to a Ri value of roughly 0.2 over the large water bodies. This pattern becomes more

inconsistent in the summer with atmospheric conditions over James Bay and Lake Superior being most stable whereas unstable conditions are still present over Lake Erie. Atmospheric conditions over the Great lakes become unstable again into the fall season with some regions having Ri values of -0.8.

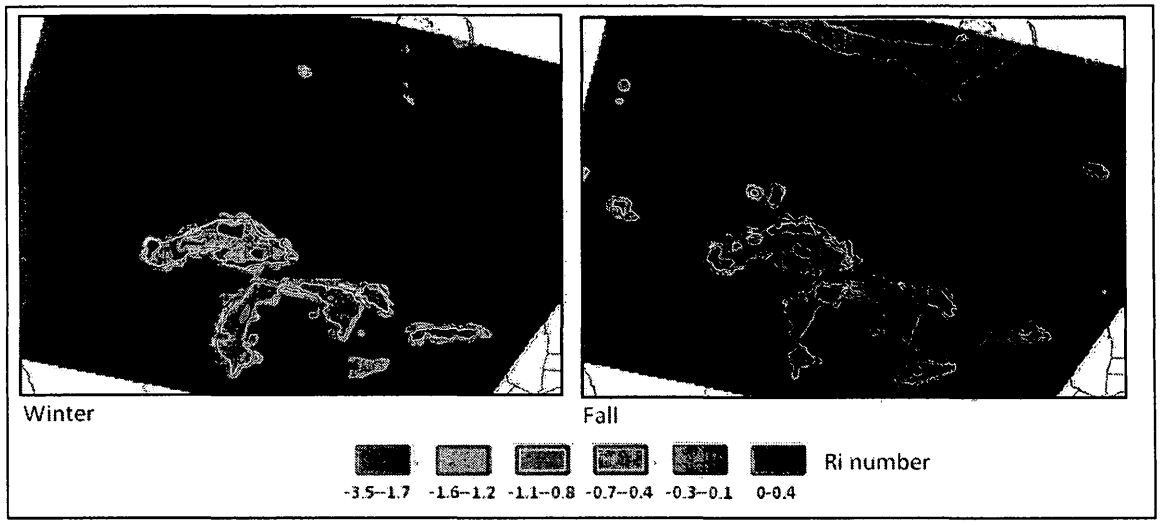

Fig. 2.14: Seasonal mean Richardson number for study area for a) Winter and b) Fall (September, October, November).

Trends in stability are near zero over much of Ontario but fluctuate in magnitude over the water bodies, with the strongest and significant ($p< 0.05$) negative trends occurring in the winter months (Fig. 2.15). Trends over the Lakes and eastern James Bay in the winter are roughly between -0.05 – 0 Ri units/yr. These trends are less negative and significant through spring, and during the summer, regions over Lake Superior can experience positive trends in stability but not at a significant level ($p< 0.05$). Trends in the fall show all the Great Lakes (excluding Lake Superior) and James Bay and the shoreline of

Hudson Bay as having negative trends in stability between -0.05 and 0 Ri units/yr. However, statistically significant trends are limited to atmospheric conditions over James Bay, Lake Michigan, Lake Erie and Ontario.

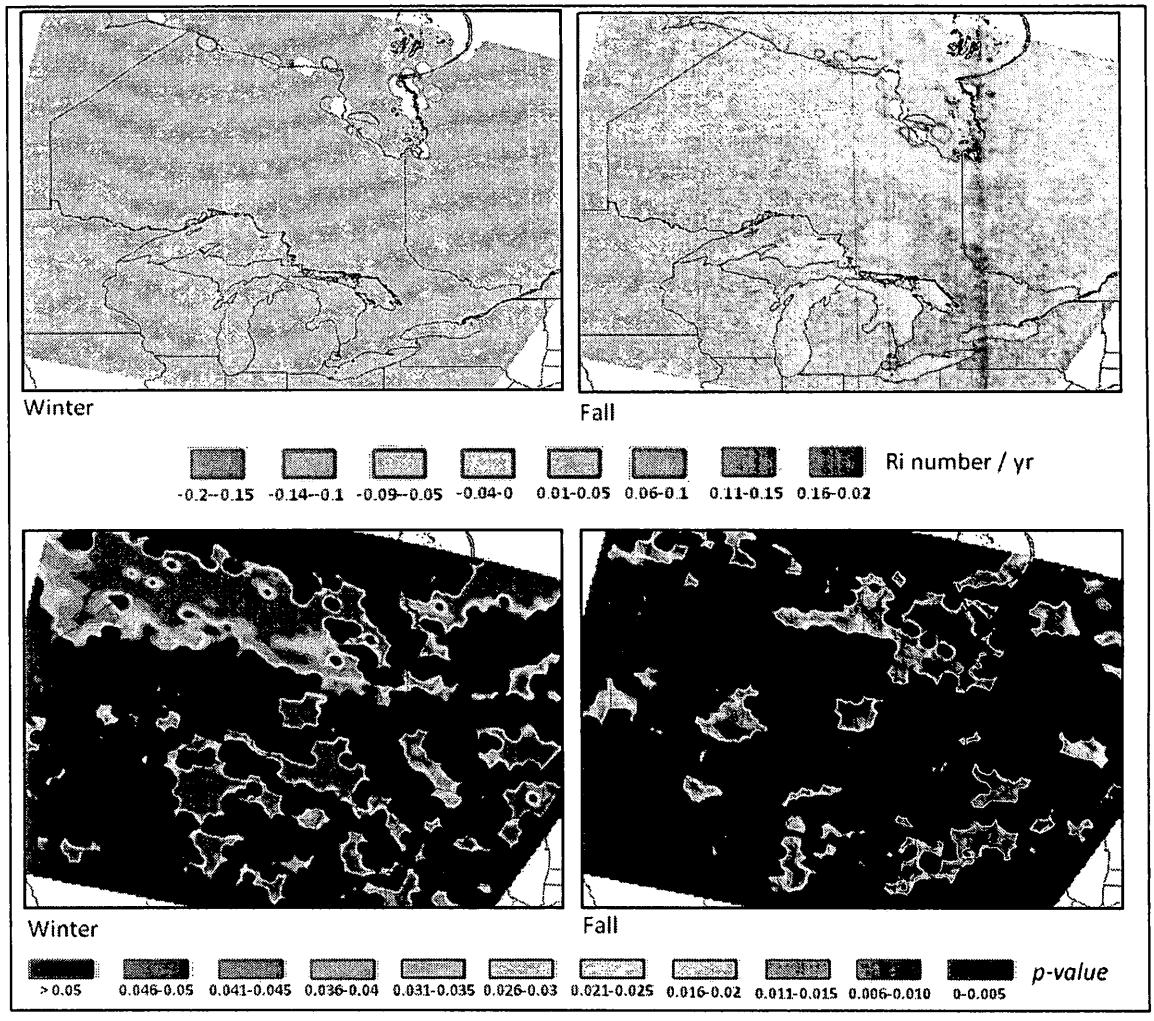

Fig. 2.15: Multi-year trends in seasonal Richardson number for study area for a) Winter (December, January, February), b) Fall (September, October, November) and Statistical significance (*p*-values) of wind energy trends for the study area for a) Winter (December, January, February), and b) Fall (September, October, November).*Coastalregions in white have been omitted due to coding error at the 30 m hub height.*

2.4.4 Albedo and wind speed

Regressional analysis with wind speeds against % albedo change give a negative relationship for much of the Great Lakes and James Bay (Fig. 2.16). An inverse relationship exists between the two parameters during the winter and wind speeds will increase with decreasing ice/snow coverage (% albedo). This trend is in the magnitude of -0.15 to -0.12 ms^{-1}/ % albedo in regions of eastern James Bay. A slope of -0.04 to -0.02 ms^{-1}/ % albedo is more common in regions surrounding the lakes, especially north of Lake Superior and Huron.

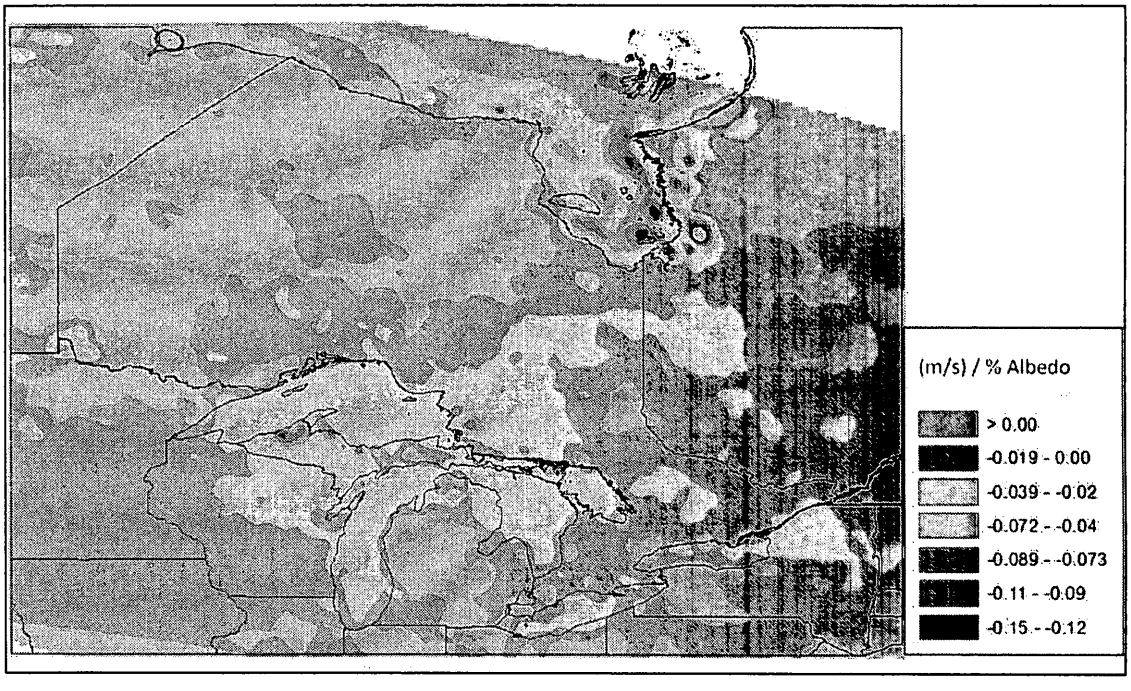

Fig. 2.16: Multi-year trends in seasonal winter mean wind speed regressed against

2.5Discussion

2.5. 1 Wind speed trends

From the analysis of the NARR data, it is clear that wind speeds are strongest over the Great Lakes than much of central and northern Ontario in the winter and fall months at both the 10 and 30 m hub heights. These wind speeds are also higher over James Bay and along the lower western Hudson Bay shoreline. This clear distinction of wind speeds is closely related to boundary conditions that exist as parcels of air transition over to land and water bodies and the physical state of described water bodies and terrain. The impact of warming temperatures on the dynamics of the Great Lakes is poorly understood but it has been recognized that the regional warming is different between the land and water (Austin and Coleman, 2007). The boundary layer that exists between the land and Lakes is most influential during the months of ice cover, ice breakup and ice re-formation. It has been noted that wind speed changes over the Lakes are being primarily influenced by changes in surface forcing (Desai and McKinley, 2009). Although the winds over the Lakes are poorly understood, it is agreed that lake ice concentrations have been on a rapid decline and this has been hypothesized to cause a destabilization in the atmospheric boundary layer (Cole *et al.*, 2007). Lake ice breakup have been linked with subsequent atmospheric temperature changes with a five-day change in break-up date would represent a 1.0° C change in April temperature and these energy balance changes may

influence wind patterns as well (Magnuson et al., 2000; Robertson *et al.*, 1992; Palecki and Barry, 1986).

Mean wind speed over the Lakes are not as high or distinct from the surrounding land during the summer months although similar patterns as seen in winter exist during the spring. As ice breakup of the lakes occur, atmospheric stability over the lakes is affected and thermal gradients may persist, driving onshore and offshore winds. These gradients weaken due to surface forcing from the loss of lake ice as water temperatures rise which has been noted for Lake Superior where summer temperatures have increased by roughly 3.5°C over the last century, most of that warming occurring in the last three decades (Austin and Colman, 2008). Bathymetry of lakes also affect rates of lake ice concentrations and break up and shallower lakes such as Lake Erie and Ontario have mean wind speeds closer to the surrounding land in early seasons than the larger Laurentian Lakes. These conditions are similar to those seen over James and Hudson Bay where sea ice breakup influences atmospheric stability. Gagnon and Gough, 2005, found statistically significant trends toward earlier breakup in James Bay, along the southern shore of Hudson Bay. Break-up first occurs in eastern James Bay owing to thawing and physical erosion produced by warmer wind blowing off of northern Ontario following snowmelt (Maxwell, 1986). These patterns are similar at the 30 m hub height with greater mean wind speeds in the order of 1-2 ms^{-1} faster. Trends over the Lakes in the fall may not be directly influenced by changes in reformation of lake ice as it is suggested that

unlike break-up in the spring, fall ice formation has not seen significant deviations over the years (Duguay *et al.*, 2006).

As seasonal atmospheric boundary layers are largely influenced by the surface forcing of lake ice concentrations, the apparent trends in wind speeds seem correlated with the former parameter. Winter trends in wind speed regressed against albedo levels show that during the winter months, a statistically significant ($p< 0.005$) negative relationship exists (*ca.* -0.04 to - 0.09 ms^{-1}/.% albedo/.yr) whereby decreasing albedo is related with increasing wind speeds and this trends is strongest over the Great Lakes (mainly in February) and James Bay (mainly in December). Thus over a decade, wind speeds can change as much as 12% over the Lakes and 23% in the James Bay at the 10 m hub height with each percent of albedo change. This is in accordance with studies purporting loss of lake and sea ice with changes in atmospheric stability (Desai and McKinley, 2009; Cole *et al.,* 2007; Gagnon and Gough, 2005). This relationship is reciprocal with atmospheric conditions affecting ice conditions and it has been noted that Artic sea ice and ice changes in the Hudson Bay are a sensitive indicator of climate conditions with negative trends in ice cover being linked with increased frequency of low pressure systems (Maslanik *et al.*, 1994).

Data supporting surface forcing on wind trends through changing ice cover is further complemented by stability analysis using NARR data which found that during the winter and fall seasons, the boundary layer over the Great Lakes is becoming increasingly and

significantly instable ($p< 0.05$) with very unstable conditions existing presently, particularly over Lake Superior. As expected, the Lakes are more stable during summer months as lake ice concentrations decrease to near disappearance and thermal regimes weaken. Richardson number modeling has a good fit with wind and temperature gradient estimates (Businger *et al.*, 1971) and unique research by Richards *et al.*, 1996, using data from Lake Erie and Ontario shows that the effect of changes in atmospheric stability lead to wind speed increase over water during unstable conditions and decrease during stable conditions. Furthermore, an increase in the length of over-water fetch due to lake ice decrease contributes to an increase in wind speeds during unstable conditions. Strong winds were also found to be less influenced by changes in atmospheric instability (Richards *et al.*, 1966), helping to explain smaller trends in wind speed seen at the 30 m hub height. These trends in stability over the Laurentian Lakes and James Bay, and patterns of lake/sea ice concentrations help to explain apparent seasonal trends in wind speed increase in these regions.

Winter and fall trends in wind speed are quite strong (*ca.* 0.05 $ms^{-1}yr^{-1}$ in winter; 6% decadal increase in winter means) with some areas in the winter experiencing as high as $0.07ms^{-1}yr^{-1}$which translates into roughly a 10% decadal increase in wind speeds in some regions of the lakes particularly over Lake Superior. Decadal trends show roughly a 3-4% increase in wind speeds over Laker Superior which is close in estimation to the 5% increase found by Desai and McKinley, 2009. In the fall, wind speeds can experience *ca.* 3% decadal increase in mean wind speed over the Lakes but with trends of up to 0.12 ms^{-}

$^{1}yr^{-1}$in James Bay, wind speeds can have a highly significant ($p< 0.005$) decadal increase of 17% and have increased 57 % over the past 33 years. Regions in central and northern Ontario experience weak negative trends in the fall and winter months but these trends are not statistically significant. These trends have also been found over the great lakes at the 80 m hub height using NARR data (Li *et al.*, 2010).

2.5.2 Wind energy potential

Wind energy potential is irrefutably influenced by wind speed regimes over Ontario and trends in wind energy are in accordance with wind speed results with the strongest influence occurring during the fall and winter months over the Great Lakes and James Bay. Wind energy potential for the province is restricted to regions around the lakes and in southern Ontario where much of the land is surrounded by water bodies. This has been known for some time through previous studies (Li *et al.* 2010; Elliot *et al.*, 1991) but magnitudes have been hard to estimate through limited observational data. Much of Ontario has low wind energy potential in comparison to the Great lakes and James Bay but wind energy potential increases with hub height at 30 m. With 20-60 $MJyr^{-1}$ trends over much of the Lakes at the 10 m hub height, wind energy has an approximate decadal increase of 17% over means in some regions during the winter and this increase is roughly 10% at 30 m. Wind energy potential can be increased by approximately 50% in most areas along the coast of the Great Lakes by moving from the 10 m hub height to the

30 m. Research using the PRECIS simulation to forecast (years 2071 – 2100) wind power suggests decreasing wind speed over southern Ontario at 80 m relative to the baseline period but also show that observational data show that changes in wind speed may not be proportional to the changes of wind power (Yao *et al*, 2012). Although this study shows very small decreasing wind speed trends in southern Ontario during the summer, these trends are not necessarily significant at the 0.05 confidence spatially. The previous study was also limited by only annual data (non-seasonal) and lack of temporal variations of wind speed.

Wind energy potential is also strongest in the fall with the lowest values being found in the summer months. This is largely due to the existing thermal gradients and changes in air density with winter having higher means than the summer.

2.6 Conclusions

Wind speed trends during the winter and fall months are the greatest at both hub heights of 10 and 30 m, with the summer season giving the lowest means. These trends are highly spatial, occurring frequently over the Great Lakes, lower Hudson Bay and James Bay. Much of Ontario experience statistically insignificant wind speed trends with lower much lower means than surrounding water bodies. These trends are suggested to have a strong correlation with decreasing lake/sea ice concentrations where loss of sea ice leads to both

physical and energy balance changes which subsequently alter the stability in the atmospheric boundary due to surface forcing. Data show that this notion is supported by increasingly more unstable conditions over the Lakes and James Bay as shown by negative Richardson numbers in these regions. The relationship between albedo and wind speed also shows an inverse relationship with wind speeds increasing with decreasing % albedo. With these present trends, and with instability increasing over the large water bodies, the potential for wind energy supply is increased and trends show strong changes in wind energy means along the shorelines of the Lake and western James Bay during the winter and fall months. Trends over Lake Erie and Lake Ontario are not very substantial as compared to the other Great Lakes and thus a greater potential of wind energy production lies along northern Lake Superior and Huron. There is also potential for investment in wind energy technology in northern communities along James Bay. Although trends are not as strong at the 30 m hub height, wind speeds and available wind energy are much higher and thus electricity from wind production can be increase with greater hub height by 50% in most areas around the Lakes during the favourable seasons. Data shown are calculated based on a swept area of 1 m^2 and thus values will exponentially increase with increasing swept area. Ontario, most fortunately, is not experiencing any significant negative trends in wind speed nor power and thus the potential for wind energy industry will only increase in the coming decades as long all driving forces promoting these wind regimes continue.

2.7 References

Archer, C. L., & Jacobson, M. Z. (2003). Spatial and temporal distributions of U.S. winds and wind power at 80 m derived from measurements. *Journal of Geophysics and Resources*, **108**, 4289.doi:10.1029/ 2002JD002076.

Austin, J. A., & Colman, S. M. (2008).A century of temperature variability in Lake Superior. *Limnology Oceanography,* **53**, 2724–2730.

Austin, J. A., & Colman, S. M. (2007). Lake Superior summer water temperatures are increasing more rapidly than regional air temperatures: A positive ice-albedo feedback. *Geophysical Research Letters,* **34**, *L06604.*

Bukovsky, M. S., Karoly, D. J. (2007). A Brief Evaluation of Precipitation from the North American Regional Reanalysis. *Journal of Hydrometeorology,***8**, 837–846.

Black, T. L. (1988), The step-mountain Eta coordinate regional model: A documentation, NOAA/NWS National Meteorological Center, 47 pp. *NCEP, 5200 Auth Road, Camp Springs, MD 20746.*

Businger, J. A., Wyngaard, J. C., Izumi, Y., & Bradley, E. F. (1971). Flux profile relationships in the atmospheric surface layer. *Journal of Atmospheric Science,* **28**, 181–189.

Canadian Wind Energy Association [CanWEA]. (2012) April. Canadian Wind Energy Market. Ottawa (ON): Canadian Wind Energy Association. Available from: http://www.canwea.ca/pdf/canweafactsheet-FedProInitiatives-final.pdf.

Chuang, H.Y., Manikin, G., & Treadon, R. E. (2001). The NCEP Eta Model Post Processor: A documentation, Off. Note XXX, 52 pp., Natl. Cent. *Environ. Predict, Camp Springs, Md.* Retrieved from http://www.emc.ncep.noaa.gov/officenotes/newernotes/on438.pdf.

Cole, J. J. et al. (2007). Plumbing the global carbon cycle: Integrating inland waters into the terrestrial carbon budget. *Ecosystems,***10**, 172–185.

Desai, A. R., Austin, J. A., Bennington1, V., & McKinley, G. A. (2009).Stronger winds over a large lake in response to weakening air-to-lake temperature gradient. *Nature Geoscience,***2**, 855-858.

Dominguez, F., Kumar, P., Vivoni, E. R. (2008). Precipitation recycling variability and ecoclimatological stability—A study using NARR data. Part II: North American monsoon region. *Journal of Climate,***21**, 5187–5203.

Duguay, C.R., Terry, D., Prowse, B. R., Bonsal, R. D., Brown, M. P., La croix.,& Menard, P. (2006). Recent trends in Canadian lake ice cover. *Hydrological Processes,* **20**, 781–801.

Elliott, D. L., Wendell, L. L., & Gower, G. L. (1991) An Assessment of the Available Windy Land Area and Wind Energy Potential in the Contiguous United States, *Technical report*, Pacific Northwest Lab., Richland, WA (United States).

Fall, S., Niyogi, D., Gluhovsky, A., Pielke, R. A., Kalnay, E., &Rochon, G. (2010). Impacts of land use land cover on temperature trends over the continental United States: Assessment using the North American regional reanalysis. *International Journal of Climatology,***30**, 1980–1993.

Gagnon, A. S., Gough, W.A. (2005). Climate change scenarios for the Hudson Bay Region: An inter-model comparison. *Climatic Change,* **69**, 269–297.

Holt, E., Wang, J. (2012). Trends in wind speed at wind turbine height of 80 m over the contiguous United States using the North American Regional Reanalysis (NARR). *Journal of Applied Meteorological and Climatology,* **51**, 2188- 2202.

Hundecha, Y., St-Hilaire, A., Ouarda, T. B. M. J., El Adlouni, S., &Gachon, P. (2008).A nonstationary extreme value analysis for the assessment of changes extreme annual wind speed over the Gulf of St. Lawrence. *Journal of Applied Meteorology and Climatology,* **47**, 2745–2759.

Independent Electricity System Operator, IESO (2012). Supply Overview. Retrieved from http://www.ieso.ca/imoweb/media/md_supply.asp, December 18, 2012.

Janjić, Z. I. (1994). The step-mountain Eta coordinate model: Further developments of the convection, viscous sublayer, and turbulence closure schemes. *Monthly Weather Review,* **122**, 927–945.

Klink, K. (1999). Trends in mean monthly maximum and minimum surface wind speeds in the coterminous United States, 1961 to 1990. *Climate Research,* **13**, 193–205.

Lambert, S. J. (1995).The effect of enhanced greenhouse warming on winter cyclone frequencies and strengths. *Journal of Climate,* **8**, 1447–1452.

Li, M. (2005). Investigation of wind characteristics and assessment of wind energy potential for Waterloo region, Canada.

Li, M., & Li, X. (2005).Investigation of wind characteristics and assessment of wind energy potential for Waterloo region, Canada. *Energy Conversion and Management,* **46**, 3014-3033.

Li, X., Zhong, S., Bian, X., Heilman, W. E., Luo, Y., & Dong, W. (2010).Hydroclimate and variability in the Great Lakes region as derived from the North American regional reanalysis. *Journal of Geophysical Research,* **115**, 1-14.

Lobocki, L. (1993). A procedure for the derivation of surface-layer bulk relationships from simplified 2nd-order closure models. *Journal of Applied Meteorology,* **32**, 126 – 138.

Lorenz, D. J., & De Weaver, E. T. (2007). Tropopause height and zonal wind response to global warming in the IPCC scenario integrations. *Journal of Geophysical Research,* **112**, D10119.doi:10.1029/2006JD008087.

Lu, X., McElroy, M. B., Kiviluoma, J. (2011).Global potential for wind-generated electricity. *Proceedings of the National Academy of Sciences of the United States of America.*

Magnuson, J. J., Robertson, D. M., Benson, D. J., Wyne, R.H., Livingstone, D. M., Arai, T., Assel, R. A., Barry, R. G., Card, V., Kuusisto, E., Granin, N. G., Prowse, T. D., Stewart, K. M., &Vuglinski, V. S. (2000). Historical trends in lake and river ice cover in the Northern Hemisphere. *Science,* **289**, 1743–1746.

Markovic, M., Jones, C. G., Winger, K., &Paquin, D. (2009). The surface radiation budget over North America: Gridded data assessment and evaluation of regional climate models. *International Journal of Climatology,***29**, 2226–2240.

Maslanik, J. A., Serreze, M.C., & Barry, R.G. (1996). Recent decreases in Arctic summer ice cover and linkages to atmospheric circulation anomalies. *Geophysical Research Letters,* **23**, 1677–1680.

Maxwell, I.B., (1986) A Climate Overview of the Canadian Inland Seas.In Canadian Inland Seas. *Elsevier Oceanography Series*, **44**, 79-99

Mesinger, F., Janjić, Z. I., Nickoviċ, S., Gavrilov, D., &Deaven, D. G. (1988). The step-mountain coordinate: Model description and performance for cases of Alpine lee cyclogenesis and for a case of an Appalachian redevelopment. *Monthly Weather Review,* **116**, 1493–1518.

Mesinger, F., Di Mego, G., Kalnay, E., Mitchell, K., Shafran, P. C., Ebisuzaki, W., Jovic, D., Woollen, J., Rogers, E., Berbery, E. H., Ek, M. B., Fan, Y., Grumbine, R., Higgins, W., Li, H., Lin, Y., Manikin, G., Parrish, D., & Shi, W. (2006). North American regional reanalysis: A long-term, consistent, high-resolution climate dataset for the North American domain, as a major improvement upon the earlier global reanalysis datasets in both resolution and accuracy. *Bulletin of American Meteorology Society,***87**, 343–360.

Palecki, M. A., & Barry, R.G. (1986). Freeze-up and break-up of lakes as an index of temperature changes during the transition seasons: A case study for Finland. *Journal of Climate and Applied Meteorology,* **25,** 893–902.

Pryor, S. C., Barthelmie, R. J., Young, D. T., Takle, E. S., Arritt, R. W., Flory, D., Gutowski, Jr W. J., Nunes, A., & Roads, J. (2009). Wind speed trends over the contiguous United States. *Journal of Geophysical Research,***114**, 1-18.

Pryor, S. C., &Ledolter, J. (2010).Addendum to "Wind speed trends over the contiguous United States." *Journal of Geophysical Research, **115***, D10103.doi:10.1029/2009JD013281.

Pryor, S. C., Barthelmie, R. J. (2010). Climate change impacts on wind energy: A review. *Renew Sustainable Energy Review,* **14**, 430–437.

Richard, T. L., Dragert, H., &McIntyre, D. R. (1966). Influence of atmospheric stability and over-water fetch winds over the lower Great Lakes. *Monthly Weather Review,* **7**,448-453.

Robertson, D. M., Ragotzkie, R. A., & Magnuson, J. J. (1992). Lake ice records used to detect historical and future climatic changes. *Climatic Change,* **21**,407–427.

Ruiz-Barradas, A., & Nigam, S. (2006). Great Plains hydro-climate variability: The view from North American regional reanalysis. *Journal of Climate,***19**, 3004–3010.

Yao, Y., Huang, H. G., Lin, Q. (2012). Climate change impacts on Ontario wind power resource. *Environmental System Research,* **1**, 1-11.

CHAPTER 3

FEASIBILITY OF MICRO-SCALE WIND TURBINES IN ONTARIO: INTEGRATING POWER CURVES WITH WIND TRENDS.

Feasibility of Micro-scale Wind Turbines in Ontario: Integrating Power Curves with Wind Trends.

Masaō Ashtine[a]

a Department of Geography, York University, 4700 Keele Street, Toronto, Ontario, Canada.

*Corresponding authors: mashtine@yorku.ca, bello@yorku.ca

3.1 Abstract

Micro-scale wind turbines, unlike utility-scale turbines, produce electricity at a rate of 300W to 10kW at their rated wind speed and are typically below 30m in hub height. These wind turbines have much more flexibility in their costs, maintenance and siting owing to their size and can provided wind energy in areas much less suited for direct supply to the grid system. The small wind industry has been substantially slow to progress in Ontario, Canada and there is much debate over their viability in a growing energy dependent economy. In an effort to diversify the energy sector in Canada, it is crucial that preliminary research be conducted and this study seeks to demonstrate the performance of two tested micro-wind turbines both spatially and temporally in Ontario using NARR data as an observational reference. The assessment of efficiencies of a Skystream 3.7 – 2.4 kW and a Bergey Excel 1 kW wind turbine and the pre-established Kortright Centre for Conservation wind test site. It was noted that while wind power around the Great Lakes and eastern James Bay are increasing in the seasonal months of winter and fall, these turbines are also seeing increased electrical output within wind regimes suited for their performance but electrical output for smaller rated power wind turbines may provide less than preferable energy supplies.

3.2 Introduction

Much of the modern wind turbines representing the renewable energy landscape consist of utility-scale wind turbines which can produce electricity in the magnitudes of MW and do so by taking advantage of stronger winds aloft with higher hub heights and larger rotor diameters. Substantial Canadian investment in wind turbines saw a 20% growth in clean wind energy production in 2012. This growth represents over $2.5 billion in investment and Canada's current installed capacity is just over 6,500 MW whereas globally, in 2012 wind energy capacity grew by 19%, with the global wind industry installing approximately 44,711 MW of wind power (CanWEA, 2012) and today there are over 150,000 wind turbines operating around the world in over 90 countries. The province of Ontario has 2,043 MW of installed wind capacity, *ca* 31% of Canada's total capacity (IESO, 2012). The micro-scale wind industry however is focused on the installation of wind turbines which produce electricity on average between 300W to 10kW rated power with hub heights that are generally below 30m. Although these turbines have been around for arguably millennia, they have failed to dominate the wind energy sector owing to increasing doubts on their performance, technological advancements, field testing and feasibility in a changing climate.

Micro-scale wind turbines produce more costly electricity than their utility scale counterparts, especially in poor wind sites. When tailored to specific wind regimes and used at optimal conditions through wind site assessment, micro-scale wind turbines can be a reliable energy source and can provide socio-economic benefit to regions that are far

away from the grid power and seen in the industry's increasing benefit to electrical supply in developing countries (Celik, 2003). The micro-scale industry has been especially hindered in Canada with currently between 2,200 and 2,500 turbines installed in Canada, 90% of which fall into the mini wind turbine category (< 1 kW rated power). The total combined capacity of all SWTs is estimated to be between 1.8 MW and 4.5 MW, equivalent to the capacity of one to three modern utility-grade wind turbines and their total annual output is roughly 7.5 GWh per year, or the amount of electricity consumed by approximately 750 Canadian homes (CanWEA, 2012).

The small wind industry has afforded the renewable energy sector with the benefits of energy independence for the consumer, remote electricity production in regions off-grid and a more diversified energy supply which can be complemented with solar energy and utilized by businesses and households. However, this industry is faced with many challenges, particularly the lack of standardized field testing of these wind turbines that result in uncertainty in performance claims by manufacturers. A vast amount of the testing done to establish micro-wind turbine rated power and power curves are done in wind tunnels and has substantial focus on the electrical components of the wind turbines and does not realistically assess how the turbine performs in the field.

As environmental factors such as temperature, radiation and wind variability can affect turbine performance, field testing is essential. Studies assessing the performance of micro-scale wind turbines in the field are often focused with the turbine's effect on the local environment or turbulence patterns produced by secondary rotor effects (Lubitz,

2012; Matsushima *et al.,* 2006; Eggers *et al.,* 2000; Bechly *et al.,* 1996; Bose, 1992; Hogstrom *et al.,* 1988). The potential of these turbines is yet to be assessed in Ontario and currently there are no standardized testing regulations for their calibration and power output in the North American wind industry (Li and Li, 2005) although many more advances have been made within the American micro-scale wind turbine industry.

The Kortright Centre for Conservation has been at the forefront of renewable energy initiatives in Toronto, Ontario and hope to be the first field standardization test site for micro-scale wind turbines in Ontario with the only other test site in Canada being located in Prince Edward Island. Two leading industry standard turbines were assessed in this study, the Bergey Excel 1 kW and the Skystream 3.7 – 2.4 kW wind turbines with hub heights of 16.8 m and 15.2 m respectively. These turbines have varying specifications as listed in Table 1.1.

Table 3.1: Wind turbine specifications for Skystream and Bergey turbine at the Kortright field testing site. Information obtained from manufacturer description.

		Bergey	Skystream
Structural	Hub Height	17.37 m	15.24 m
	Turbine type	HAWT, upwind	HAWT, downwind rotor with stall regulation control
Manufacturer rating	Rated Power	1 kW	2.4 kW
	Rated Wind Speed	11 ms^{-1}	13 ms^{-1}
Rotor specifics	Rotor Diameter	2.5 m	3.72 m
	Swept Area	4.91 m^2	10.87 m^2
	Rotor Speed (RPM)	490 (rated rotor speed, no range applied)	50 – 330
	Blade Material	Pultruded fiberglass	Fibreglass reinforced composite
Wind	Cut-in Wind Speed	2.5 ms^{-1}	3.5 ms^{-1}
	Cut-out Wind Speed	None	25 ms^{-1}
	Max Design Wind Speed	54 ms^{-1}	63 ms^{-1}
Protection	Furling Wind Speed	13 ms^{-1}	No furling
	Overspeed protection	Auto tail furl, electrical breaking system	Electronic stall regulation

3.2.1 NARR dataset

Field data from the assessed wind turbines were incorporated into wind data from the North American Regional Reanalysis dataset to analyze turbine performance both

spatially and temporally over Ontario and the Great Lakes. The NCEP-NARR is a long-term, dynamically consistent, high-resolution, high-frequency, atmospheric and land surface hydrology dataset (Mesinger *et al.*, 2006) and at present this dataset comprises reanalysis data for the time period of 1979–present and within this study, data from 1980-2012 were used. The NARR model uses the enhanced spatial resolution of NCEP Eta Model (32km, 45 layers) together with the Regional Data Assimilation System (RDAS) which, substantially assimilates precipitation along with other variables (Mesinger *et al.*, 2006; Janjić, 1994;Mesinger *et al.*, 1988; Black, 1988). NARR is widely known for its successful assimilation of high-quality and detailed precipitation observations into the atmospheric analysis which was previously lacking from many global models. This research focused on the electrical output potential over Ontario through investment in small wind turbines using the NARR wind data for the tropospheric heights of 10m and 30 m. However, owing to preliminary coding error at the 30m level, grid cells along the southern Hudson Bay shoreline have been erroneous in their wind speed estimation due to their low lying elevation (marginally above sea level; http://www.emc.ncep.noaa.gov/mmb/rreanl/faq. html#zero-30m-winds). These 43 grid cells were precisely defined, non-influential on neighbouring cells, and represented less than 0.01% of the study scope (Appendix A).

3.2.2 Power Curves

Power curves produced by turbines (Equations 3.1 and 3.2) describe how the turbines perform over a series of wind speed bins can be used to model wind power generation at measured wind speeds and thus gives NARR the ability to map out wind power over the past 33 years and across Ontario and the Great Lakes.

Bergey 1 kW

$$\text{Wind Power (W)} = -0.1007x^4 + 2.02x^3 - 2.8783x^2 - 2.1873x + 2.7317 \qquad (3.1)$$

Skystream 2.4 kW

$$\text{Wind Power (W)} = -0.1442x^4 + 2.9853x^3 - 8.2462x^2 + 9.3011x - 3.9783 \qquad (3.2)$$

Applying these power curves to each 3-hr wind sample allowed for a near 'real-time' assessment of wind energy output for the studied wind turbines over Ontario, and for the spatial representation of this wind energy and any occurring trends. This analysis however is limited to the sample size and distribution of wind speeds collected from the test site and must be taken as modeled data when applied to NARR. The Kortright test site is conveniently located north of Toronto, with an open fetch, having a predominantly southeast and northwest wind pattern. However, surface roughness was not accounted for when applying turbine power curves to other geographic regions in Ontario and many regions will differ in localized wind profiles.

Results correlate with previous studies (Li *et al.*, 2010; Desai *et al.*, 2009) and showing increasing wind patterns over the Great Lakes and micro-scale wind turbines have the benefit of accessing this potential in remote regions not suitable for wind farms. Further research into these micro-scale wind turbines should be done on higher rated power wind turbines and on the cost benefit analysis of the industry given electrical output results.

3.3Methods

3.3.1 Power curves

Meteorological and electrical output data was captured for both turbines between 7 November 2012 and 30 April 2013. This data provided 5 second readings of wind speed at 8 levels above ground, temperature, wind direction and electrical output readings (Bergey and Skystream) for approximately 6 months. Analysis of this data was used to produce performance data through power curve analysis (Fig. 3.1) which demonstrated how the Bergey and Skystream wind turbines performed at differing wind speeds. Applying a best fit curve, quadratic equations were produced for each turbine that best described the ability of the turbine to convert wind energy into electrical power in Watts (Equations3.1, Bergey and 3.2, Skystream).

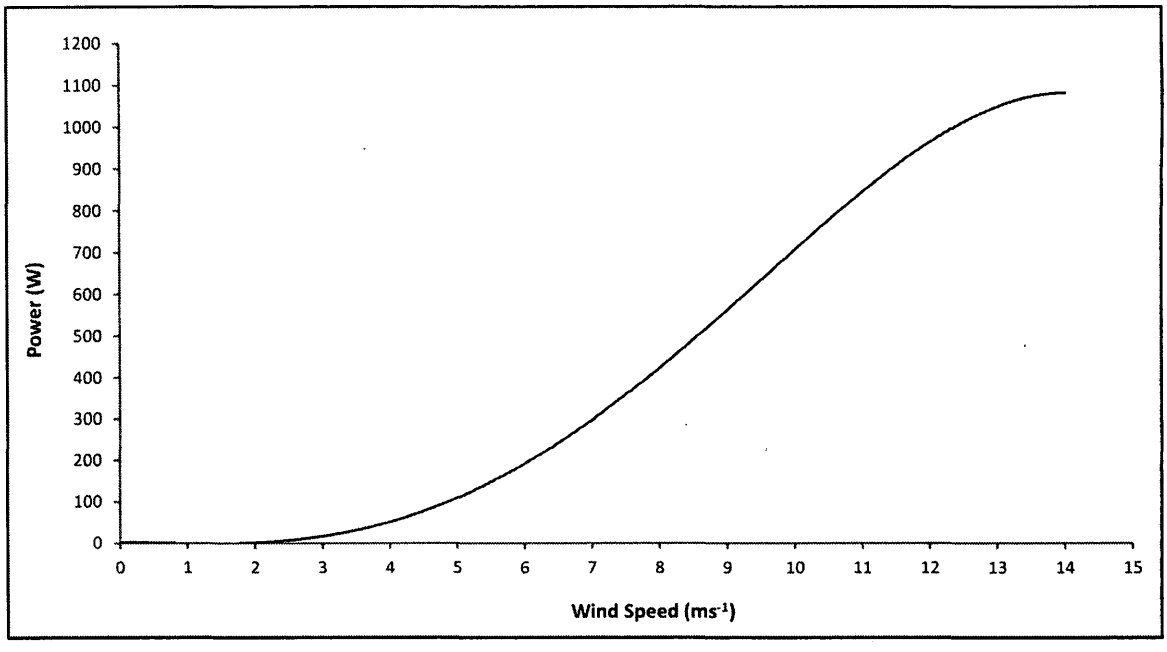

Fig. 3.1: Computed power curve for the Bergey Excel 1 kW small wind turbine. Data was collected between Nov. 2012 – April 2013.

3.3.2 Applying power curves to NARR

As the NARR data gave u and v, directional wind speeds, the moment magnitude wind speed U (ms^{-1}) for each grid cell and both tropospheric levels of 10 and 30m was calculated using the standard magnitude formula as represented by the following Equation 3.3:

(3.3)

Wind speeds at 10 and 30 m heights were derived for every 3-hr measurement from the corresponding NARR wind data from 1980 to 2012. Monthly mean wind speeds for years 1980 to 2012 were computed and 33-yr monthly averages were also computed and seasonal means were finally derived for winter (December, January, February), spring (March, April, May), summer (June, July, August) and fall (September, October, November). It is to be noted that a coding error as listed by (http://www.emc.ncep.-noaa.gov/mmb/rreanl/faq.html#zero-30m-winds) prevented a full assessment of wind speed means at the 30 m hub height in low lying regions restricted to the lower Hudson Bay shoreline. These regions were not taken into consideration in analysis.

The power curve equations for the Bergey and Skystream wind turbines were then applied to the analyzed wind speed data from NARR, however, only data for the Bergey 1 kW wind turbine is presented as it was found that the Skystream 2.4 kW power curve closely represented the Bergey's due to its underperformance. Using the hourly (3-hr) wind speeds for each month over the period of 1980 – 2012, the Bergey turbine power curve was used to compute the electrical output for each 3-hr reading from the NARR dataset was calculated in megajoules (MJ) and the summed electrical output for each month was averaged based on 33 years of wind speed data. Long-term seasonal means were subsequently derived and thus, the resultant output showed the mean, summed electrical output in MJ for each grid cell within the NARR study scope (3364 cells) with particular interest in Ontario and the Great Lakes. This method was repeated at the 30m hub height as well and thus electrical output was given at two atmospheric heights for

each wind turbine. Plots of spatial differences in performance between the hub heights of 10 and 30m were made, showing regions where increases in hub height have proven more effective than in other regions.

3.3.3 Trends in electrical output and wind speed

Trend analysis in electrical output over Ontario and the Great Lakes from each wind turbine was computed with the OLS method and interannual variability of wind power was also assessed through the standard deviation of 33 year monthly averages. Plots of significant trends were also conducted through *t*-test analysis and statistically significant *p*-values were reported on a seasonal basis.

3.4 Results

3.4.1 Wind Speed Trends

The NARR reanalysis dataset gives a clear indication that winds over the Great Lakes and James Bay are the greatest in magnitude in comparison with surrounding regions in Ontario. Through analysis done over 33 years of data and both 10 and 30 m hub heights, seasonal trends in wind speed show a common occurrence of higher mean wind speed over the Great Lakes, particularly over Lake Superior (Fig. 3.2 and 3.3). During the

winter (defined as the months of December, January and February), mean wind speed over the Great Lakes vary in the range of 5.5 ms^{-1} to 7.5 ms^{-1}, values which are substantially higher than seen across central and northern Ontario (4.5 ms^{-1}) and are more frequent over the larger Great Lakes than with Lake Erie or Ontario.

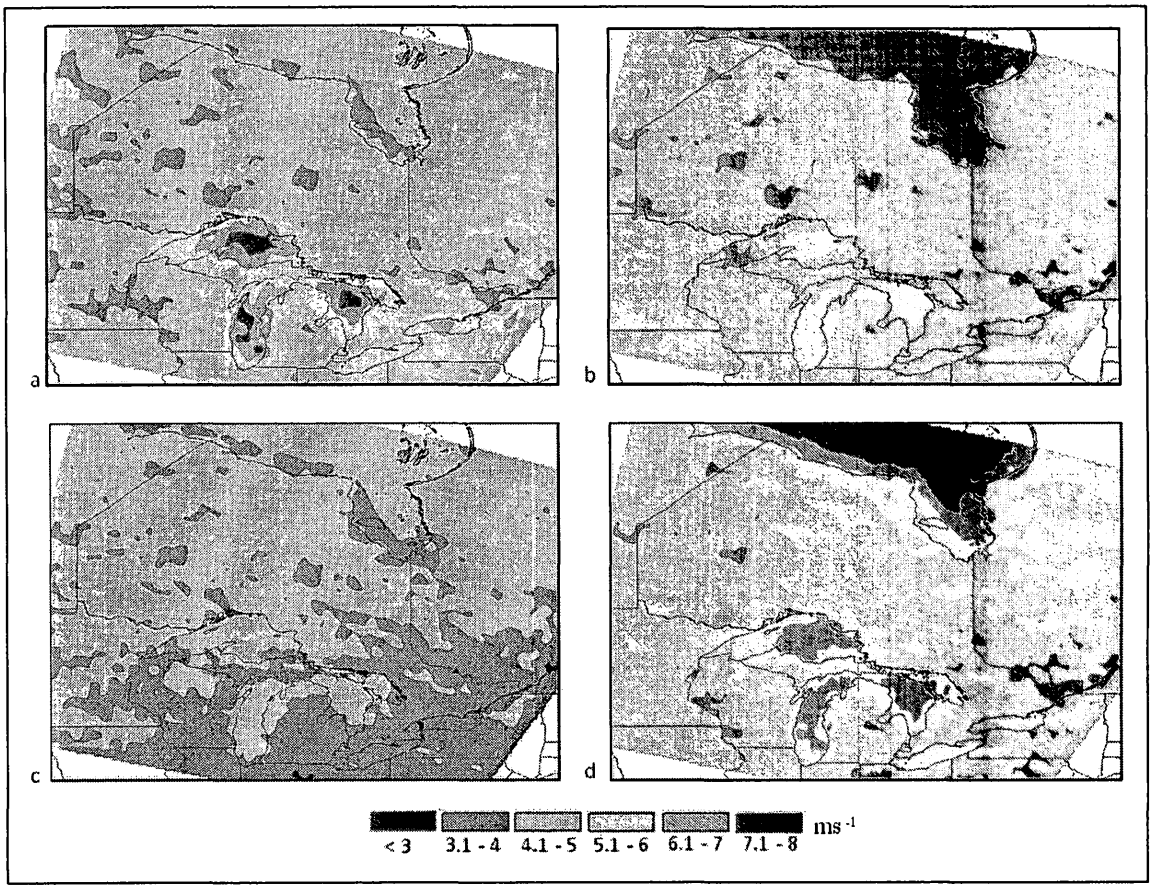

Fig. 3.2: Seasonal mean wind speeds for study area at 10 m for a) Winter (December, January, February), b) Spring (March, April, May), c) Summer (June, July, August), d) Fall (September, October, November).

Spring winds are reduced over the Great Lakes and while wind speeds over central and northern Ontario stay consistent from the previous seasons, the winds over the Great Lakes have largely died down, with wind speeds over Lake Superior being the highest of the Lakes but still lower than spring means. These wind speed means are further reduced in the summer and the Great Lakes have become much less distinct in wind speed means in comparison to the surrounding land and south of Ontario experiences lower wind speeds, *ca.* 3 ms^{-1}. Wind speed means increase substantially over Hudson Bay and the majority of the Great Lakes have mean of approx. 6 - 6.5 ms^{-1}.

Wind regimes at the 30 m hub height show very similar patterns with slight spatial and temporal variations. During the winter months, mean wind speeds over central and northern Ontario blowing at roughly 2 ms^{-1} higher at 30 m and the same occurs over the Lakes where the latter appear more even in wind speed distribution. Throughout each season, the wind speed boundaries between the Great lakes and land become less defined at the 30 m height and winds become more uniform over Ontario. The largest variation in mean wind speeds with hub height exist during the winter months with an approximate increase in wind speeds by 30% and wind speeds over much of Ontario increase by roughly 1 ms^{-1} at the 30 m hub height.

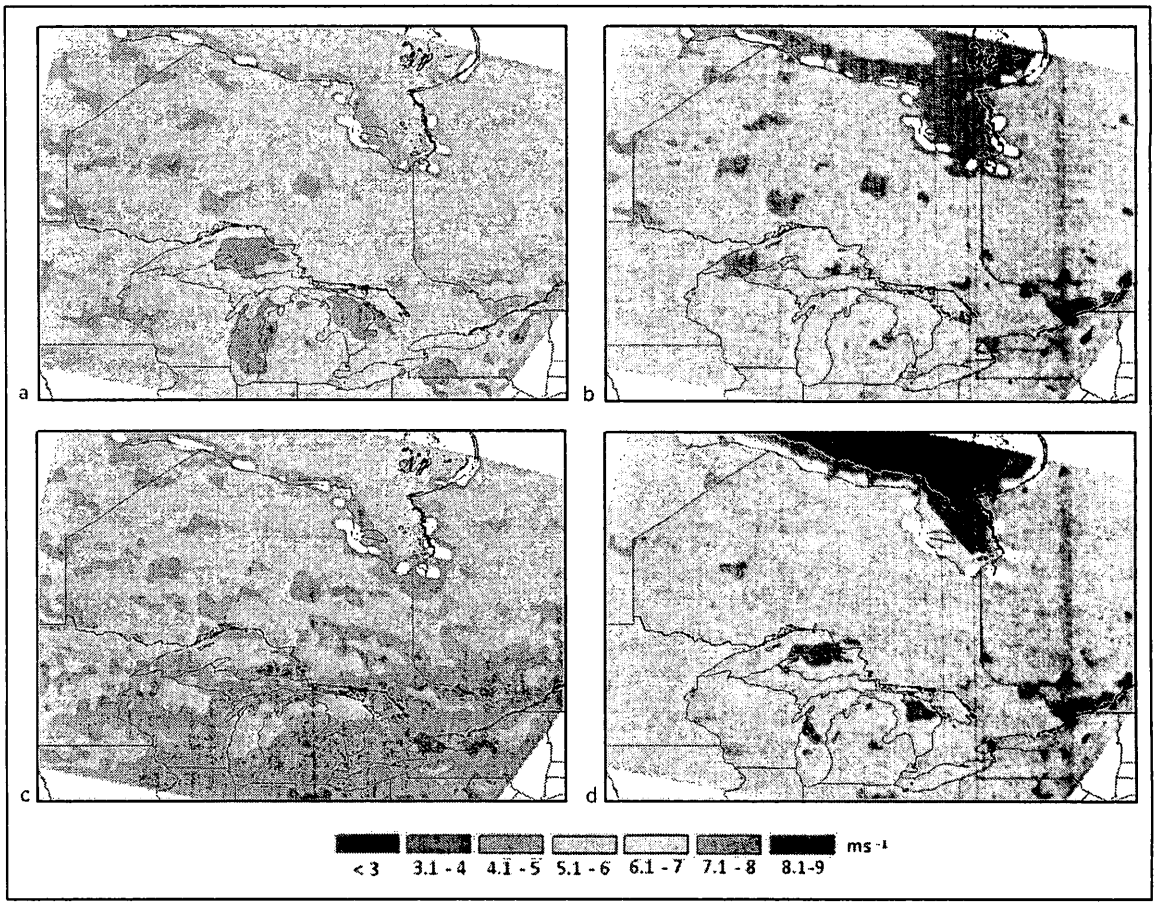

Fig. 3.3: Seasonal mean wind speeds for study area at 30 m for a) Winter (December, January, February), b) Spring (March, April, May), c) Summer (June, July, August), d) Fall (September, October, November). *Coastalregions in white have been omitted due to coding error at the 30 m hub height.*

James Bay has the highest wind speed trends at the 10 m hub height (maximum of *ca.* 0.1 $ms^{-1}yr^{-1}$, particularly over eastern James Bay) during winter (Fig. 3.4). Trends over the Great Lakes are also strong (*ca.* 0.05 $ms^{-1}yr^{-1}$ with some areas experiencing around 0.07 $ms^{-1}yr^{-1}$) and trends over Lake Erie and Ontario are not as strong as the larger Lakes. This trend over the Lakes changes in spring where Lake Superior has higher wind trends, but most of the lake has lower trends than during winter and Lake Erie and Ontario appear to have slightly negative trends but at means very close to 0 $ms^{-1}yr^{-1}$. Increases in wind

speed appear to be greatest over James Bay in the fall where trends indicate wind speed rates between 0.1 and 0.12 $ms^{-1}yr^{-1}$ in some regions. That represents an approximate 50% increase in wind speeds versus the mean over 33 years or *ca.* 15% increase per decade. The opposite is true for the Lakes during the summer where trends over the lakes appear no different from the surrounding land with very low rates of change. The wind speed trends are also apparent at the 30 m hub height with no substantial increase or decrease in trends (Fig. 3.5).

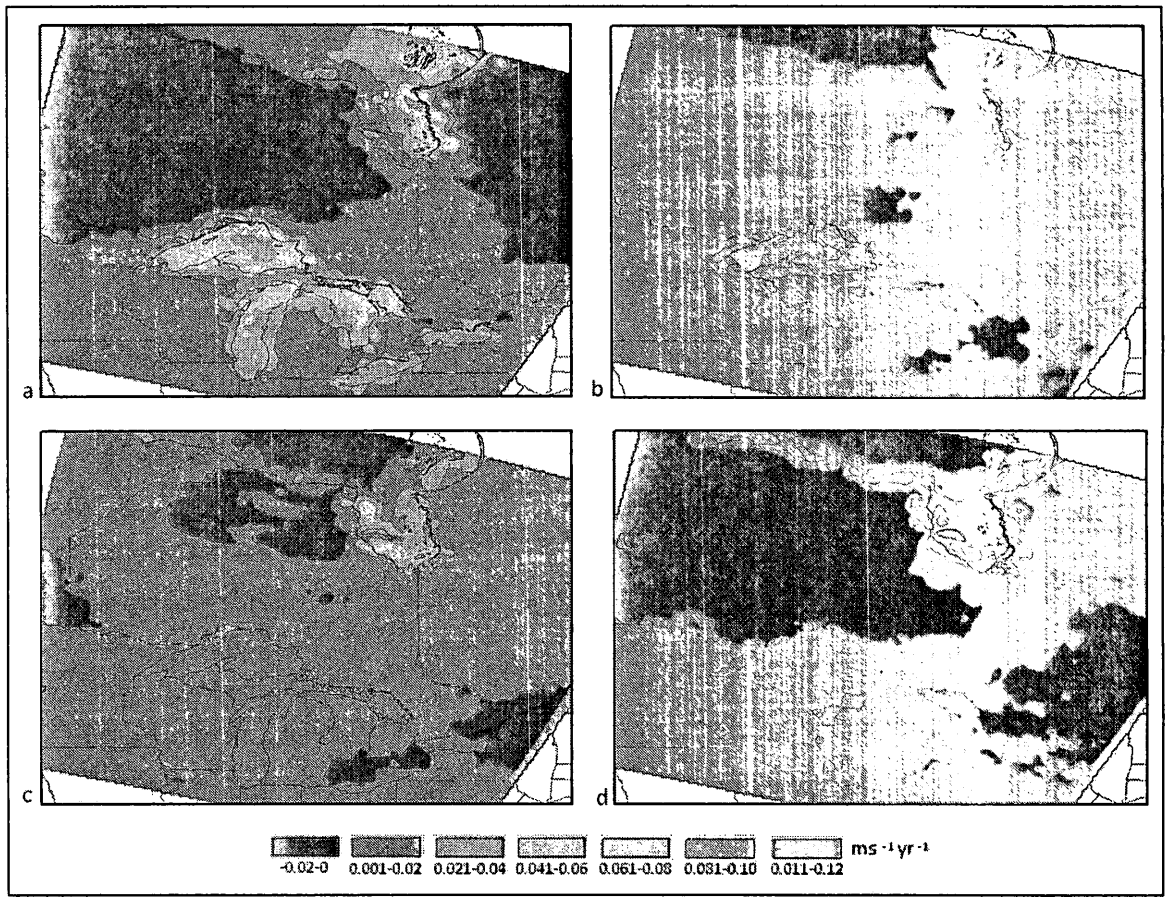

Fig. 3.4: Multi-year trends in seasonal wind speeds for study area at 10 m for a) Winter (December, January, February), b) Spring (March, April, May), c) Summer (June, July, August), d) Fall (September, October, November).

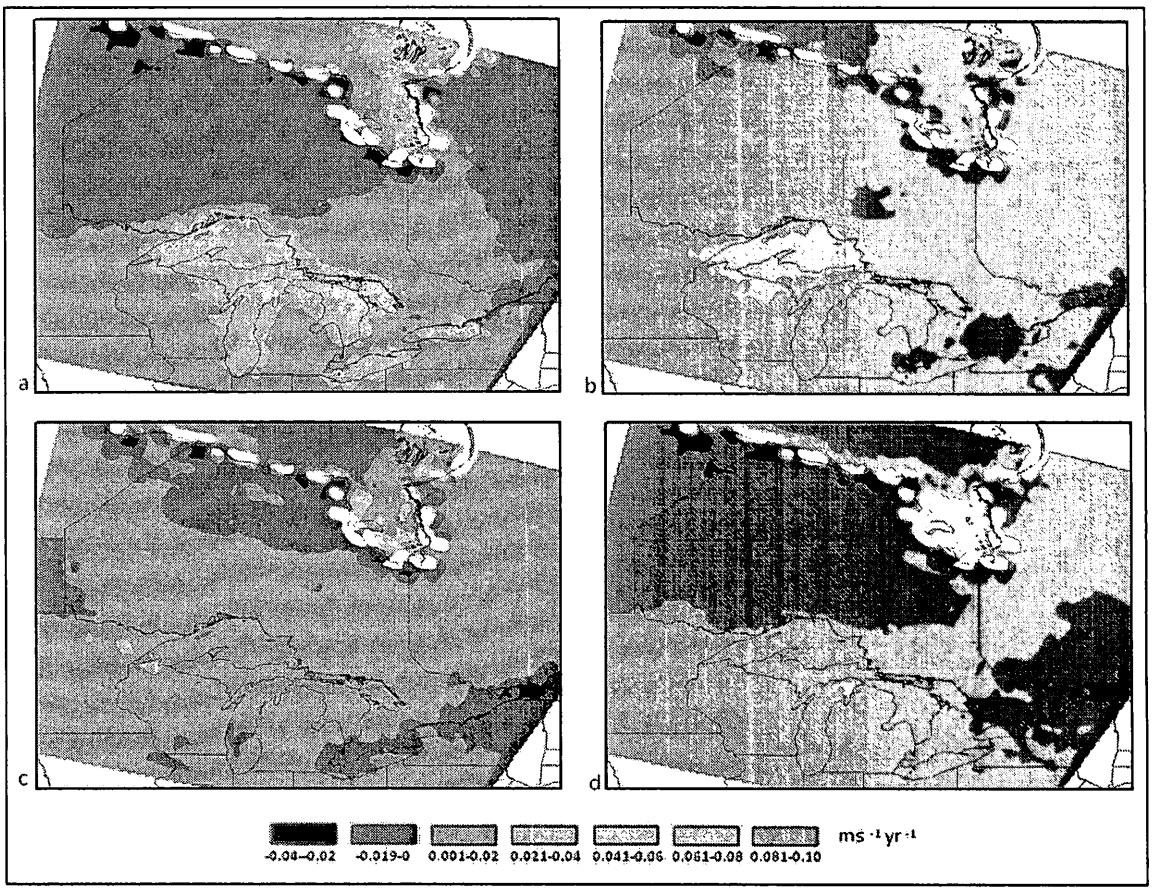

Fig. 3.5: Multi-year trends in seasonal wind speeds for study area at 30 m for a) Winter (December, January, February), b) Spring (March, April, May), c) Summer (June, July, August), d) Fall (September, October, November).*Coastalregions in white have been omitted due to coding error at the 30 m hub height.*

For most seasons, many of the trends experienced were highly significant ($p< 0.005$) over the Great Lakes and James Bay at both hub heights (Fig. 3.6). Spring does not experience significant trends ($p< 0.05$) over all the Great Lakes but these are limited to regions over Lake Superior and southern Lake Michigan, and during the summer, this statistical significance is localized mainly to James Bay and some of the Great Lakes (Huron, Erie and Ontario). Regression analysis with wind speeds against % albedo change give a negative relationship for much of the Great Lakes and James Bay (Fig. 3.7). This trend

implies an inverse relationship exists between the two parameters during the winter and wind speeds will increase with decreasing ice/snow coverage (% albedo). This regressional trend is in the magnitude of -0.15 to -0.12 ms^{-1}/ % albedo in regions of eastern James Bay. Trends of -0.04 to -0.02 ms^{-1}/ % albedo are more common in regions surrounding the lakes, especially north of Lake Superior and Huron.

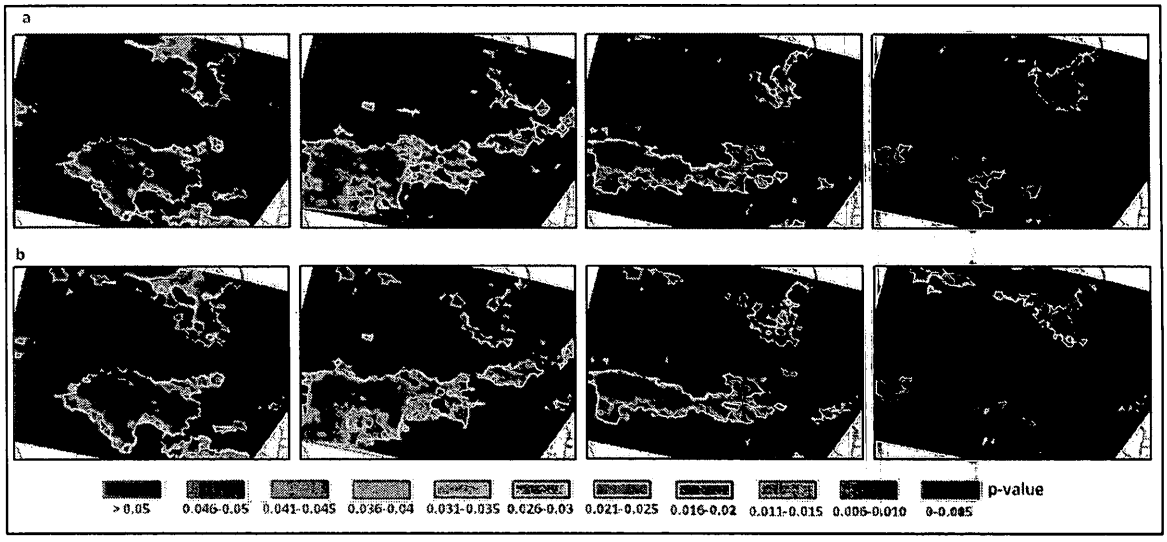

Fig. 3.6: Statistical significance (*p*-values) of multi-year trends in seasonal wind speed for the study area at a) 10 m and b) 30 m for Winter (December, January, February), Spring (March, April, May), Summer (June, July, August), Fall (September, October, November) from left to right respectively.

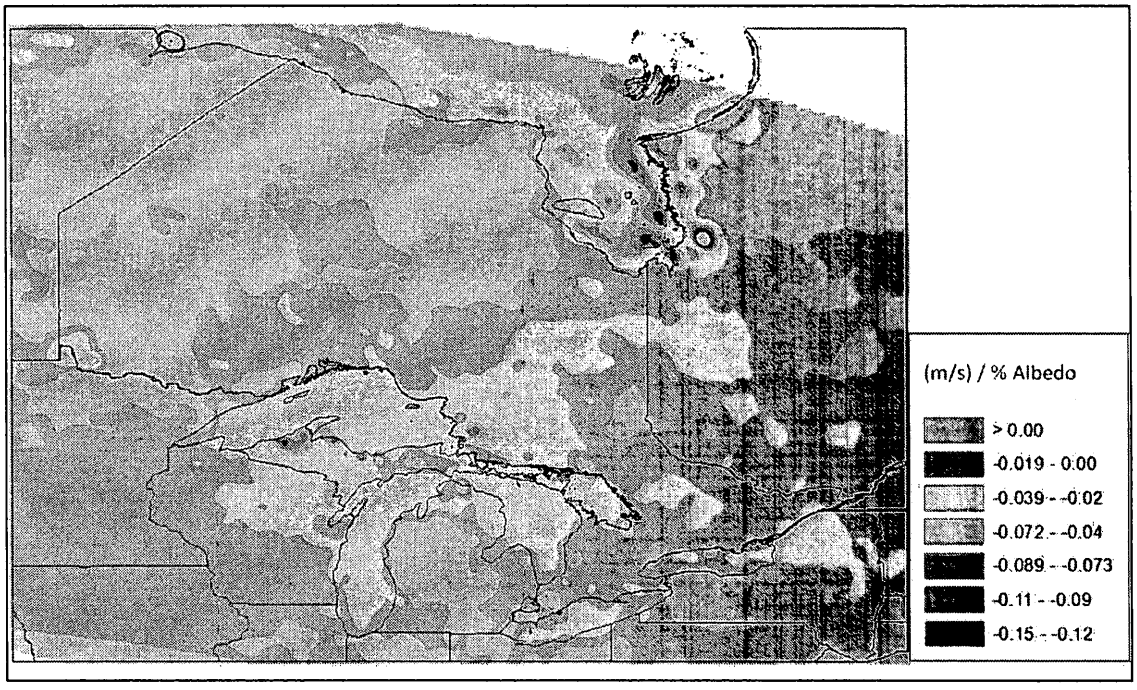

Fig. 3.7: Multi-year trends in seasonal winter mean wind speed regressed against

3.4.2 Seasonal turbine electrical output

Power curve produced for the Bergey 1 kW (Fig. 3.1) wind turbine was in close accordance to power curves of this turbine from field testing as well (Seitzler, 2009; Summerville, 2005). The Bergey reaches its maximum power output of 1.1 kW at 13.5 $ms^{-1}$with a cut-in wind speed of 2.5 ms^{-1}. Turbine output closely follows patterns in wind speed means with the Lakes and James Bay producing the greatest amount of electrical energy for both turbines during the winter and fall seasons (Fig. 3.8). Much of central and northern Ontario has low means of seasonal electrical output with southern Ontario

having higher means. Electrical energy produced over the Lakes during the winter is high over central regions with means *ca.* 3000 MJ and 1500 MJ in surrounding regions.

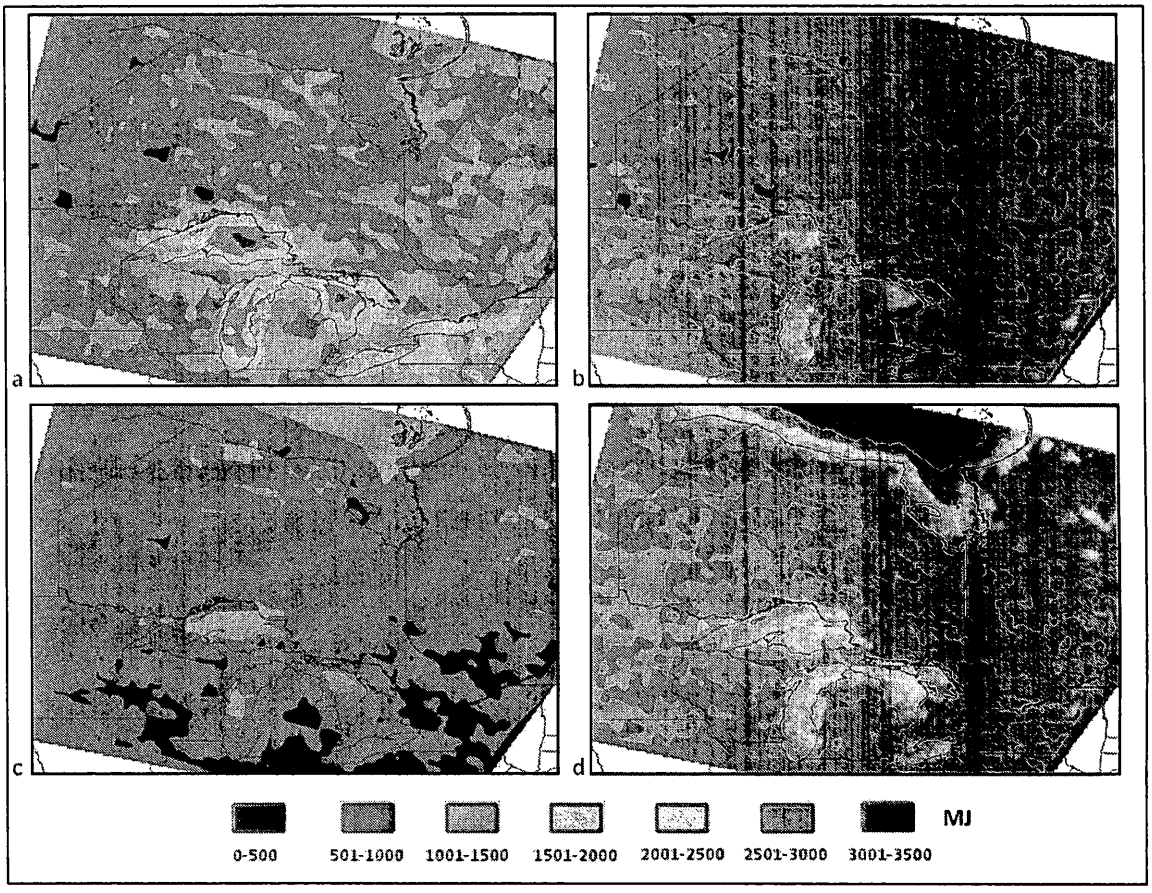

Fig. 3.8: Seasonal total mean turbine energy output (MJ) for the Bergey Excel 1 kW wind turbines for study area at 10 m for a) Winter (December, January, February), b) Spring (March, April, May), c) Summer (June, July, August), d) Fall (September, October, November).

The Bergey turbine produces less electricity around Lake Erie and Ontario but Lake Ontario shows more promising yields during the winter of approximately 25% more electrical output. Spring values are much less regionally with electrical production

becoming more uniform across the province and the Lakes have reduced output with regions surrounding the lakes having a mean of 1000-1200 MJ produced. This pattern of more uniform production is further seen during the summer where means have fallen to 800 MJ over most of Ontario, with regions around Lake Superior have the highest yields. Northern Ontario benefits in the summer with regions producing between 1000 to 1200 MJ. Energy output increases for northern Ontario along the Hudson Bay coastline and western James Bay during the fall as output can vary within 1500-2000 MJ.

The Lakes obtain higher yields in the fall with roughly 1500-2000 MJ produced by the Bergey turbine in surrounding areas and yields are fairly evenly distributed amongst the Lakes with Lake Ontario giving slightly lower output. Electrical output patterns are similar at the 30 m hub height with total energy production being higher, particularly in winter and fall seasons (Fig. 3.9).

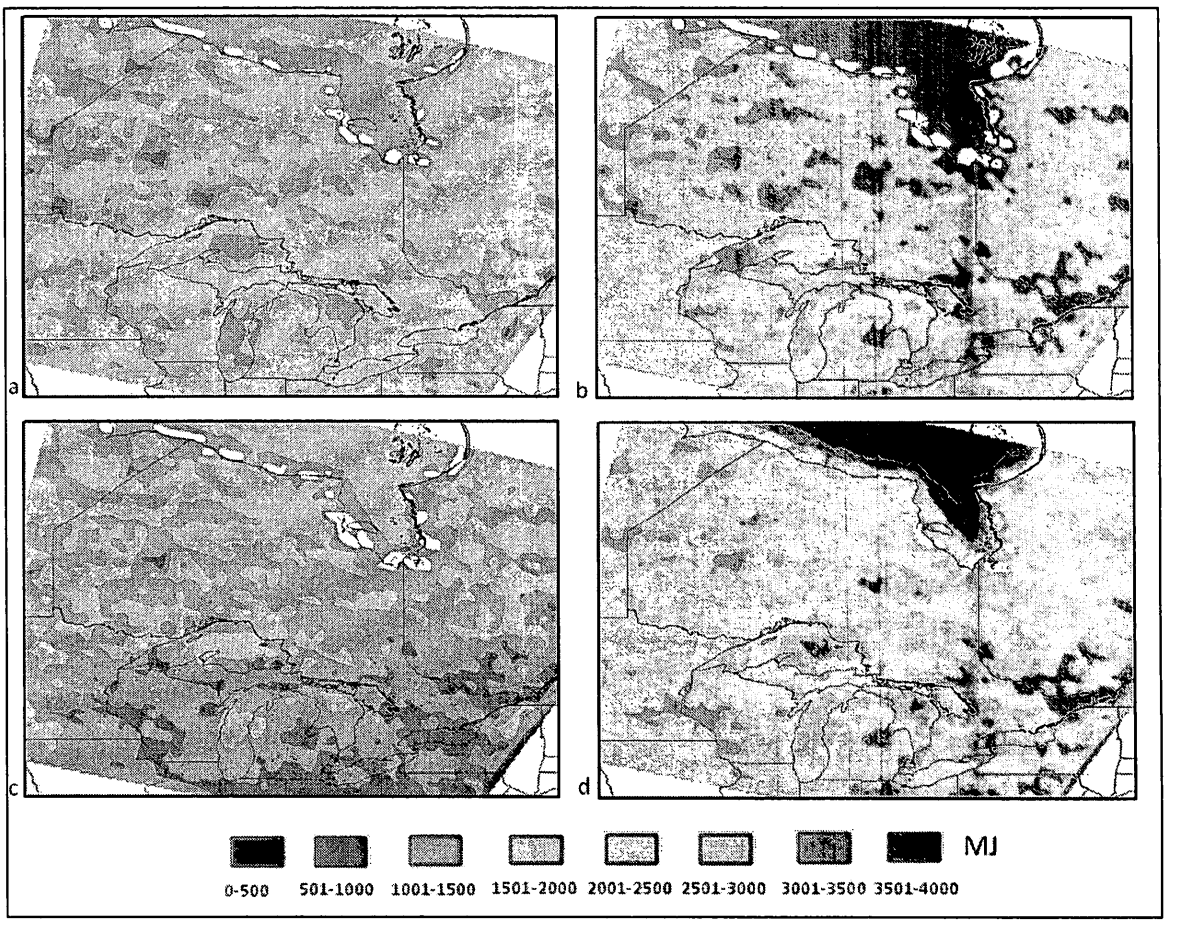

Fig. 3.9: Seasonal total mean turbine energy output (MJ) for the Bergey Excel 1 kW wind turbines for study area at 30 m for a) Winter (December, January, February), b) Spring (March, April, May), c) Summer (June, July, August), d) Fall (September, October, November). *Coastal regions in white have been omitted due to coding error at the 30 m hub height.*

Intuitively, trends in electrical output closely represent wind speed trends with the largest trends occurring in the winter and fall seasons (Fig. 3.10). Winter can see positive trends in turbine electrical output at 10 m of roughly 7 $MJyr^{-1}$ (5% decadal increase) over regions close to the Lakes and up to 20 $MYyr^{-1}$ along the eastern James Bay coast (20% decadal increase). Fall averages are different with the trends over the Lakes being not as strong (0-5 $MJyr^{-1}$) whereas regions over the western James Bay coastline can see trends

of 25 $MJyr^{-1}$ which translates to a 10% increase over means per decade. Winter trends persist into the spring season but are more limited to Lake superior and eastern James Bay whereas as summer trends show the highest increases for western James Bay (8 $MJyr^{-1}$) and the lower Hudson bay coastline.

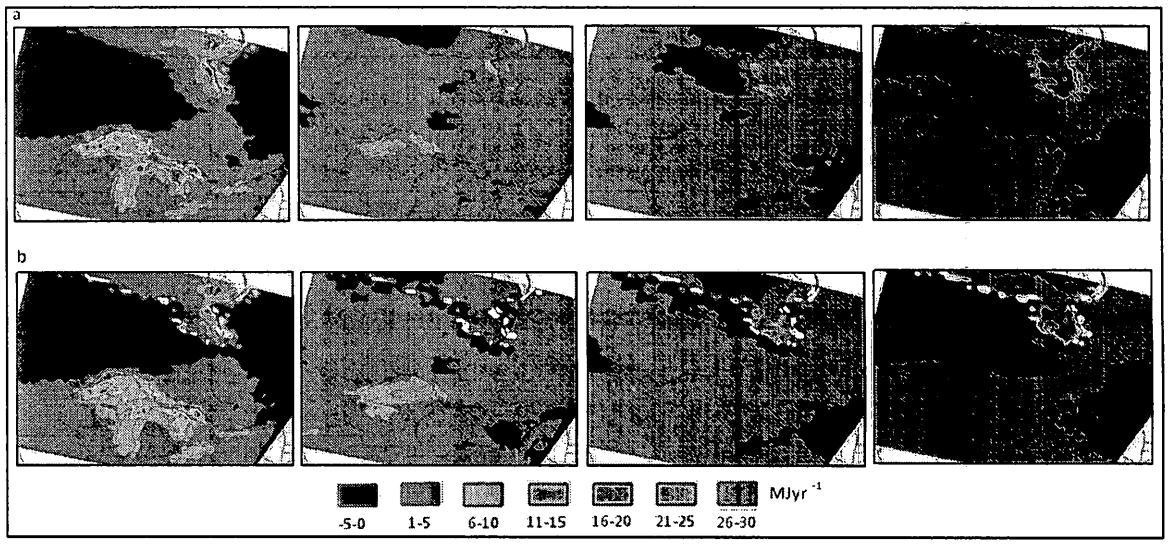

Fig. 3.10: Multi-year trends in seasonal total mean turbine energy output (MJ) for the Bergey Excel 1 kW wind turbines for study area at a) 10 m and b) 30 m for Winter (December, January, February), Spring (March, April, May), Summer (June, July, August), Fall (September, October, November) from left to right respectively. *Coastalregions in white have been omitted due to coding error at the 30 m hub height.*

Trends at the 30 m hub height follow a similar pattern but are not as strong as those at 10 m hub height. The aforementioned trends seen during the winter and fall around the Lakes and James Bay are highly significant ($p< 0.005$) at both hub heights.

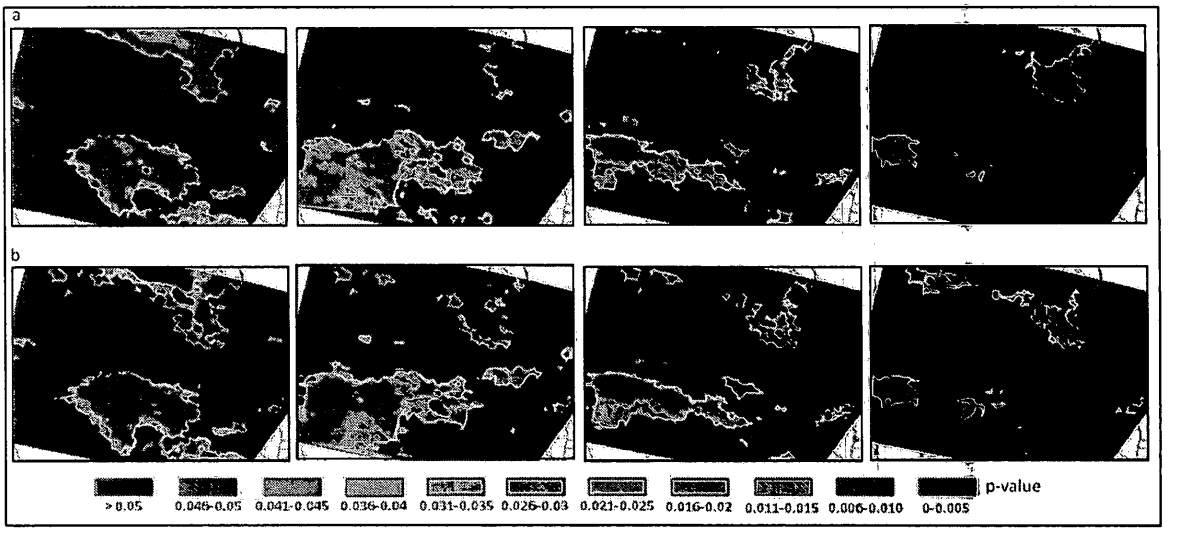

Fig. 3.11: Statistical significance (*p*-values) of multi-year trends in seasonal turbine output for the Bergey Excel 1 kW turbine for the study area at a) 10 m and b) 30 m for Winter (December, January, February), Spring (March, April, May), Summer (June, July, August), Fall (September, October, November) from left to right respectively.

Increasing the hub height of the Bergey turbine during the winter gives slightly higher output during the winter than in the fall where up to 100% increase in wind speeds can be experienced over much of Ontario in the winter versus approximately 80% in the fall (Fig. 3.12). Differences in electrical production are much less near the Lakes with surrounding regions seeing *ca.* 60% and 20% over the Lakes themselves. Winter means are slightly lower with height over the Lakes than in fall. Hub height increase to 30 m can enhance electrical output by 60-80% during the spring with less spatial variability across Ontario. The summer presents a more spatially heterogeneous account of output as while much of northern and central Ontario increase output by 80% at 30 m but this change can be within 100-120 % in regions in southern Ontario, particularly in proximity to Lake Erie and Ontario.

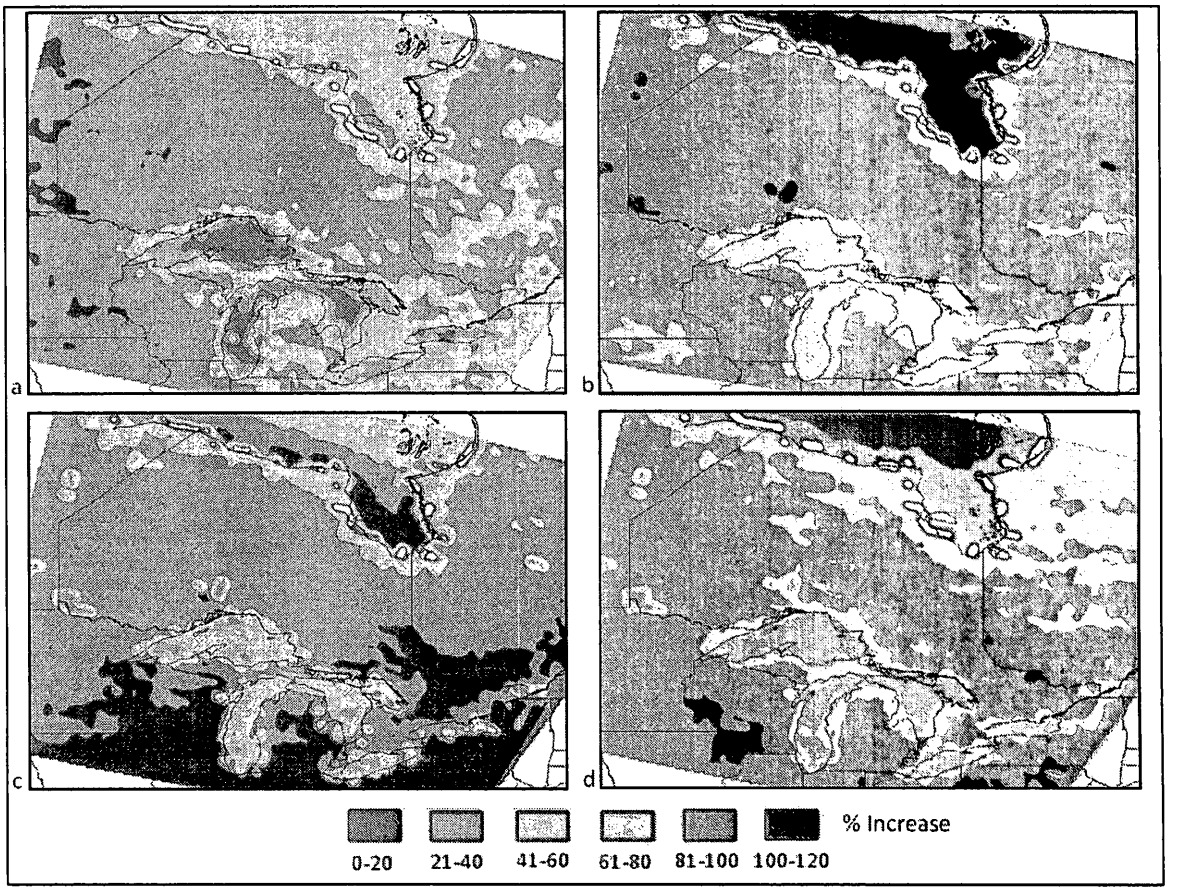

Fig. 3.12: Seasonal differences in turbine electrical output for the Bergey Excel 1 kW wind turbine between the 10 m and 30 m height fora) Winter (December, January, February), b) Spring (March, April, May), c) Summer (June, July, August), d) Fall (September, October, November).. Values express the percent increase in turbine output as hub height increases to 30 m. *Coastal regions in white have been omitted due to coding error at the 30 m hub height.*

Annual averages (Fig. 3.13) remain consistent in patterns of electrical production for the Bergey 1 kW wind turbine with regions surrounding the Great Lakes having an annual average of total electrical energy production*ca.* 1250 kWh with central, northern and southern Ontario have averages close to 500-1500kWh at the 10 m hub height. Energy production is more evenly produced at the 30 m hub height with most of Ontario

producing between 2000-2500kWh and regions around the Lakes having higher means in electrical output than regions in central and northern Ontario.

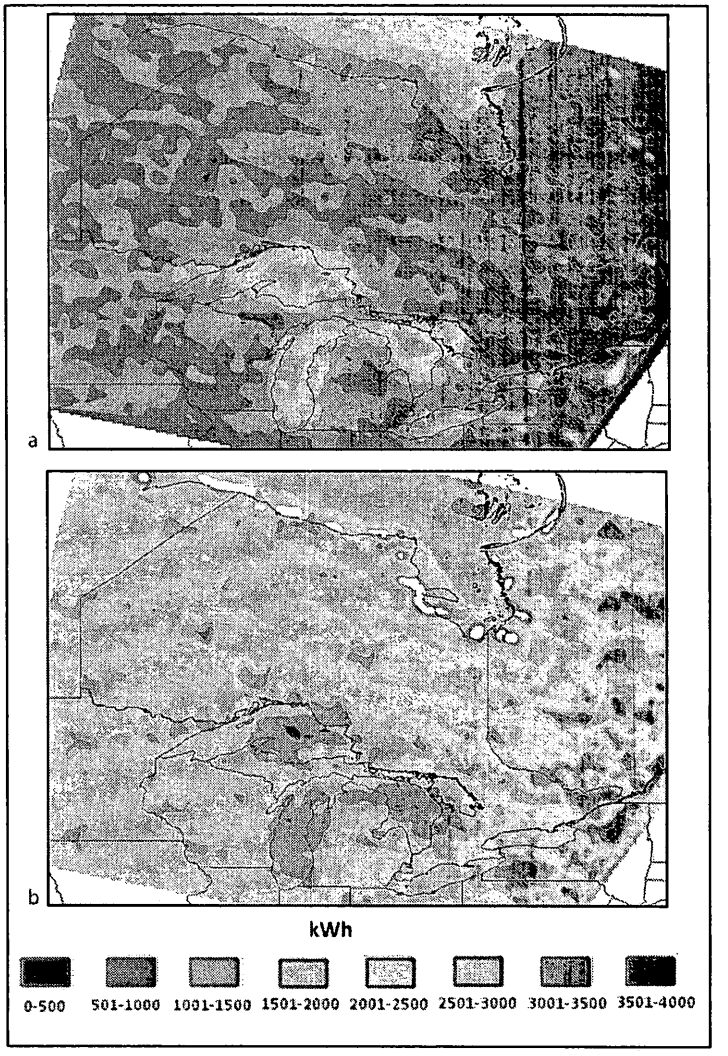

Fig. 3.13: Annual total mean turbine energy output (kWh) for the Bergey Excel 1 kW wind turbine for a) 10 m and b) 30 m hub heights. *Coastal regions in white have been omitted due to coding error at the 30 m hub height.*

3.5 Discussion

3.5.1 Wind trends at hub height

Wind speed trends and means show greatest change and highest wind speeds in regions surrounding the Laurentian Lakes and James Bay in northern Ontario at both the 10 and 30 m hub height. Wind patterns change in distribution and speed when transitioning from large water bodies to land as the latter landscapes have very distinct properties that influence the atmosphere above. Wind speeds of the Lakes are highest over the lakes owing to surface forcing of the atmosphere above by lake ice (Gagnon and Gough, 2005). Changing dynamics in lake/sea ice cover and their respective breakup and reformation dates can influence atmospheric conditions and stability (Desai and McKinley, 2009; Cole *et al.*, 2007; Gagnon and Gough, 2005) and it is suggested and these changes can lead to changes in wind speed over the Lakes and Hudson Bay region. Lake ice has been declining over the past decades (Austin and Colman, 2008) with negative trends in ice cover being linked with increased frequency of low pressure systems and temperature increase in northern regions (Duguay *et al.*, 2006; Magnuson *et al.*, 2000; Cohen *et al.*, 1994; Maslanik *et al.*, 1994; Palecki and Barry, 1986).

Mean wind speeds over the Lakes are not as high or distinct from the surrounding land during the summer months although similar patterns as seen in winter exist during the spring. As ice breakup of the lakes occur, atmospheric stability over the lakes is affected

and thermal gradients may persist, driving onshore and offshore winds. These conditions are similar to those seen over James and Hudson Bay where sea ice breakup influences atmospheric stability. Gagnon and Gough (2005) found statistically significant trends toward earlier breakup in James Bay, along the southern shore of Hudson Bay. Winter trends in wind speed regressed against albedo levels show that during the winter months, a statistically significant ($p< 0.005$) negative relationship exists (*ca.* -0.04 to - 0.09 ms^{-1}/% albedo/yr) whereby decreasing albedo is related with increasing wind speeds and this trends is strongest over the Great Lakes (mainly in February) and James Bay (mainly in December).

Winter and fall trends in wind speed are quite strong (*ca.* 0.05 $ms^{-1}yr^{-1}$ in winter; 7% decadal increase in winter means) with some areas in the winter experiencing as high as $0.07ms^{-1}yr^{-1}$ which translates into roughly a 10% decadal increase in some regions of the lakes particularly over Lake Superior. Decadal trends show roughly a 3-4% increase in wind speeds over Lake Superior which is close in estimation to the 5% increase found by Desai and McKinley (2009). In the fall, wind speeds can experience *ca.* 3% decadal increase in mean wind speed over the Lakes but with trends of up to 0.12 $ms^{-1}yr^{-1}$ in James Bay, wind speeds can have a very significant ($p< 0.005$) decadal increase of 17% and have increased 57% over the past 33 years. Regions in central and northern Ontario experience slightly negative trends in the fall and winter months but these trends are not statistically significant. These trends have also been found over the great lakes at the 80 m hub height using NARR data (Li *et al.*, 2010).

3.5.2 Trends in electrical output

Turbine output is greatest during the winter and fall seasons with the winter season seeing high yields in regions surrounding the Lakes and James Bay during the winter. These yields are expected owing to the higher trends in wind speed seen during these seasons. Summer and spring yields are lower owing to weakening wind gradients, with spring having higher output for most of Ontario than in summer. It is evident that the majority of electrical energy produced by the turbine is seasonal and spatially dependent and thus not all of Ontario will benefit from small wind turbine implementation. Southern regions in Ontario are surrounded by Lakes Erie, Huron and Ontario and benefit from wind patterns persisting in this region and thus this area has the highest concentration of utility scale wind farms in Ontario. Analysis in the Waterloo region (southern Ontario) has shown that the windiest months where wind energy potential is the greatest are from November to May (Li, 2005). It is widely noted that increases in turbine hub height increases electrical yields from the turbines as faster winds are captured at higher hub heights owing to the reduced effect of wind shear from the terrain (Lu et al., 2002). Although the same patterns in electrical output by the analyzed micro-scale Bergey 1 kW wind turbine at the 10 m hub height also exist at 30 m, the yield is not always spatially and temporally consistent. Increasing the hub height in the winter can see up to 100% increase in wind speeds over much of Ontario versus 80% in the fall as the turbine extract more energy from higher speed winter winds aloft as wind gradients are slightly steeper.

Although focus is given to micro-scale wind turbines and not offshore production, it is useful to note that electrical output is increased by 20% over the lakes at the 30 m hub height versus up to 60% in regions surrounding the lakes. Surface roughness causes winds closer to the terrain to lose more momentum than over water bodies. Furthermore, wind profiles are steeper over the land, thus too is wind energy potential (Hicks, 1976). Southern Ontario, particularly regions closer to Lake Erie and Ontario most benefit from increases in hub height to 30 m as capturing lake winds can raise yields by 100-120%. These southern regions will benefit more from turbines of a higher hub height, potentially reducing the need for more turbines such as in regions where only 60% increase with hub height is experienced. With the 10 m hub height, decadal trends indicate increases in electrical output by approximately 6% over regions close to the lakes and up to 20% along the eastern James Bay coast in the winter, wind trends are increasing wind energy production temporally. Ontario will most benefit from James Bay trends in the fall where regions over the western James Bay coastline can see up to 10% increase in means per decade. Trends at the 30 m hug height are not as strong but still suggest growing supply of wind energy temporally through the winter and fall seasons.

When looking at annual average in total electrical output for the Bergey 1 kW at 10 m hub height it is evident that regions that will most benefit from micro-scale wind turbine investment in Ontario are those surrounding the Great Lakes and regions along northern Ontario that will benefit from wind blowing to and from Hudson and James Bay. Southern Ontario also has more evenly distributed yields of higher value as it benefits

from its proximity to the Lakes. Much of Ontario will see an annual power production of 800-1200 kWh while areas surrounding Lake Superior can have high outputs of 1.6 MWh. Power production is more evenly distributed at the 30 m wind as at the high hub height, the influence of surface roughness is reduced. Much of Ontario will see power outputs of approximately 1.5 to 2.3 MWh and power output is increased for southern Ontario and around the Great Lakes as well. Using the means of 1.5 to 2.3 MWh from much of Ontario at the 30m hub height and the reported electrical cost of 8.45cents/kWh for Ontario as of May 1st, 2013 (http://www.ontariohydro.com/index.php?page=current_rates), the use of the Bergey 1 kW wind turbine can see an approximate annual saving of $130 to $200 in electrical bills per annum. However, this value is greatly limited by the fluctuating nature of electrical prices and the difference in costs between providers. Having a combination of higher hub heights and a higher rated output turbine (e.g. 10 kW, 25 kW) will surely increase annual savings but a cost-effective analysis was not performed in this study.

The Statistics Board of Canada gives an annual Ontario household consumption of 107 GJ from its last household energy census in 2007. Spatial comparison (10m hub height) of the supply of electricity from the Bergey 1 kW wind turbine to the demand of the average Ontarian household shows that the Bergey turbine is most economically viable around the lakes but will only account for up to 6% for annual energy demand (e.g. near Georgian Bay) and approximately 3.5 to 4.5% in southern Ontario whereas much of Ontario will see this turbine accounting for 2.5-4% of energy demands (Fig. 3.14). These

values are increased at the 30 m hub height with much of Ontario now experiencing between 5 and 7% of energy demand from the Bergey turbine and regions around Lake Superior can meet energy demands of up to 9-10% in some regions.

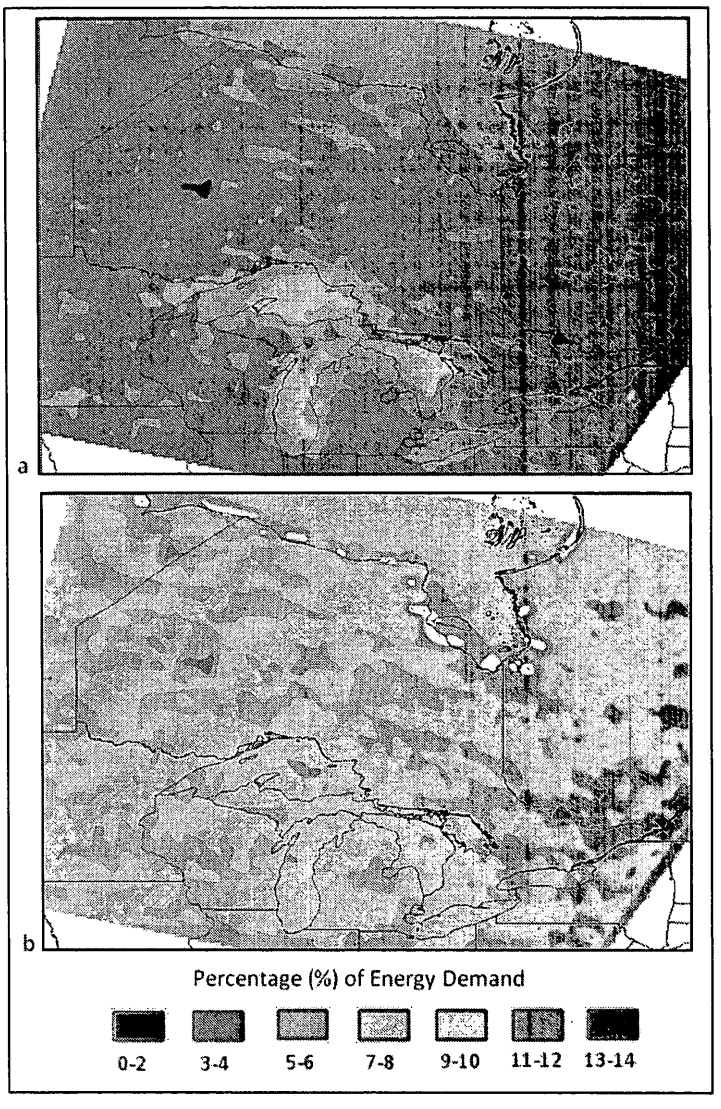

Fig. 3.14: Annual percentage of energy demands met for an average Ontarian household by the Bergey Excel 1 kW wind turbine for a) 10 m and b) 30 m hub heights. The average annual energy demand for a household in Toronto is reported as 107 GJ (Statistics Canada, 2007). *Coastal regions in white have been omitted due to coding error at the 30 m hub height.*

3.6 Conclusion

Wind speed trends during the winter and fall months are the greatest at both hub heights of 10 and 30 m, with the summer season giving the lowest means. These trends are highly spatial, occurring frequently over the Great Lakes, lower Hudson Bay and James Bay. Much of Ontario experiences statistically insignificant wind speed trends with lower much lower means than surrounding water bodies. It is purported that a strong correlation with decreasing lake/sea ice concentrations and increasing wind speeds exists where loss of sea ice leads to both physical and energy balance changes, which subsequently alter the stability in the atmospheric boundary due to surface forcing. Through turbine analysis, I postulate that the micro-scale wind turbine industry will be most feasible at a higher hub height of 30 m and utilizing turbines of a higher rated output. Even with a 1 kW wind turbine (< 0.001% of most utility scale wind turbines), annual savings of $130-$200 can be possible for much of Ontario at the 30 m hub height with energy demands being met by approximately 5 and 7%. These statistics however, are derived from general energy usage averages and apply a basic energy demand to Ontario whereas true estimates are heterogeneous and not spatially even as energy demands are surely higher in southern populated regions. The Bergey turbine is only at 1kW rated output and other turbines can be at rated outputs of 10 kW and 25 kW as commonly seen in the micro-scale turbine industry and will lead to higher turbine output. Limitations in the estimation of turbine electrical power exists as power curves are inherently based on data collected

and sample size of such data. However, this study's analysis produced a power curve which was a good representation of the Bergey manufacturer power curve.

3.7 References

Austin, J. A., & Colman, S. M. (2008).A century of temperature variability in Lake Superior. *Limnology Oceanography,* **53**, 2724–2730.

Bechly, M. E., Clausen, P. D., Lindeyer, J., & Wood, D. H. (1997).The Fort Scratchley wind turbine. *Proceedings of the 35th ANZSES Conference, 1–3 December, Canberra, ACT.*

Black, T. L. (1988), The step-mountain Eta coordinate regional model: A documentation, NOAA/NWS National Meteorological Center, 47 pp. *NCEP, 5200 Auth Road, Camp Springs, MD 20746.*

Bose, N. (1992). Icing on a small horizontal-axis wind turbine—Part 1: Glaze ice profiles. *Journal of wind engineering and industrial aerodynamics*, **45**, 75-85.

Canadian Wind Energy Association [CanWEA].(2012) April.Canadian Wind Energy Market. Ottawa (ON): Canadian Wind Energy Association. Available from: http://www.canwea.ca/pdf/canweafactsheet-FedProInitiatives-final.pdf.

Celik, A. N. (2003). Energy output estimation for small-scale wind power generators using Weibull-representative wind data. *Journal of Wind Energy and Industrial Aerodynamics,***91**, 693–707.

Cohen, S., Agnew, T., Headley, A., Loute, P., Reycroft, J., & Skinner, W. (1994).Climate variability, climatic change, and implications for the future of the Hudson Bay bioregion. *The Hudson Bay Programme.*

Cole, J. J. et al. (2007). Plumbing the global carbon cycle: Integrating inland waters into the terrestrial carbon budget. *Ecosystems,***10**, 172–185.

Desai, A. R., Austin, J. A., Bennington1, V., & McKinley, G. A. (2009).Stronger winds over a large lake in response to weakening air-to-lake temperature gradient. *Nature Geoscience,***2**, 855-858.

Duguay, C.R., Terry, D., Prowse, B. R., Bonsal, R. D., Brown, M. P., La croix.,& Menard, P. (2006). Recent trends in Canadian lake ice cover. *Hydrological Processes,* **20**, 781–801.

Eggers, A. J. (2000).Modeling of yawing and furling behavior of small wind turbines.*2000 ASME Wind Energy Symposium, 19th, AIAA, Aerospace Sciences Meeting and Exhibit, 38th, Reno, NV,* 1-11.

Gagnon, A. S., Gough, W.A. (2005). Climate change scenarios for the Hudson Bay Region: An inter-model comparison. *Climatic Change,***69**, 269–297.

Hicks, B. B. (1976). Wind profile relationships from the 'Wangara' experiment. *Quarterly Journal of Royal Meteorological Society,***102**, 535-551.

Högström, U. (1988). Non-dimensional wind and temperature profiles in the atmospheric surface layer: a re-evaluation. *Boundary Layer Meteorology,* **42**, 55–78.

Independent Electricity System Operator, IESO (2012). Supply Overview. Retrieved from http://www.ieso.ca/imoweb/media/md_supply.asp, December 18, 2012.

Janjić, Z. I. (1994). The step-mountain Eta coordinate model: Further developments of the convection, viscous sublayer, and turbulence closure schemes. *Monthly Weather Review,* **122**, 927–945.

Li, M. (2005). Investigation of wind characteristics and assessment of wind energy potential for Waterloo region, Canada.

Li, M., & Li, X. (2005).Investigation of wind characteristics and assessment of wind energy potential for Waterloo region, Canada.*Energy Conversion and Management,* **46**, 3014-3033.

Li, X., Zhong, S., Bian, X., Heilman, W. E., Luo, Y., & Dong, W. (2010).Hydroclimate and variability in the Great Lakes region as derived from the North American regional reanalysis. *Journal of Geophysical Research,* **115**, 1-14.

Lu, L., Yang, H., Burnett, J. (2002). Investigation on wind power potential on Hong Kong islands—an analysis of wind power and wind turbine characteristics. *Renewable Energy***27**, 1–12.

Lubitz, D.W. (2012). Impact of ambient turbulence on performance of a small wind turbine. *Renewable Energy*. Retrieved from http://dx.doi.org/10.1016/j.renene.2012.08.015

Magnuson, J. J., Robertson, D. M., Benson, D. J., Wyne, R.H., Livingstone, D. M., Arai, T., Assel, R. A., Barry, R. G., Card, V., Kuusisto, E., Granin, N. G., Prowse, T. D., Stewart, K. M., &Vuglinski, V. S. (2000). Historical trends in lake and river ice cover in the Northern Hemisphere. *Science,* **289**, 1743–1746.

Maslanik, J. A., Serreze, M.C., & Barry, R.G. (1996). Recent decreases in Arctic summer ice cover and linkages to atmospheric circulation anomalies. *Geophysical Research Letters,* **23**, 1677–1680.

Matsushima, T., Takagi, S., & Muroyama, S. (2006). Characteristics of a highly efficient propeller type small wind turbine with a diffuser. *Renewable energy*, **31**, 1343-1354.

Mesinger, F., Janjić, Z. I., Nicković, S., Gavrilov, D., &Deaven, D. G. (1988). The step-mountain coordinate: Model description and performance for cases of Alpine lee cyclogenesis and for a case of an Appalachian redevelopment. *Monthly Weather Review,* **116**, 1493–1518.

Mesinger, F., Di Mego, G., Kalnay, E., Mitchell, K., Shafran, P. C., Ebisuzaki, W., Jovic, D., Woollen, J., Rogers, E., Berbery, E. H., Ek, M. B., Fan, Y., Grumbine, R., Higgins, W., Li, H., Lin, Y., Manikin, G., Parrish, D., & Shi, W. (2006). North American regional reanalysis: A long-term, consistent, high-resolution climate dataset for the North American domain, as a major improvement upon the earlier global reanalysis datasets in both resolution and accuracy. *Bulletin of American Meteorology Society,***87**, 343–360.

Ontario Hydro, (2013).Ontario Hydro Electricity Rates.Retrieved from http://www.ontario-hydro.com/index.php?page=current_rates, June 18, 2013.

Palecki, M. A., & Barry, R.G. (1986). Freeze-up and break-up of lakes as an index of temperature changes during the transition seasons: A case study for Finland. *Journal of Climate and Applied Meteorology,* **25,** 893–902.

Seitzler, M. (2009). The electrical and mechanical performance evaluation of a roof mounted, one-Kilowatt wind turbine. *Report CWEC-2009-003*. Davis CA, USA: California Wind Energy Collaborative, University of California, Davis

Summerville, B. (2005). Small wind turbine performance in Western North Carolina, report. Boone, NC: Appalachian State University. Retrieved from http:// www.wind.appstate.edu/reports/researcharticlesmallwindperformanceBJS.

CHAPTER 4

TECHNICAL REPORT FOR THE TORONTO AND REGION CONSERVATION AUTHORITY

Technical Report for the Toronto and Region Conservation Authority

July 2013

Kortright Centre for Conservation Wind Test Site: Preliminary Site Assessment

Masaō Ashtine[a]

a Department of Geography, York University, 4700 Keele Street, Toronto, Ontario, Canada.

*Corresponding authors: mashtine@yorku.ca, bello@yorku.ca

4.1 Site Summary

The Kortright Centre for Conservation is located 10 minutes north of Toronto, on 325 hectares of woodland. With ample area for the testing of small wind turbines, the conservation presents the unique opportunity for the standardized testing of wind turbines pending site assessment. Data collected for this report was obtained between November 2012 and May 2013. The test site is located immediately east of the archetype house and consists of one meteorological tower (housing wind speed, wind direction and temperature sensors) and four small wind turbines (two out of commission due to damages). Preliminary results indicate that a strong wind regimes from the south east and north west bearings and an average wind speed of 4 ms^{-1} and a maximum wind speed of 18 ms^{-1} at the 30.5 m hub height.

4.2 Table of Contents

4.2.1 List of Figures

representing the four coordinal sectors of north east, south east, south west and north west.

Fig. 4.9: Power curve for Bergey Excel 1 kW derived from data collected between Nov 2012 – May 2013. Data from April 2013 was excluded due to technical problems in data collection. Equation defining power curve: $y = -0.1007x4 + 2.02x3 - 2.8783x2 - 2.1873x + 2.7317$, where y is the power produced by the Bergey wind turbine. Rated power is produced at a rated wind speed of 12.3 ms^{-1}. Furling wind speed is shown at 14 ms^{-1}.

Fig. 4.10: Power curve for the Bergey XL.1 turbine. Included are the wind speeds for cut-in, rated power, and auto-furling. Source: Supplied by Bergey Windpower.

Fig. 4.11: Power curve for Skystream 2.4 kW derived from data collected between Nov 2012 – April 2013 and as report by SWCC*. Equation defining power curve produced from field collected data: $y = -0.1442x4 + 2.9853x3 - 8.2462x2 + 9.3011x - 3.9783$, where y is the power produced by the Skystream wind turbine. Rated power for the tested Skystream 2.4 kW is 1.2 kW and rated wind speed is 13.5 ms^{-1}.

Fig. 4.12: Power curves at each wind direction for Bergey Excel 1 kW derived from data collected between Nov 2012 – May 2013. NE: north east; SE: south east; SW: southwest; northwest. All represents data from all directions.

Fig. 4.13: Power curves at each wind direction for Skystream 2.4 kW derived from data collected between Nov 2012 – April 2013. NE: north east; SE: south east; SW: southwest; northwest. All represents data from all directions.

Fig. 4.14: Power curves computed for each month for Bergey 1 kW derived from data collected between Nov 2012 – May 2013. Data from April 2013 was excluded due to technical problems in data collection.

Fig. 4.15: Power curves computed for each month for Skystream 2.4 kW derived from data collected between Nov 2012 – April 2013.

Fig. 4.16: Power curves at varying standard deviations of wind speed for Bergey Excel 1 kW derived from data collected between Nov 2012 – May 2013.

Fig. 4.17: Average coefficient of power (C_p) for the Bergey Excel 1 kW versus binned wind speed.

Fig. 4.18: Average coefficient of power (C_p) for the Skystream 2.4 kW versus binned wind speed.

Fig. 4.19: Deviation in output power from the Bergey Excel 1 kW turbine against standard deviation of measured wind speed. Power deviations were derived from the difference of modeled power (calculated from a line-of-best-fit) and measured power in Watts.

Fig. 4.20: Deviation in output power from the Skystream 2.4 kW turbine against standard deviation of measured wind speed. Power deviations were derived from the difference of modeled power (calculated from a line-of-best-fit) and measured power in Watts.

Fig. 4.21: Deviation in output power from the Bergey Excel 1 kW turbine against measured wind speed. Power deviations were derived from the difference of modeled power (calculated from a line-of-best-fit) and measured power in Watts.

Fig. 4.22: Deviation in output power from the Skystream 2.4 kW turbine against measured wind speed. Power deviations were derived from the difference of modeled power (calculated from a line-of-best-fit) and measured power in Watts.

Fig. 4.23: Standard deviation of power from the Bergey Excel 1 kW turbine against standard deviation in wind speed.

Fig. 4.24: Standard deviation of power from the Skystream 2.4 kW turbine against standard deviation in wind speed.

Fig. 4.25: Deviation in output power from the Bergey Excel 1 kW turbine against calculated slope in wind speed. Power deviations were derived from the difference of modeled power (calculated from a line-of-best-fit) and measured power in Watts. Slope readings are taken from wind speed data over three consecutive minutes.

Fig. 4.26: Deviation in output power from the Skystream 2.4 kW turbine against calculated slope in wind speed. Power deviations were derived from the difference of modeled power (calculated from a line-of-best-fit) and measured power in Watts. Slope readings are taken from wind speed data over three consecutive minutes.

Fig. 4.27: Adapted plot of Bergey Excel 10 kW turbine power curves during variable wind and steady wind conditions. *Source: www.wind-power-program.com*

4.2.2 List of Tables

4.3 Site Description

The Toronto and Region Conservation Authority (TRCA) has proposed the Kortright Centre for Conservation as the prototype site for the testing and standardization of micro-scale wind turbines. The proposed testing site is immediately east of the Archetype House and the area is an open grassy field within the Kortright Centre for Conservation (43°49'54" N and 79°35'16" W) and has a very wide and open fetch area with a surface roughness profile that is yet to be determined (Fig. 4.1). The dominant vegetation within this area is that of low lying grasses (maximum 0.2 m) and shrubs along with trees which border the field. The area below the wind turbine in regularly maintained and vegetation height is very close to the surface.

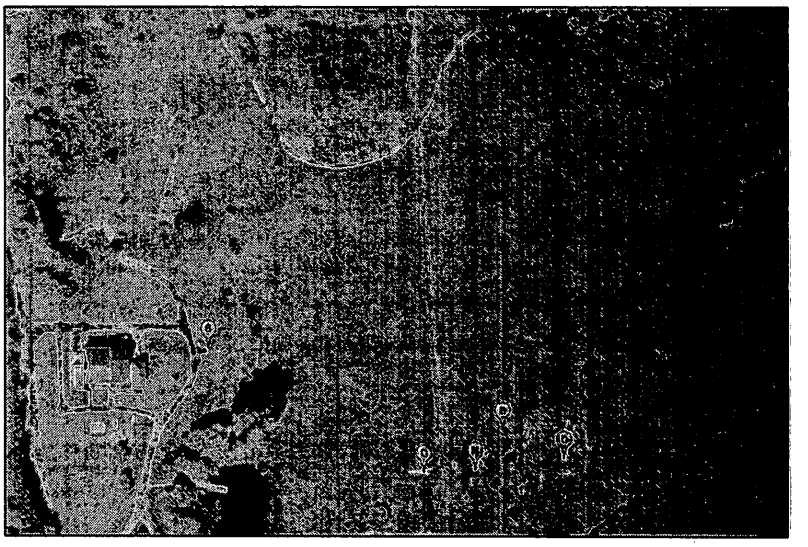

Fig. 4.1: Satellite image of the test site at the Kortright Centre for Conservation. Red markers represent locations of small wind turbines with D demarcating turbines that have been out of commission due to damages.* S: Skystream 3.7 – 2.4 kW; B: Bergey Excel 1 kW

The Kortright field testing site (elevation, 188 m) is situated approximately 25 km from the Toronto city center and thus shares similar weather patterns. Lake Ontario serves to moderate Toronto's weather to the point that its climate is one of the mildest in Canada. Spring and summer temperatures range from 15 °C to 25 °C and during winter months, the average daytime temperature, with the exception of January, the coldest month, hovers just slightly below freezing. Wind speeds vary from an average of 3.5 ms^{-1} in the summer months to 5 ms^{-1} in winter. Preliminary analysis showed that the average wind speed at the 16.8m hub height was 3.2 ms^{-1}, with a max wind speed at 12 ms^{-1} at 1 minute average readings. It is assumed that nearby tree boundaries do not obscure the dominant wind direction nor wind profile and the field testing site is fairly uninhibited from surface roughness influences. Surface roughness influence for the Bergey wind turbine will be greatest during period of southwestern winds which blow over a narrow ridge of trees. This influence is greatest for the Skystream wind turbine during periods of wind blowing from the west over the Archetype house and from the south as wind blow over a patch of Birch trees.

4.4 Meteorological Tower and Turbine Setup

4.4.1 Meteorological Tower

A 30 m tall meteorological tower was erected in early July, 2012 in the test field containing the small wind turbines (Fig 4.2). The main instrumentation on the tower mast

is that of the eight calibrated anemometers at the heights of 6.1 m, 10 m, 12.2 m, 15.2 m (Skystream hub height), 17.4 m (Bergey hub height), 18.3 m, 24.4 m and 30.5 m. Four anemometers were attached to the mast at the hub height corresponding to each of the turbines (two no longer operational) and one anemometer was mounted at the 10 m environmental standard. These anemometers are strategically placed to capture vertical variations in wind and were used to describe wind distribution and profiles at the Kortright testing site.

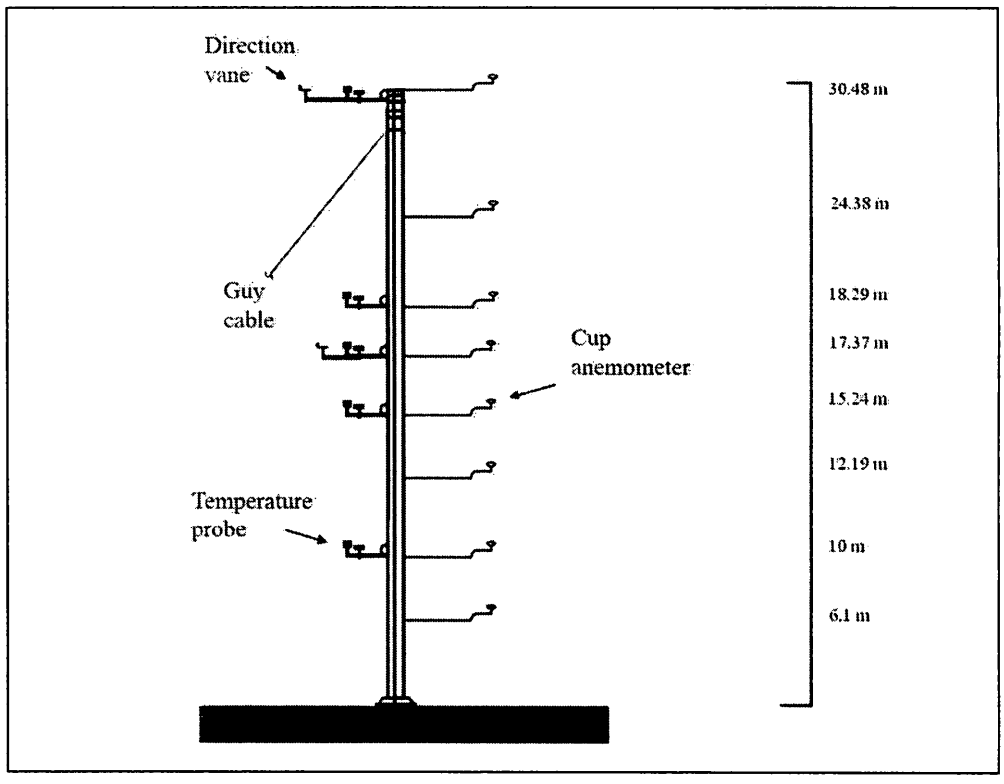

Fig.4.2: Simplified diagram of mounted instruments on the test site Meteorological tower.

Ambient air temperature is measured at five heights of 10 m (environmental standard), 15.2 m (Skystream hub height), 17.4 m (Bergey hub height), 18.3 m and 30.5 m as temperature is important when factoring the influences of air density. As the directionality of wind has an important role in establishing site characteristics and wind patterns, two wind vanes were mounted on the tower mast at heights of 15.2 m and 30.5 m. Further specifics of the mounted instrumentation are provided in Table 4.1.

Table 4.1: Specifications for mounted sensors on meteorological tower at the Kortright testing site.

	Mounted Height	Model	Operational Range	Data Capture
Anemometers	6.10 m, 10 m, 12.19 m, 15.24 m, 17.37 m, 18.29 m, 24.38 m, 30.48 m	8 NRG #40c 3-cup anemometers,	1 ms^{-1} to 96 ms^{-1}	5-second recording, 0.1 ms^{-1} accuracy (5 ms^{-1} to 25 ms^{-1})
Temperature Sensors	10 m, 15.24 m, 17.37 m, 18.29 m, 30.48 m	5 NRG #110s RTD sensor with radiation shield	-40 °C to 52.5 °C	5-second recording, +/- 0.8 °C accuracy maximum
Wind Vanes	15.24 m, 30.48 m	2 NRG #200p Wind Vane	360° mechanical, continuous rotation	5-second recording

The data acquisition unit for the meteorological tower is a National Instruments CFP-1804 which is housed in a nearby instrumentation house. This is a slave unit for the controllers based in the Archetype house, and is access from the main computer with a

wireless bridge. The individual modules of the CFP (Compact Field Point) system accept different signal parameters and three modules on the CFP were used for the anemometer, RTD (temperature) and wind vane sensors and the wind turbine inverters. Data was recorded at 5 second intervals and the parameters recorded were that of date stamp, wind speed (ms^{-1}), wind direction (degrees), ambient air temperature (°C), and Bergey inverter voltage (Volts) and current (Amps) readings for the turbine, battery and battery-dump. The Skystream wind turbine was not connected to the main meteorological tower wiring owing to its position within the field test site. Data from the Skystream wind turbine were acquired wirelessly using a Southwest Windpower USB radio receiver which was mounted on the east facing wall of the Archetype house with a direct line of sight to the Skystream wind turbine nacelle. This data were then instantaneously processed with the Skyview 2.0 software on the main computer. Data were also recorded on a 5 second time basis and were also further extracted from SQL format for analysis.

Data acquisition for the Skystream 2.4 kW wind turbine started as of 25 September 2012, and the Bergey 1 kW wind turbine data began recording as of 7 November 2013 owing to unforeseen delays in mounting of the meteorological tower and instrument setup.

4.4.2 Small Wind Turbines

The Skystream wind turbine, located on the north western side (292 degrees and 117 m away) of the meteorological tower, is a HAWT manufactured by Southwest Windpower and has a hub height of 15.24 m with a rated power of 2.4 kW. The Bergey wind turbine is located much closer to the meteorological tower with a distance of 18 m and bearing of 32 degrees. The latter wind turbine is a HAWT with a hub height of 16.76 m with a rated power of 1 kW. Both wind turbines have specific designs that influence performance and power output (Table 4.2).Each wind turbine design (Fig. 4.3) accounts for protection of the rotor during extreme wind events. The Bergey can perform furling of its blades (blade edges face into wind) during high speeds (> 13 ms^{-1}) with a breaking system to slow or stop rotor rotation. The Skystream is incapable of furling but does possess an electronic stall regulation system to stop rotor rotation in high wind speed events (at or above 25 ms^{-1}).

Table 4.2: Wind turbine specifications for Skystream and Bergey turbine at the Kortright field testing site. Information obtained from manufacturer description.

		Bergey	Skystream
Structural	Hub Height	17.37 m	15.24 m
	Turbine type	HAWT, upwind	HAWT, downwind rotor with stall regulation control
Manufacturer rating	Rated Power	1 kW	2.4 kW
	Rated Wind Speed	11 ms^{-1}	13 ms^{-1}
Rotor specifics	Rotor Diameter	2.5 m	3.72 m
	Swept Area	4.91 m^2	10.87 m^2
	Rotor Speed (RPM)	490 (rated rotor speed, no range applied)	50 – 330
	Blade Material	Pultruded fiberglass	Fibreglass reinforced composite
Wind	Cut-in Wind Speed	2.5 ms^{-1}	3.5 ms^{-1}
	Cut-out Wind Speed	None	25 ms^{-1}
	Max Design Wind Speed	54 ms^{-1}	63 ms^{-1}
Protection	Furling Wind Speed	13 ms^{-1}	No furling
	Overspeed protection	Auto tail furl, electrical breaking system	Electronic stall regulation

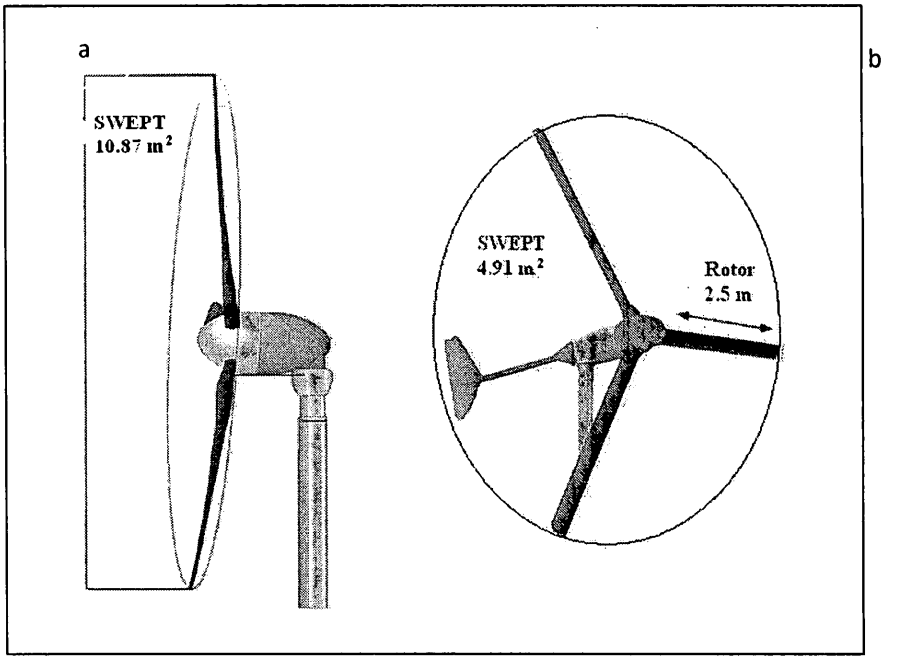

Fig.4.3: Sketch diagrams of each small wind turbine design; a) Skystream 2.4 kW b) Bergey 1 kW.

4.5 Site Wind Assessment

Wind data at the test site used in this analysis was recorded from the 7th of November, 2012 until May 31st. The data were average on a 1 minute basis from all 8 channels, not including the two wind direction channels that gave minute averages of direction in degrees with 0° and 360° representing true north. The average wind speed at the test site is approximately 3 ms^{-1} at the 15.2 m hub height (Fig. 4.4) and 4 ms^{-1} at the 30.5 m hub height (Fig. 4.5). The wind distribution at both heights takes on the typical Gaussian distribution with a right tail that skews off to a max wind speed bin of 12.5 ms^{-1} and 18.5 ms^{-1} at the 15.2 m and 17.4 m hub heights respectively. This distribution is much more

sharply defined at the 17.4 m height and has very low frequencies of faster occurring wind speeds.

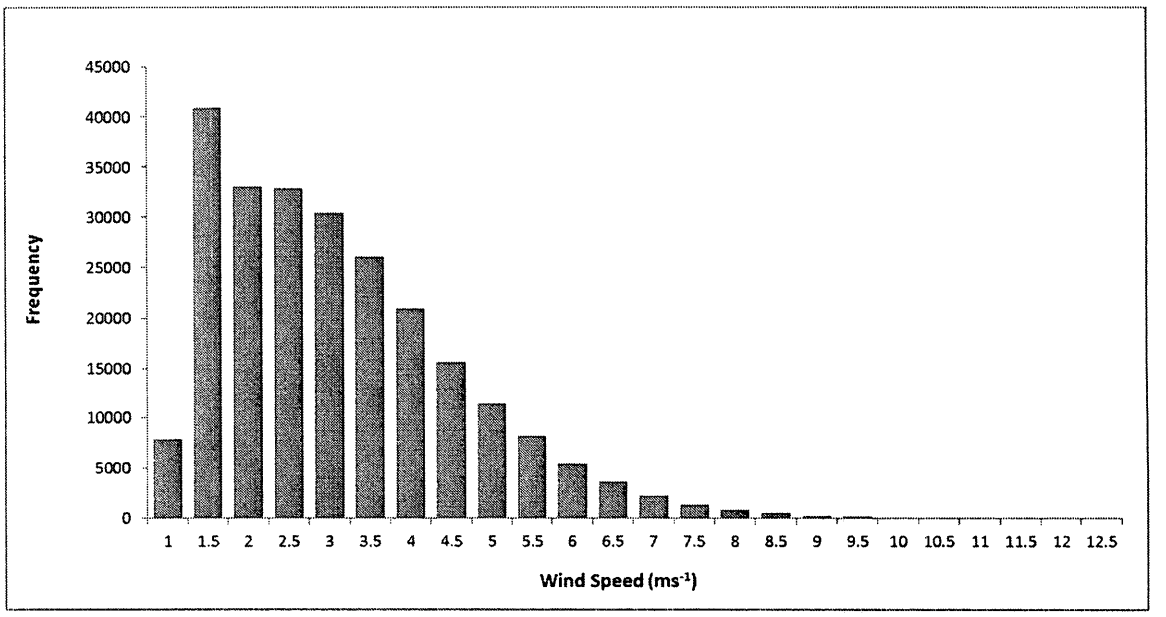

Fig. 4.4: Wind speed distribution at the 15.2 m hub height. Mean wind speed is highlighted as the red column.

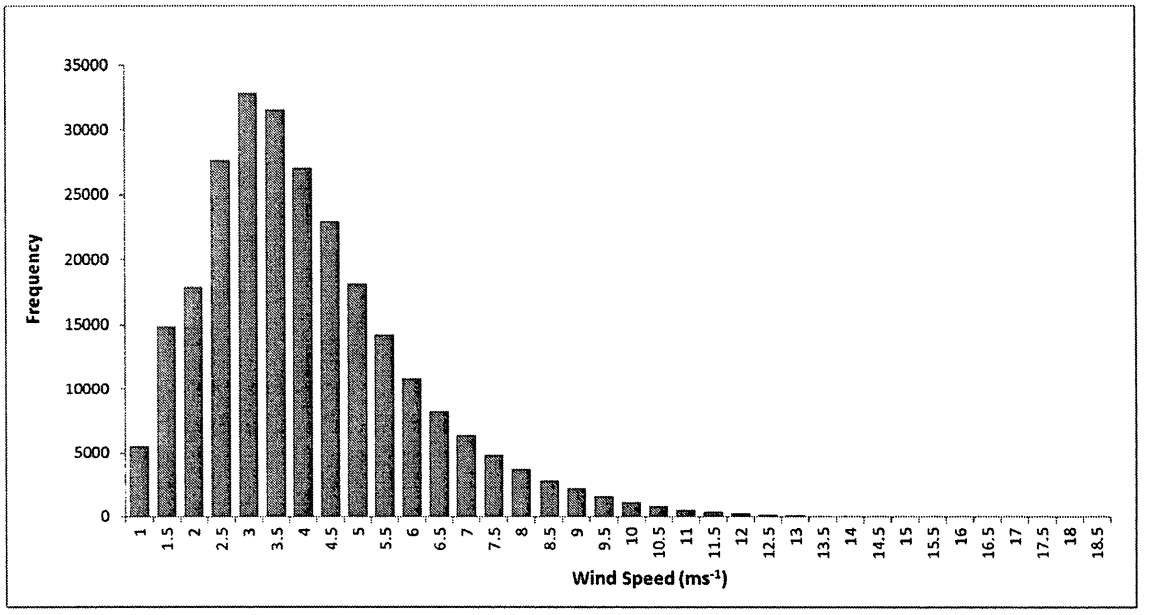

Fig. 4.5: Wind speed distribution at the 30.5 m hub height. Mean wind speed is highlighted as the red column.

Wind direction data show a substantial portion of winds blowing from north-westerly and south-easterly directions (Fig. 4.6). Very little wind is captured within the north-east and south-west sectors with the former having the least frequency of wind data. Prevailing winds come from a north-westerly direction at both hub heights.

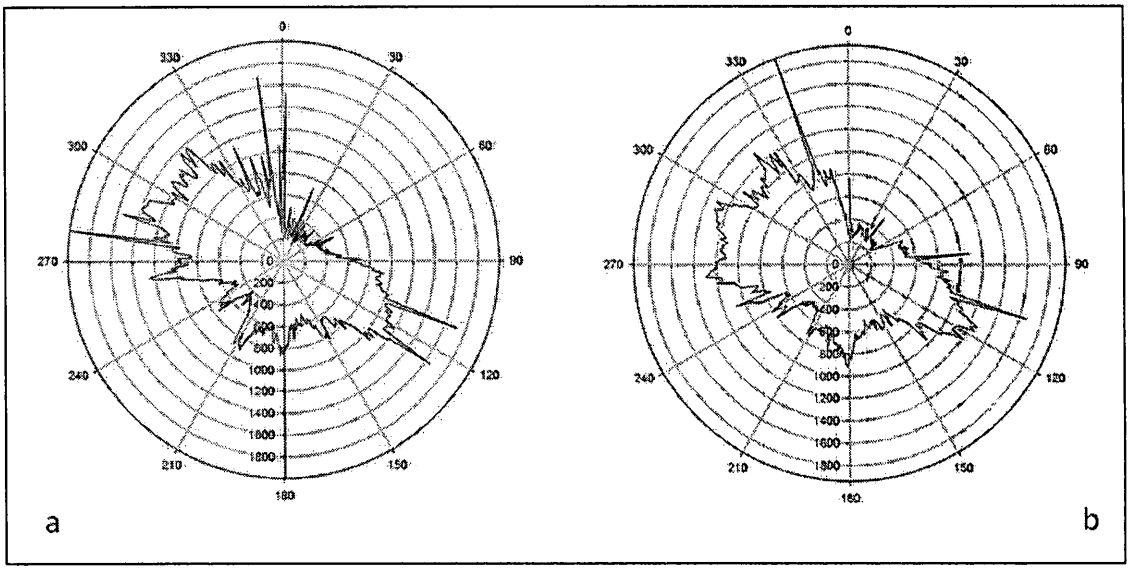

Fig. 4.6: Frequency polar plot of wind direction distributions for a) 15.2 m hub height and b) 30.5 m hub height. Bearings are given as 0° – 360° representing the four coordinal sectors of northeast, southeast, southwest and northwest.

With respect to average wind speed distribution, the north-eastern sector is shadowed in its average wind speed experienced when compared to the other directions (Fig. 4.7). This north-eastern sector has an average wind speed of approximately 2 ms^{-1} and 2.5 ms^{-1} at the 15.2 m and 17.4 m hub heights respectfully whereas the prevailing wind sector (north-west) has an average wind speed of $3m^{-1}$at the 15.2 m hub height and 4 ms^{-1} at 17.4m. Although the south-western sector is underrepresented in measured wind, this sector experiences average wind speeds much like the other directions. However, particularly at 15.2 m, the north-eastern cohort has lower reported wind speeds than any other sector. The north-western and south-eastern bearing experience the highest average wind speeds at both hub heights.

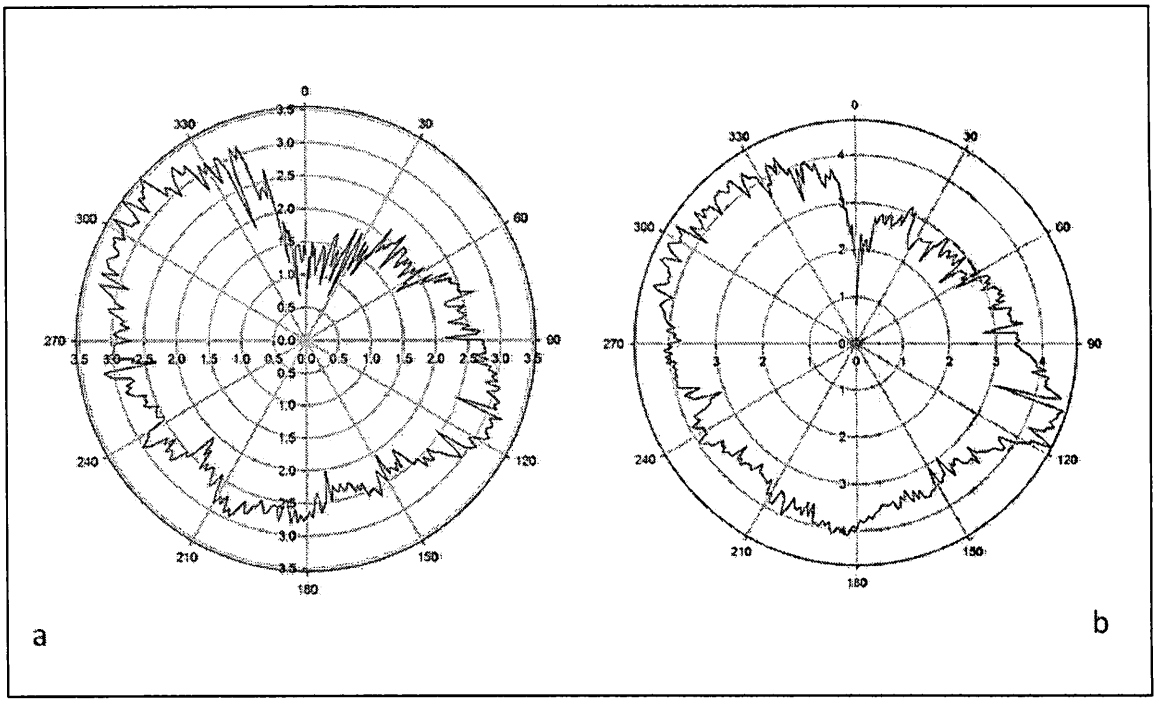

Fig. 4.7: Frequency polar plot of wind speed distributions for a) 15.2 m hub height and b) 30.5 m hub height. Bearings are given in 360° notation representing the cardinal sectors. Plots show direction of wind source.

The maximum wind speed frequency distribution wind rose show that the lower hub height has a much lower maximum wind speed of distribution for all wind sectors when compared to the 30.5 m hub height (Fig. 4.8). The north east sector is not only limited by its wind frequency but also the frequency of higher wind speeds.

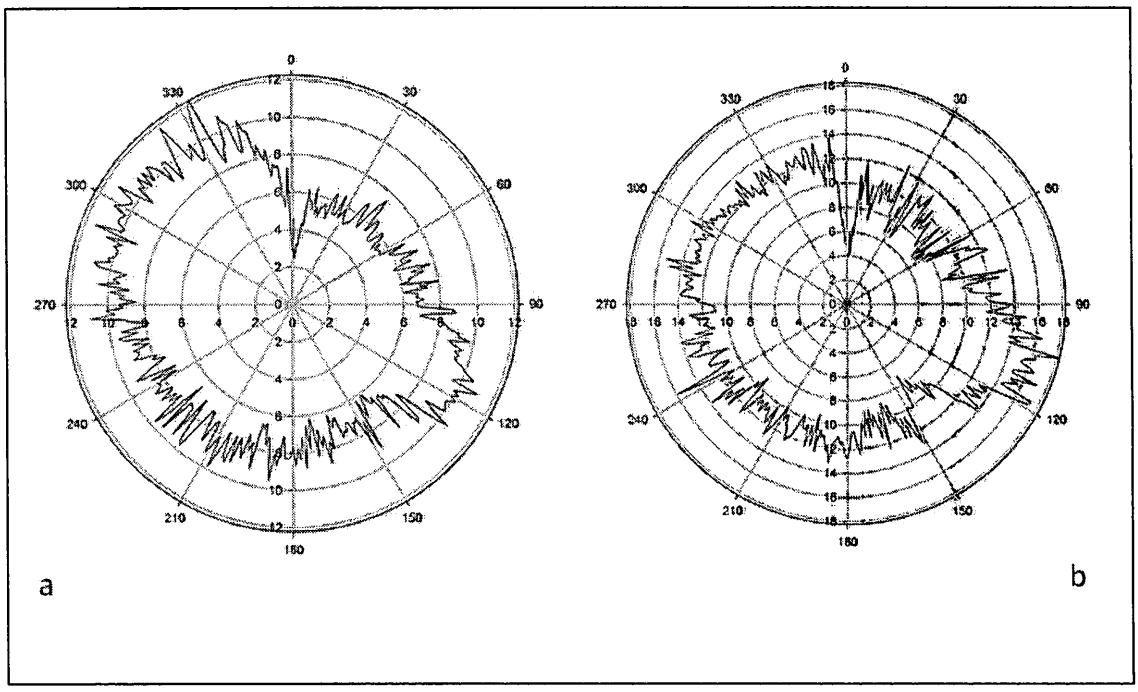

Fig. 4.8: Frequency polar plot of maximum wind speed distributions for a) 15.2 m hub height and b) 30.5 m hub height. Bearings are given in 360° notation representing the cardinal sectors. Plots show direction of wind source.

4.6 Power Curves

4.6.1 Field tested power curves

Power curves are unique to a wind turbine and describe the power output from the turbine at varying wind speeds. They are often used to define cut-in and cut-out wind speeds, rated power output, rated wind speed and furling wind speed amongst many other

parameters used to identify a turbine's efficiency. Within this study, power curves were computed by plotting measured power output versus wind speed and the resultant best fit line was used to show the non-linear relationship between wind speed and power in Watts. The Bergey Excel 1 kW power curve (Fig. 4.9) was determined using data from Nov 2012 until May 2013, excluding the month of April owing to technical error in data collection. This complete power curve nonetheless shows no power output before the turbine's cut-in wind speed of 2.5 ms^{-1} and gives a rated power of approximately 1.1 kW at a rated wind speed of 14 ms^{-1}.

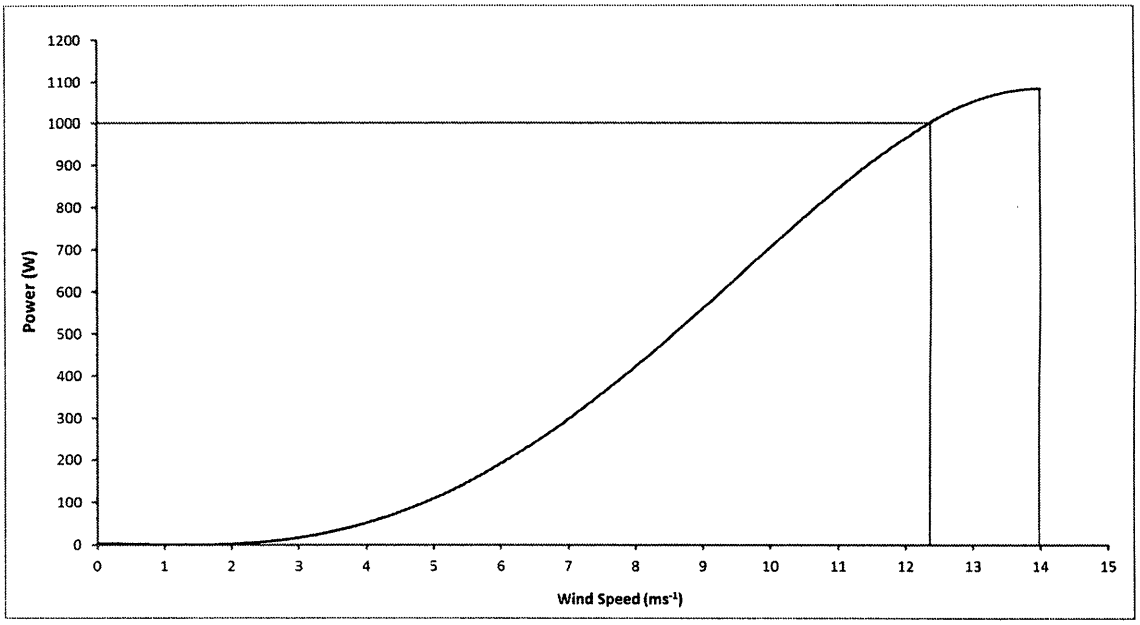

Fig. 4.9: Power curve for Bergey Excel 1 kW derived from data collected between Nov 2012 – May 2013. Data from April 2013 was excluded due to technical problems in data collection. Equation defining power curve: y = -0.1007x4 + 2.02x3 - 2.8783x2 - 2.1873x + 2.7317, where y is the power produced by the Bergey wind turbine. Rated power is produced at a rated wind speed of 12.3 ms^{-1}. Furling wind speed is shown at 14 ms^{-1}.

These results correlated very well with Bergey's reported performance data for the Excel 1 kW wind turbine and only slight discrepancies exist (Seitzler, 2009). Findings included a strong correlation between the modeled values and measured values for electrical performance and previously published data (Fig. 4.10) on the Bergey Excel 1 kW small wind turbine.

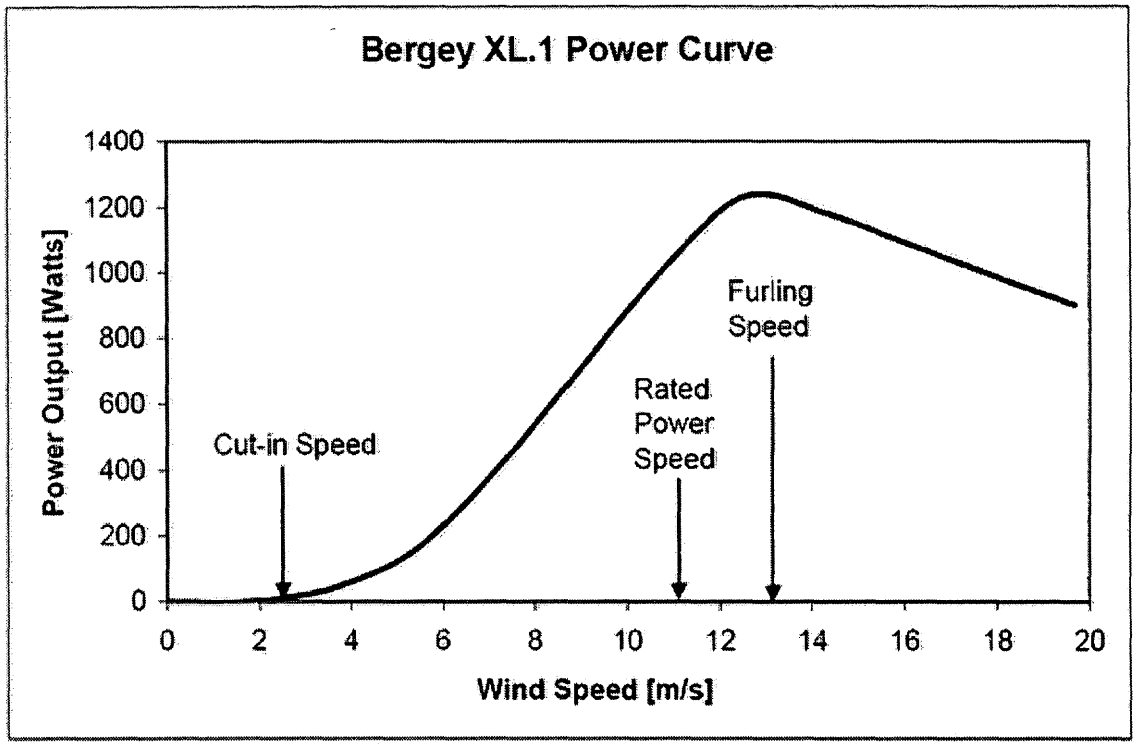

Fig. 4.10: Power curve for the Bergey XL.1 turbine. Included are the wind speeds for cut-in, rated power, and auto-furling. Source: Supplied by Bergey Windpower.

From the reported Bergey data, the Excel wind turbine reaches it rated wind power of 1 kW at 11 ms^{-1} and furls its rotors at 13 ms^{-1}. Collected data in the field at Kortright shows similar results with the field Excel turbine producing an average rated power of 1 kW at a rated wind speed of 12.3 ms^{-1} and furling at 14 ms^{-1}, indicating that the turbine is not reaching its rated power as quickly as the manufacturer has claimed. However, furling at a later speed will allow for the turbine to produce more power rather than plateauing at 13 ms^{-1}. This does prevent the Bergey Excel 1kW turbine from reaching its rated power at lower wind speeds which are more prevalent at the Kortright site.

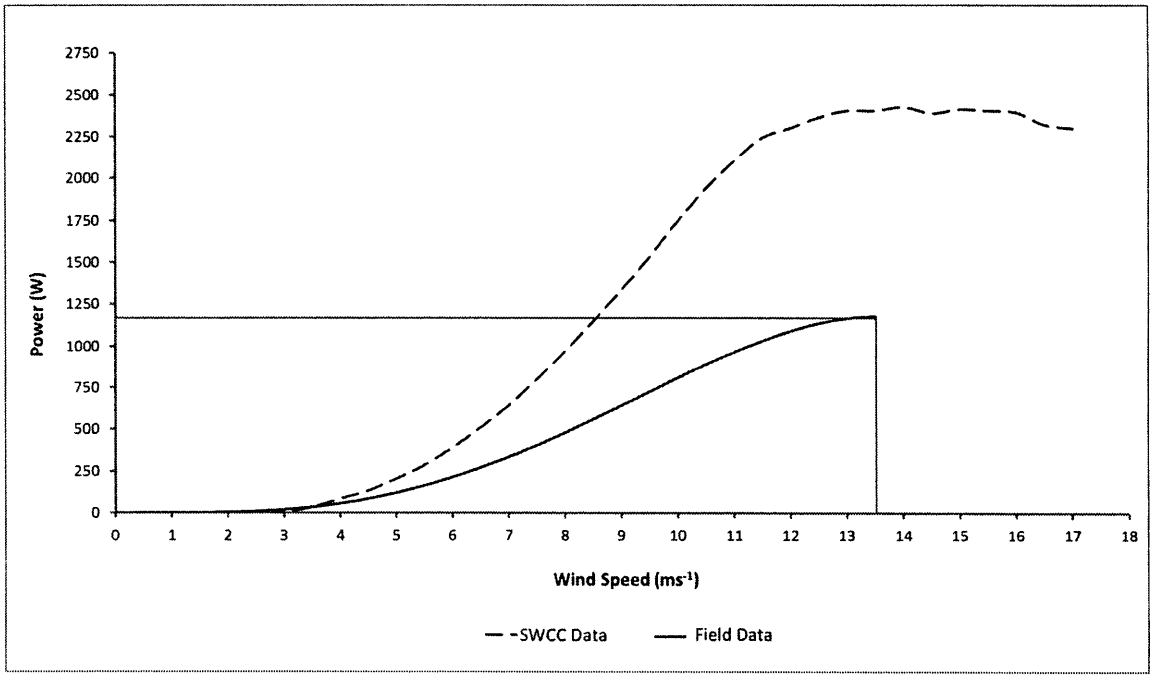

Fig. 4.11: Power curve for Skystream 2.4 kW derived from data collected between Nov 2012 – April 2013 and as report by SWCC*. Equation defining power curve produced from field collected data: y = -0.1442x4 + 2.9853x3 - 8.2462x2 + 9.3011x - 3.9783, where y is the power produced by the Skystream wind turbine. Rated power for the tested Skystream 2.4 kW is 1.2 kW and rated wind speed is 13.5 ms^{-1}.
***SWCC** is the Small Wind Certification Council

The Skystream 2.4 kW wind turbine at the Kortright test site is substantially underperforming in comparison to reported data by Southwest Windpower (Fig. 4.11). The Small Wind Certification Council, through field testing, has reported a rated power of 2.4 kW at 13 ms^{-1}which is vastly different from the data collected from the Skystream at the Kortright test site which shows a peak power output of 1.2 kW at 13.5 ms^{-1}. Variation in performance between the tested Skystream and data reported by the manufacturer is less substantial at lower wind speeds but diverges sharply with increasing wind speeds. Although the tested Skystream turbine peaks in power output at roughly the same rated wind speed as reported by the manufacturer, the wind turbine is poorly performing over a large range of wind speeds. It is also important to note that the power curve shown here is a line of best fit which was modeled from the data collected from the 1-minute average of power produced at various wind speed bins. Thus, these power curves are limited by the data collected and as the equation is polynomial (4^{th} order), will not represent the turbine's performance accurately at wind speeds where no data was collected.

4.6.2Variation in Power Curves and Wind Direction

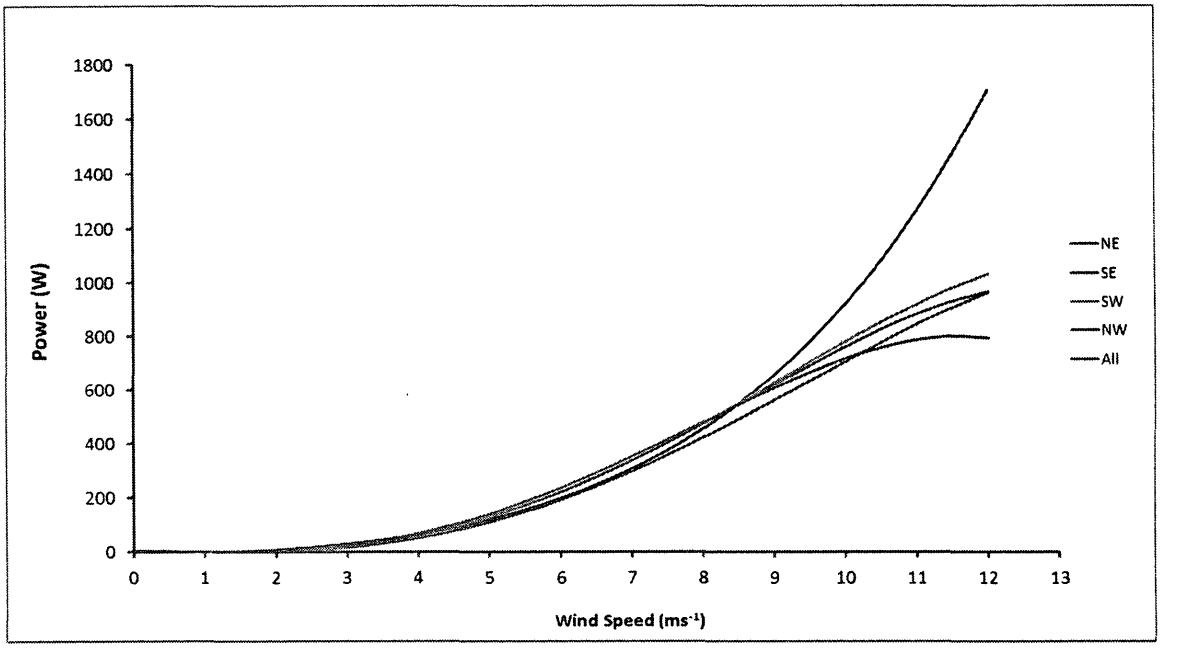

Fig. 4.12: Power curves at each wind direction for BergeyExcel 1 kW derived from data collected between Nov 2012 – May 2013. NE: northeast; SE: southeast; SW: southwest; northwest. All represents data from all directions.

With respect to a small wind turbine's design, as the wind turbine adjusts with changing wind directions, the power produced should not vary with wind direction as the rotor is always aligned with the direction of the prevailing wind to maximize the energy extracted. However, the accuracy of the power curve is highly dependent on the availability of performance data and thus its sample size. As seen through the site's wind rose (Fig. 4.6, 4.7), the north east and south west wind sections are much more limited in the frequency of wind available than the other two sectors with the North-eastern sector have the lowest wind frequency and average wind speed. This is reflected in the produced power curve using winds from the north east sector which shows a clear over estimation

in power produced at high wind speeds (> 9 ms^{-1}; Fig. 4.12). Below 9 ms^{-1} however, all sectors produce very similar power curves with slight variation in power output for the south west and north west sectors.

The produced power curves are not only affected by the sample size of wind data but more specifically, the sample size of extreme wind data. For instance, although the South-eastern section differs slightly in frequency of wind, the number of wind readings above 10 ms^{-1} may be small enough to cause precision issues in modeling a power curve that best suits the actual wind turbine performance. This suggests that when testing wind turbines in the field, it is important to consider the wind regime and distribution of winds at the site. Prevailing winds that come from mainly one direction may provide a strong wind dataset for analysis but the frequency of higher wind speeds is also important and this may differ in direction as well.

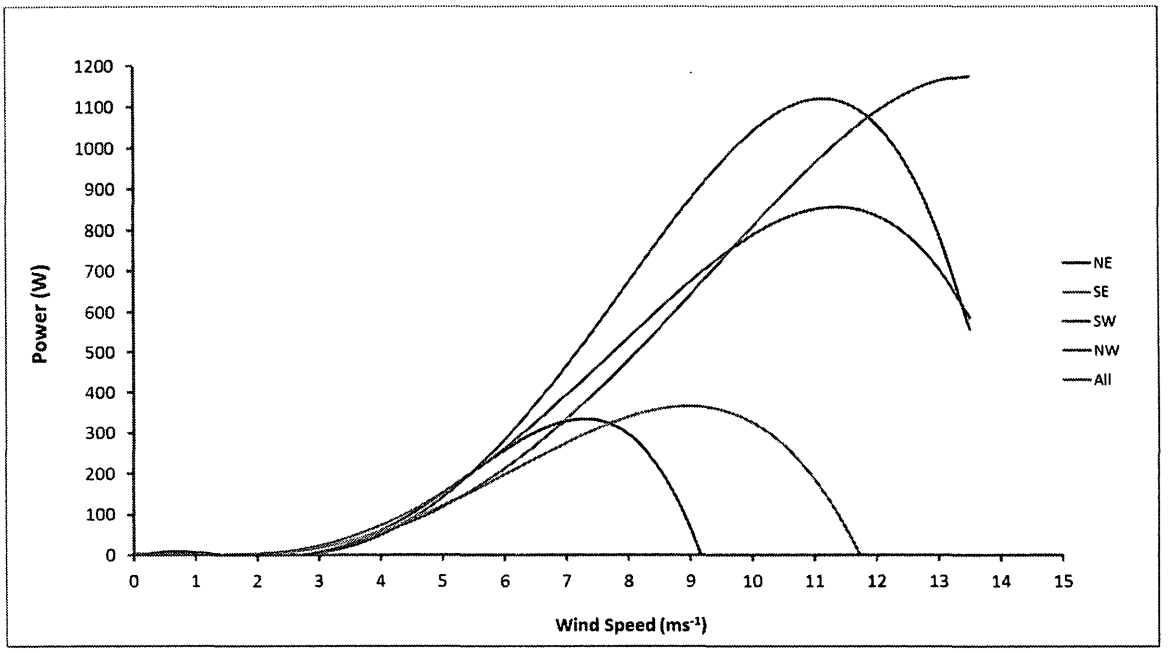

Fig. 4.13: Power curves at each wind direction for Skystream 2.4 kW derived from data collected between Nov 2012 – April 2013. NE: northeast; SE: southeast; SW: southwest; northwest. All represents data from all directions.

As shown in Fig 4.13, this sample size effect is much more pronounced when considering power curves from wind sectors produced from the Skystream 2.4 kW turbine. As this wind turbine had a unique and sporadic data acquisition which was not connected with the main recording devices, the Skystream wind turbine had many times where data was not recorded due to technical difficulties and thus the each wind sector was very different in sample size. However, it should be noted that the north east and south west sections are once again grossly under-represented and thus produced power curves which when modeled (assigned a line of best fit), underestimated power production at higher wind speeds.

4.6.3Temporal variation in power curves

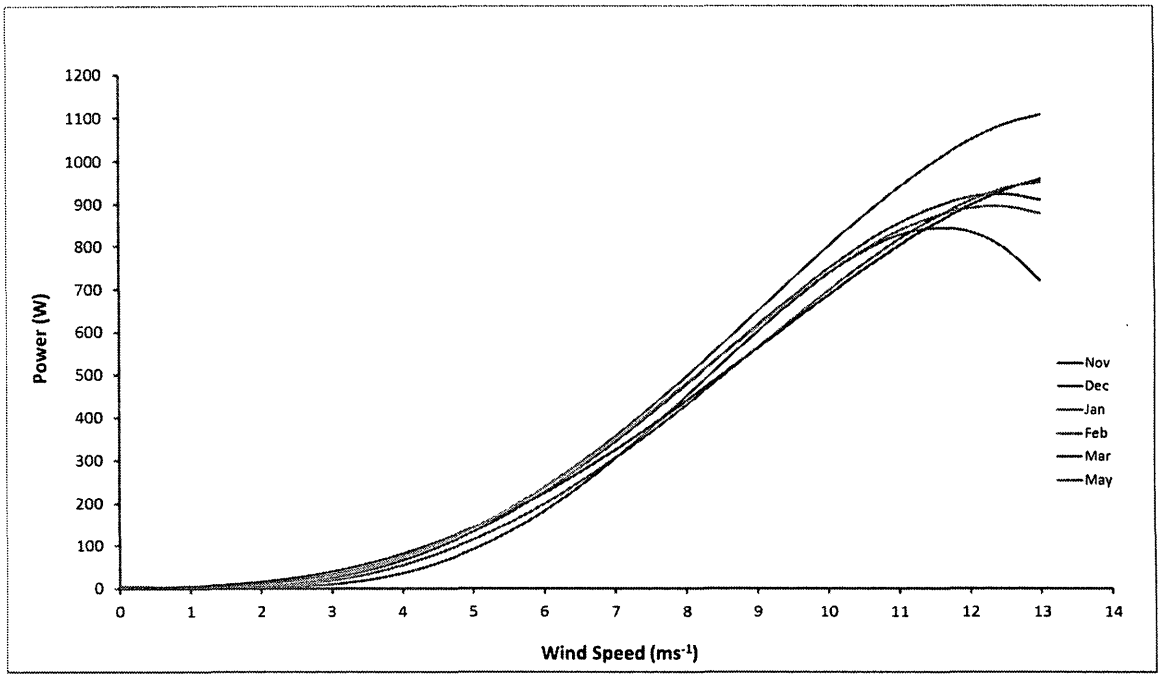

Fig. 4.14: Power curves computed for each month for Bergey 1 kW derived from data collected between Nov 2012 – May 2013. Data from April 2013 was excluded due to technical problems in data collection.

With the assumption of near-equal sample size for each month in terms of collected data (including times that the turbine was down), it is apparent that the power curve produced for each moth of data collection is very similar for the Bergey Excel 1 kW turbine with discrepancies occurring at higher wind speed bins (Fig. 4.14). Very little variation exists in produced power curves at wind speeds below 9 ms^{-1}, but more spread occurs in the data above this wind speed. This is particularly evident with the January dataset which shows an overestimation in power output at 9 ms^{-1} and onwards. Like with wind

direction. This relates to sample size and assuming at all months collected the same hours of wind data, the sample size affects power curve shape when it is limited by the sample size of extreme or higher wind speed data. As these wind speeds are less frequent and vary from month to month, producing a power curve in one month can vary at higher wind speeds than one produced from another month.

Like the month of January, a lack of wind speed readings above $11 ms^{-1}$ could have caused an underestimation at these wind speeds based on the power curve produced. As previously stated, this effect is not as prominent at lower wind speed bins which are more frequent. With this in mind, it is important to produce win turbine power curves from data collected over several months as to avoid issues with sample size. This is very important for the higher wind speed readings and instantaneous gusts of wind will be buffered out at the 1-minute averages and thus more time allotted for data collection will increase the frequency of sustained winds at higher speeds captured. This effect is once again more pronounced with the Skystream turbine (Fig. 4.15) where irregularities in data collection account for widely varying sample sizes between months.

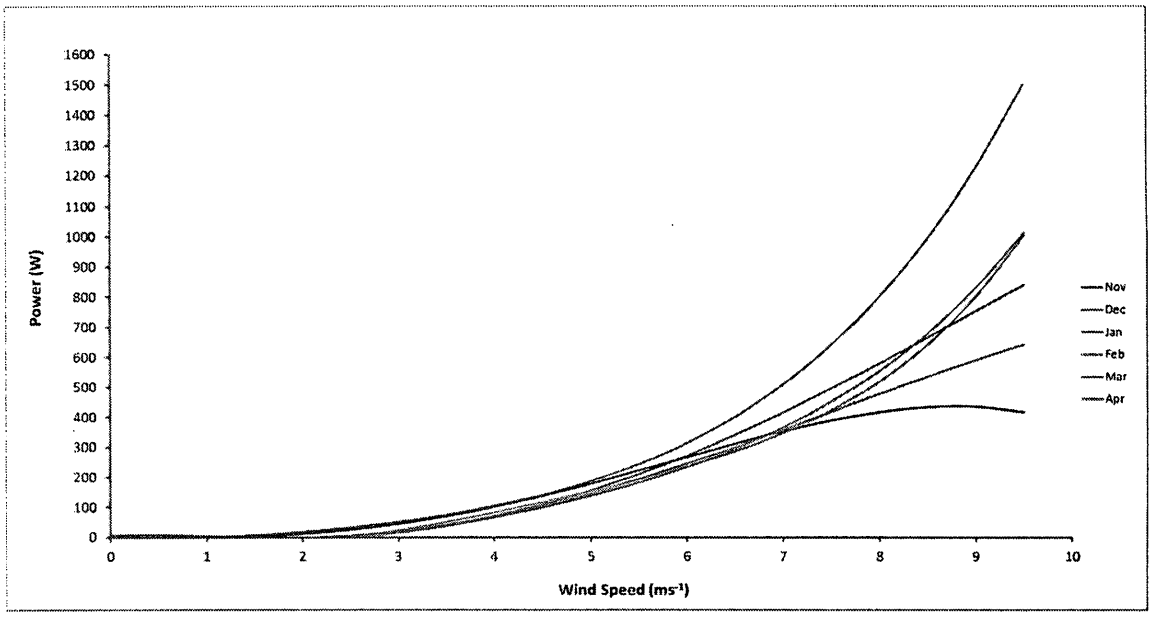

Fig. 4.15: Power curves computed for each month for Skystream 2.4 kW derived from data collected between Nov 2012 – April 2013.

4.6.4Power curves under varying standard deviations of wind speed

Standard deviation of measured wind speed is a good indicator of the variations in the wind which is an important factor when considering the response of the turbine and the subsequent power produced. During periods when the wind is more variable, it is expected that the turbine will perform differently than when the turbine is experiencing steady-flowing winds. Fig 4.16 shows that winds of a median standard deviation of 2-3 ms^{-1} experience produce a power curve which is almost identical to that the power curve produced from the complete dataset. It also suggests that at lower wind speeds, winds that flow very steadily produce a power curve that slightly underestimates the power output of

the turbine and more variable wind produces overestimating power curves. Once again, these power curves are limited by their sample size at higher wind speeds. This indicates that the Kortright test site has a wind regime with a predominant standard deviation of 2-3 ms^{-1} and that winds of varying standard deviation (particularly higher ones) can lead to deviations in power output from the wind turbine and thus discrepancies in power curves. Variance in the wind speed to lead to higher power output averages depending on the frequency of gusts which can keep the rotor spinning faster during lulls in the wind than would be experienced during steady wind flow.

Owing to the discrepancies in data collected from the Skystream, this analysis was not performed for this turbine.

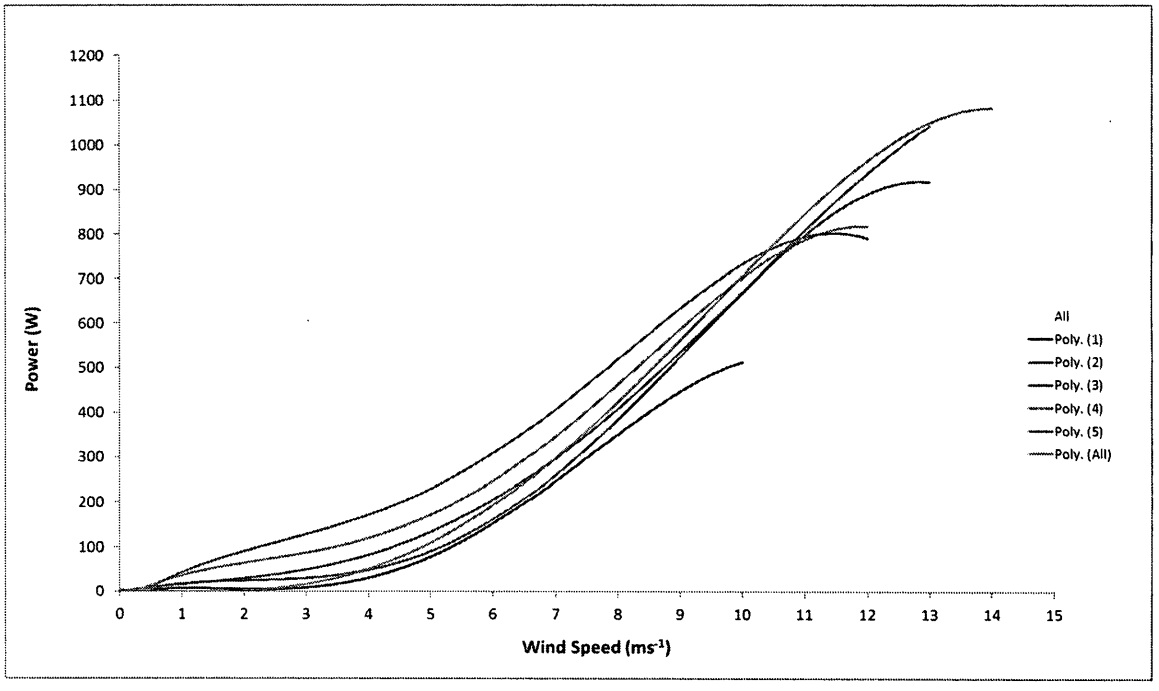

Fig. 4.16: Power curves at varying standard deviations of wind speed for Bergey Excel 1 kW derived from data collected between Nov 2012 – May 2013.

4.7 Turbine efficiency: Coefficient of Power, C_p

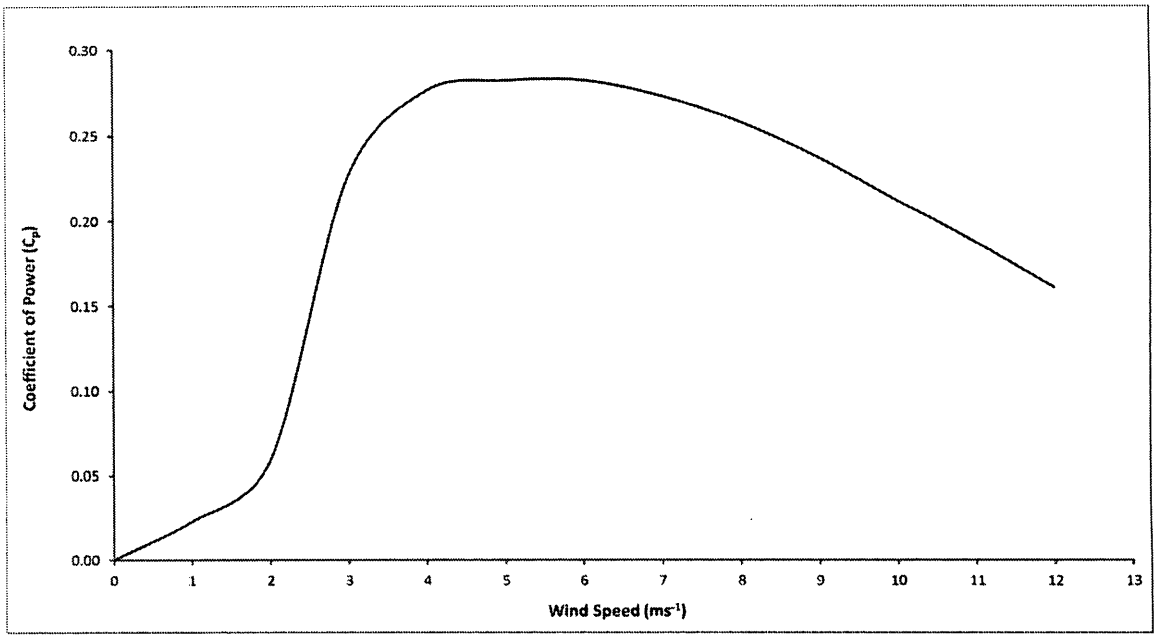

Fig. 4.17: Average coefficient of power (C_p) for the Bergey Excel 1 kW versus binned wind speed.

The coefficient of performance (C_p) is a dimensionless measure of how well the turbine is extracting wind energy from the available wind resource. This parameter is derived from the ratio of the power available in the wind to the actual power extracted by the wind turbine. A C_p of 1.0 suggests that a wind turbine is performing 100% efficiency where it extracts all of the available energy from the wind. This however is not possible through current wind turbine design as the maximum rate at which a turbine can extract wind energy is 0.59, the Betz limit. This limit describes the maximum performance at which a conventional HAWT can perform based on aerodynamic principles which govern the

passing of wind through the wind turbine's rotor. Small wind turbines can reach an average maximum performance in the range of 20 –40% with the utility-scale wind turbine models performing slightly better in most instances. The average C_p for the Bergey Excel 1 kW is shown in Fig. 4.17 and gives a maximum coefficient of performance of 0.28 which is achieved at low wind speeds of 4 ms^{-1} and is maintained until 6 ms^{-1} where it begins to decline to its lowest measured performance of 0.16 and 12 ms^{-1}. These results are fairly similar to those published in the technical report by Seitlzer (2009), where a maximum performance of 0.28 was recorded. However, this coefficient of performance was not achieved as quickly. There is no known published data by SWCC or Bergey showing how the C_p of the Bergey Excel 1 kW varies with time.

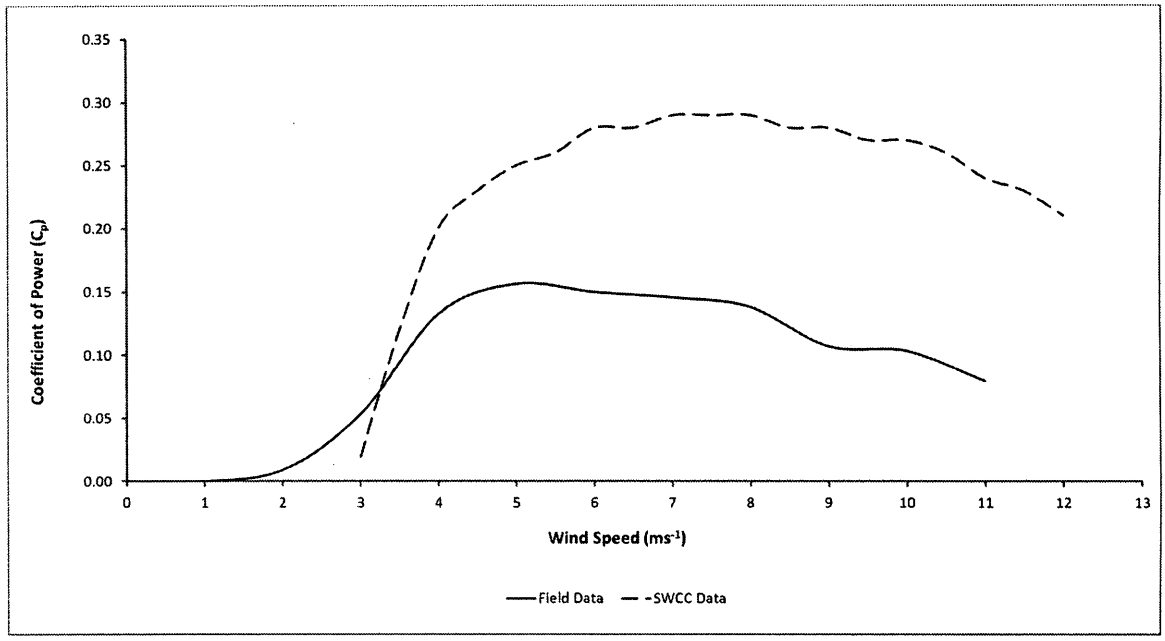

Fig. 4.18: Average coefficient of power (C_p) for the Skystream 2.4 kW versus binned wind speed.

As expected, based on the results of the Skystream power curve, the Skystream 2.4 kW wind turbine is underperforming in comparison to data published by SWCC (2009) (Fig. 4.18). Here, our field Skystream reaches an average maximum C_p of only 0.16 compared to a maximum of 0.29 as reported by SWCC.

4.8 Analysis of Power Output

It is important to understand how the wind turbines perform at varying wind speeds and how much noise exists in the data. A turbine that produces a power curve with very little scatter will have a more accurate assessment of performance and will produce to more stabilized and precise power outputs in varying wind regimes. For this analysis, the spread in measured data around the modeled data (line-of-best-fit) provided the deviation in power output, an important parameter when investigating how the wind turbine performs with wind speed. This is calculated from the difference of modeled power and measured power and a positive deviation states that the turbine power curve is overestimating based on the actual power measured and a negative deviation implies the reciprocal.

As previously noted, the standard deviation in the wind (ms^{-1}) is a measure of the winds variability and "gustiness". Plotting the deviation in power output versus the standard deviation in wind speed gives an indication of the spread in data (noise) that the turbine

experiences with variability in the wind. For instance, if there is low spread in the data during periods of very variable winds, the turbine is able to buffer the gustiness of the wind while producing electricity. The opposite occurs when the turbine responds very quickly to slight wind fluctuations and may be oversensitive in its performance.

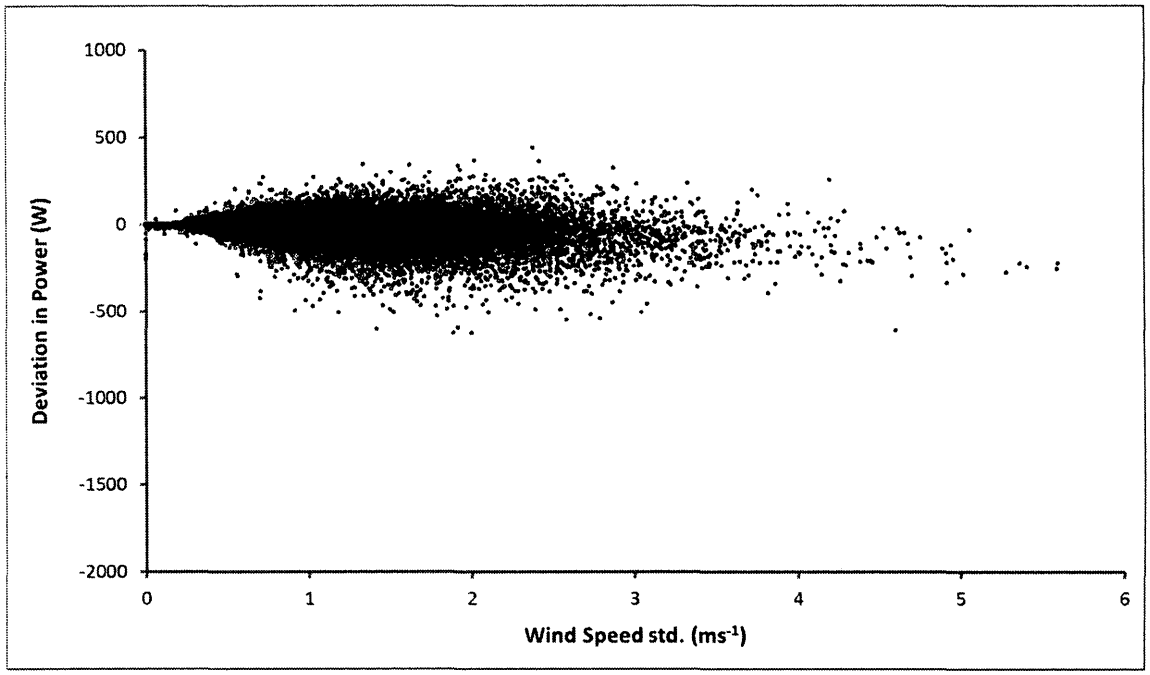

Fig. 4.19: Deviation in output power from the Bergey Excel 1 kW turbine against standard deviation of measured wind speed. Power deviations were derived from the difference of modeled power (calculated from a line-of-best-fit) and measured power in Watts.

The plot of deviation in power output versus the standard deviation of wind speed for the Bergey Excel 1kW turbine shows that with increasing variability in the wind, there is more noise in the data and it becomes less precise in modeling power output (Fig. 4.19).

The greatest noise in data occurs at lower wind variability (1 – 2 ms^{-1}) where power output can range as much as 1000 kW. At much higher standard deviations of wind speed, the spread in data points tails out and tends to a slightly negative deviation in power which shows that the modeled power curve is underestimating the power that is actually produced by the Bergey turbine but not substantially (< 250 kW).

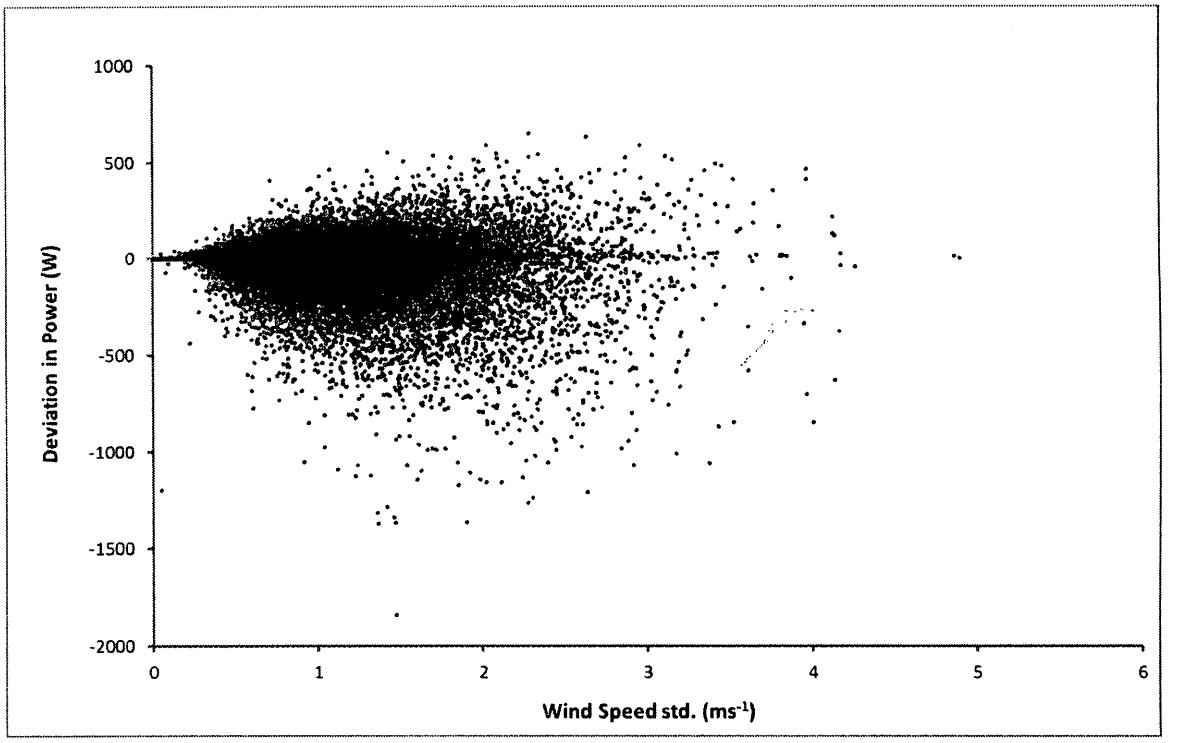

Fig. 4.20: Deviation in output power from the Skystream 2.4 kW turbine against standard deviation of measured wind speed. Power deviations were derived from the difference of modeled power (calculated from a line-of-best-fit) and measured power in Watts.

As seen with the Bergey wind turbine, much of the data points in the plot of deviation in power output versus standard deviation in wind speed for the Skystream 2.4 kW turbine are clustered around zero (Fig. 4.20). However, there is far greater spread in the data with much more points existing in the negative values. Much of the noise in the data is occurring between 2 and 4 ms^{-1} in standard deviation of wind speed and there can be as much as 1.5 kW difference in the modeled power curve versus measure power output. The Skystream is performing much more poorly than the Bergey as seen before, with inconsistent power outputs over wind speed.

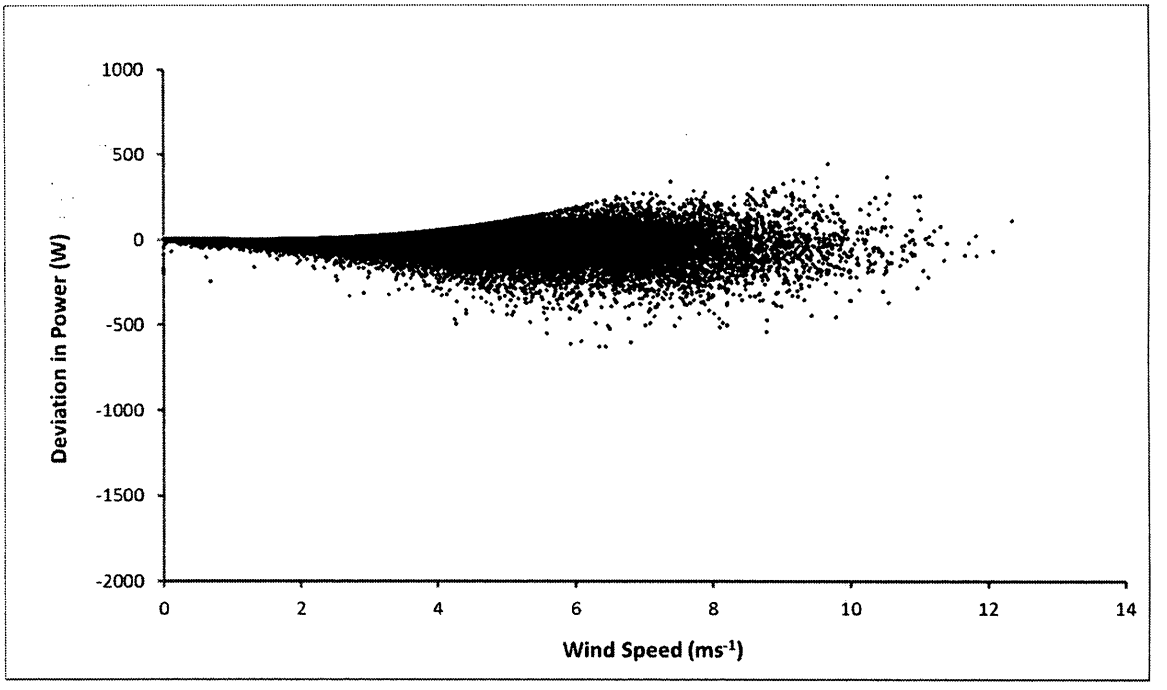

Fig. 4.21: Deviation in output power from the Bergey Excel 1 kW turbine against measured wind speed. Power deviations were derived from the difference of modeled power (calculated from a line-of-best-fit) and measured power in Watts.

The above graph shows how the deviation in power output changes with increasing wind speeds for the Bergey 1kw wind turbine (Fig. 4.21). As the deviation in power is calculated from modeled wind power minus the measurement wind power, the maximum deviation in power is limited by the modeled power with increasing wind speed and this is represented by the uniform pattern in data above zero. The plot indicates that the power produced by the Bergey wind turbine is most variable between the wind speeds of 4 – 8 ms^{-1} and the spread in data becomes less again as wind speed increases beyond 8 ms^{-1}. However, the overall noise in the data suggests that the Bergey turbine produces very similar power outputs at similar wind speeds.

A similar pattern is observed when describing the deviation in power versus wind speed for the Skystream 2.4 kW (Fig. 4.22) wind turbine but there is a far greater spread in data at each wind speed as compared to the Bergey turbine performance. For instance, at 6 ms^{-1}, the Skystream turbine can produce a deviation in power as great as 1.8 kW with no clear indication that this deviation becomes smaller at higher wind speeds.

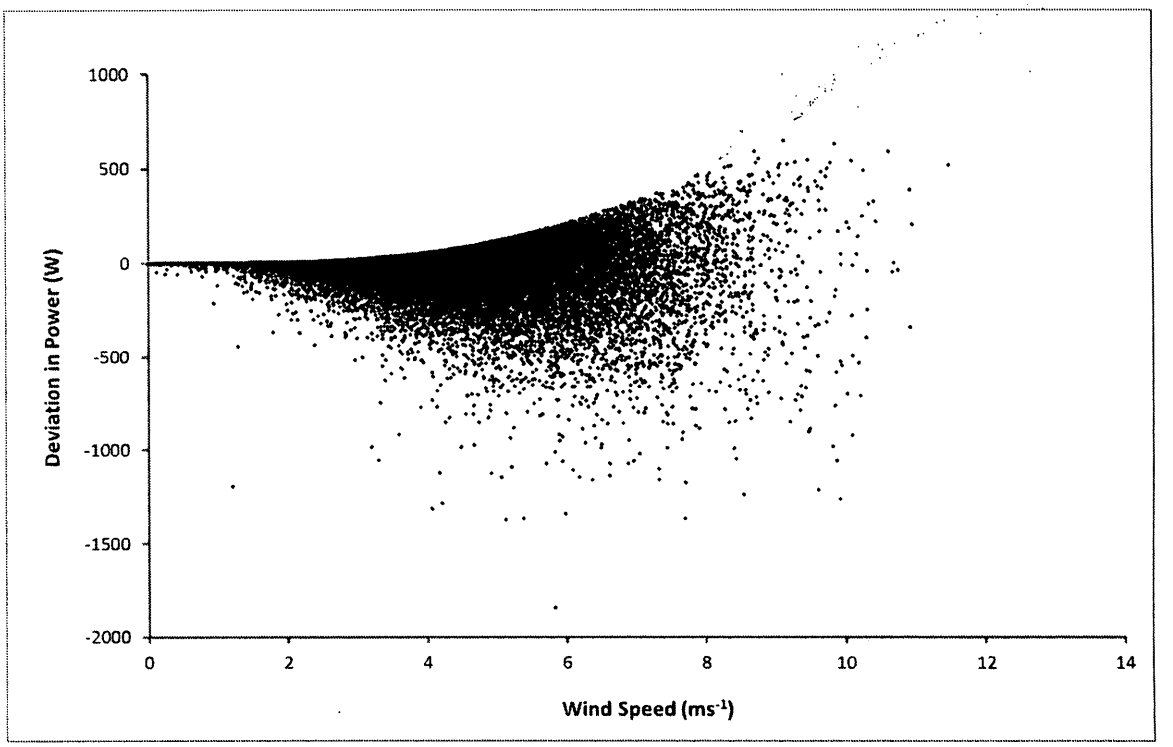

Fig. 4.22: Deviation in output power from the Skystream 2.4 kW turbine against measured wind speed. Power deviations were derived from the difference of modeled power (calculated from a line-of-best-fit) and measured power in Watts.

Another important analysis in helping to establish the suitability of the Kortright site and its associated wind turbines is how variability in the wind affects variability in power output. As seen in Fig. 4.23, variability in power increases with increasing variability in the wind for the Bergey turbine with a limit of 600 W in power standard deviation at higher variability in wind speed. As the Bergey has a rated power output of 1.1 kW (tested), this maximum variability is roughly 55% of the rated power output.

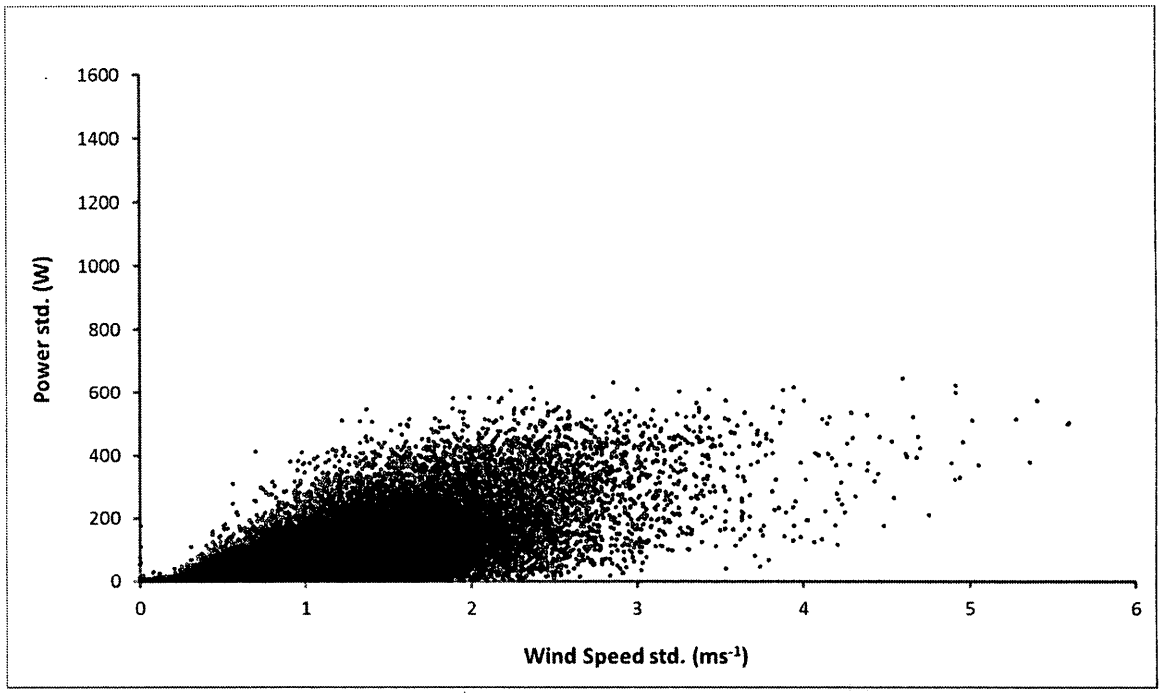

Fig. 4.23: Standard deviation of power from the Bergey Excel 1 kW turbine against standard deviation in wind speed.

This pattern is far more pronounced with data collected from the Skystream turbine with as much as 1.6 kW of power variability occurring at wind speeds as low as $3ms^{-1}$ (Fig. 4.24). This variability represents 133% of the rated power of the Skystream turbine which is a substantial amount of variability and demonstrates the inefficiency in performance by the Skystream.

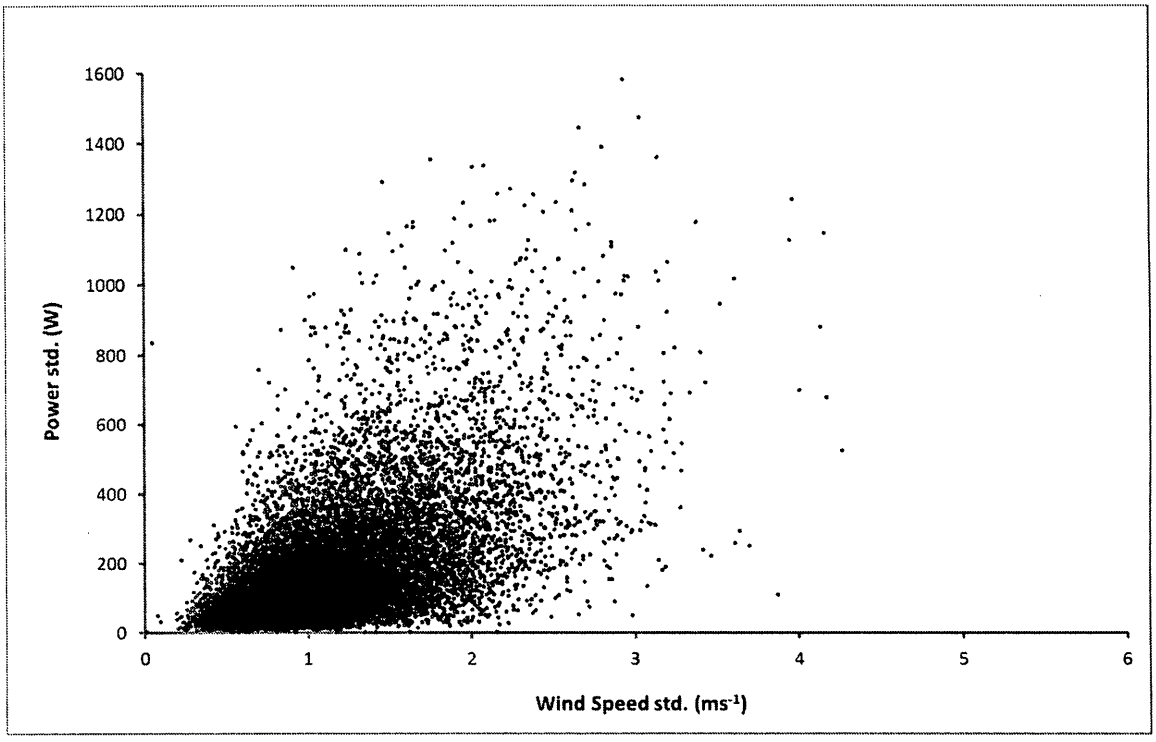

Fig. 4.24: Standard deviation of power from the Skystream 2.4 kW turbine against standard deviation in wind speed.

The deviation in power can also be represented with respect to the slope in the wind. Using continuous data measurements of wind speed, the slope (parameter used to describe if winds are accelerating or decelerating) of wind can be calculated, in this analysis, over 3-minute intervals. The slope is calculated by fitting a trend line through three 1-minute readings and the slope of the line describes the short-term trend in the wind in $ms^{-1}min^{-1}$. This slope gives an indication of the rate of wind speed increase or decrease and can be used to describe how the wind turbine responds accordingly in terms of the power output produced. If a turbine responds differently during accelerating wind speeds versus decelerating wind speeds then a bias in power produced with occur

depending on the nature of the winds blowing. The plot for deviation in power versus slope for the Bergey turbine shows a very symmetrical plot with most of the data points tailing off from the origin (Fig. 4.25). This shows that the wind turbine is performing equally the same when the rate of change in the wind is positive and when it is negative.

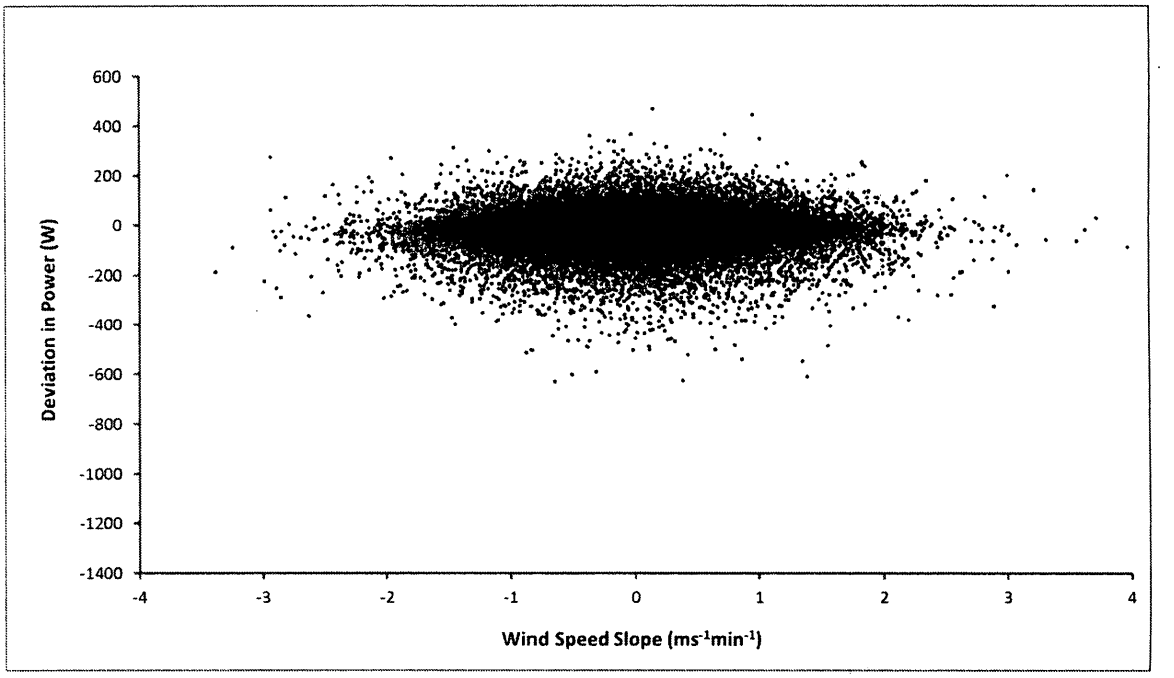

Fig. 4.25: Deviation in output power from the Bergey Excel 1 kW turbine against calculated slope in wind speed. Power deviations were derived from the difference of modeled power (calculated from a line-of-best-fit) and measured power in Watts. Slope readings are taken from wind speed data over three consecutive minutes.

As the Skystream was more intermittent in its data collection, there were shorter periods of continuous wind speed data and thus a smaller sample size but the general trend exists

with the turbine performing the same at varying rates of change in the wind speed (Fig. 4.26).

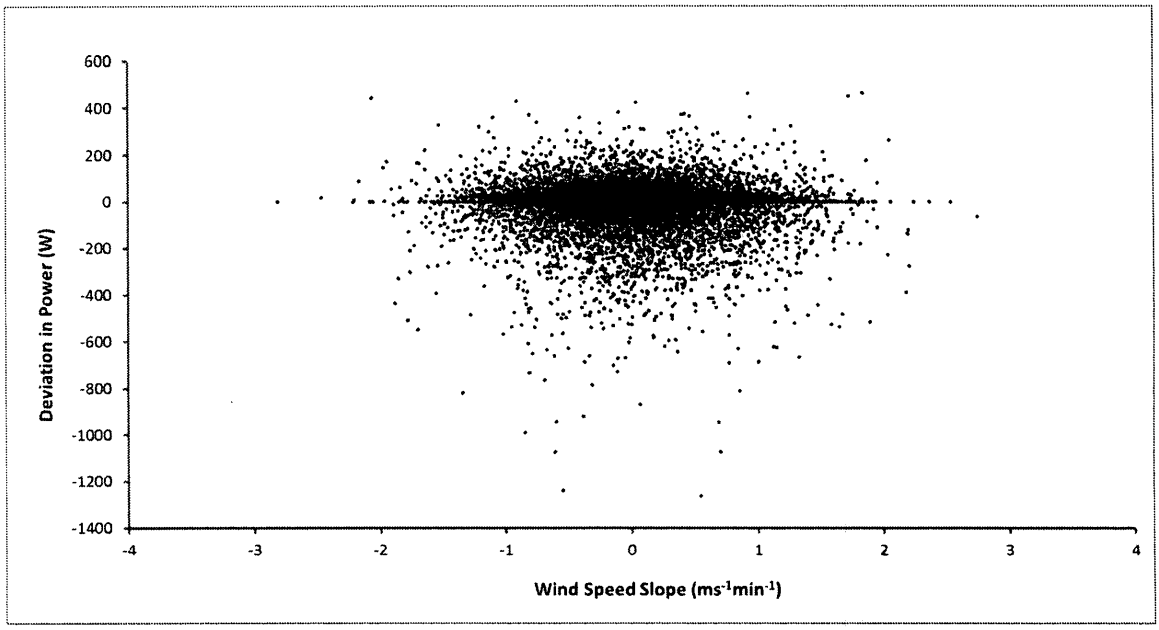

Fig. 4.26: Deviation in output power from the Skystream 2.4 kW turbine against calculated slope in wind speed. Power deviations were derived from the difference of modeled power (calculated from a line-of-best-fit) and measured power in Watts. Slope readings are taken from wind speed data over three consecutive minutes.

4.9 Summary

4.9.1 Wind distribution

Analysis of wind distribution patterns at the Kortright tests site reveal a predominantly North-westerly and South-easterly wind regime. Winds blowing from the north-east are substantially less frequent and have sub-average wind speeds. This is in agreement with direction data given by Environment Canada with a prevalent northwest wind dominating Toronto throughout most of the year. The Kortright test site also experiences an average wind speed of 3 ms^{-1}(12.5 ms^{-1} maximum) and 4 ms^{-1}(18.5 ms^{-1} maximum) at the 15.2 m and 30.5 m hub height respectively. These wind speeds are below the annual average for Toronto as given by Environment Canada, with an annual wind speed of 3.8 ms^{-1} at the environmental standard of 10 m. The maximum wind speed at lower tower heights can also limit performance testing as higher wind speeds are not frequent. Although SWCC does not certify an average wind speed for test sites, sites with an average wind speed of 5 ms^{-1} at the 30 m hub height have a strong wind resource for turbine testing, however, based on the performance results collected within this study, the Kortright Centre test site is mainly limited by the frequency of higher wind speeds. Although there is an environment of gustiness in wind at the test site, these wind speeds are buffered out at 1-minute average used for performance analysis.

As no wind turbines were tested at the 30 m hub height due to damages, describing performance at this height is difficult but the test site does show a promising wind distribution to support further testing and a maximum of 18.5 ms^{-1} wind speed will suffice for most small wind turbines in trying to understand how they perform at higher wind speeds. Furthermore, this study was completed largely in the winter and stormy months of spring which may give bias to the available wind resource. With summer winds being calmer, wind patterns may change and the possibility exists where testing of small wind turbines at lower hub heights may not be feasible.

Although the northwest and south east wind directions are most dominant at the test site, there is no conclusive data to suggest that turbulence effects, wind profile skewing or wind funneling have distorted wind patterns in any way. The bank of vegetation lying south of the meteorological tower do not appear to create enough turbulence as to distort southerly winds (with the possibility of turbulence created as wind blows over the trees from the south west) and the wide open fetch in the north east sector does not explain the poor wind resource for this bearing. Nonetheless, a separate terrain assessment and turbulence analysis of potential obstructions in the future will further define any areas that can pose an issue for performance testing. Intertek reports (Intertek Testing Services, 2012) show that site calibration and obstacle assessment can narrow down sectors from which to apply wind data in performance analysis and can be done to meet with IEC (International Electrotechnical Commission) standard for terrain assessment for turbine performance testing (IEC 61400-12-1). This testing would be particularly important in

determining the effects of turbulence created from South-westerly winds blowing over the Archetype House.

4.9.2 Power Curves

The power curve obtained for the Bergey Excel 1kW wind turbine was in agreement with other studies that have tested its performance in the field (Seitzler, 2009; Summerville, 2005). This leads welcoming support to the notion of small wind testing at Kortright with the wind resource available. However, it must be noted that the power curves are greatly affected by sample size. For instance, it has been shown that testing over short time frames can lead to insufficient wind data for performance analysis, particularly with regards to analysis of turbine performance at higher wind speeds. Furthermore, months experiencing lower than average wind speeds will not allow for an accurate assessment of performance. Wind direction also plays an important role in same size of wind data as a turbine situated in a location with a poorly fed wind sector, will experience greater noise in data and will be limited by the number of data points at the 1-minute average.
It has also been shown that power curves can vary with the variance in wind speed, with medium to low variance in wind speed giving more precise measurements of performance whereas winds with higher standard deviations can lead to slight overestimation of power output, also seen in other small wind turbine test reports (Fig. 4.27).

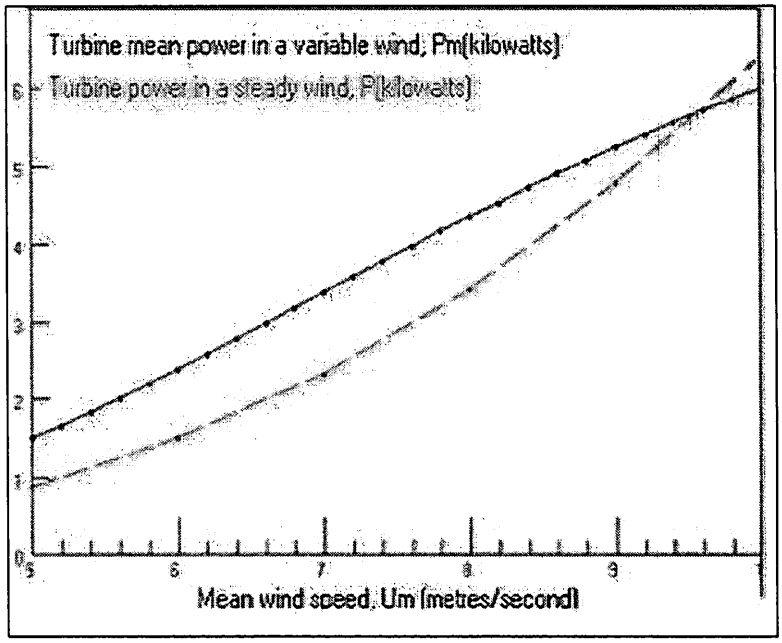

Fig. 4.27: Adapted plot of Bergey Excel 10 kW turbine power curves during variable wind and steady wind conditions. *Source: www.wind-power-program.com*

The Bergey Excel 1 kW wind turbine has a very different power curve from that of the Skystream 2.4 kW wind turbine. For reasons unknown based on collected data, the Skystream wind turbine is severely underperforming with a rated power of only 50% of its factor certified rated power of 2.4 kW. A few factors appear most plausible in these underlying differences. The Skystream wind turbine is much further from the meteorological tower than the Bergey turbine and as instantaneous gust of wind can be 'localized' at the test site, there may be a delay in wind speeds translating to wind power by the Skystream and the actual wind speed measured. This can create noise in the data which would make the Skystream power curve harder to derive. The data acquisition method for the Skystream turbine is also very unreliable and thus, the wind data is very

'choppy' and many important periods of wind extremes may have been missed while the system was down and not recording. As sample size play such a crucial factor in power performance analysis, loosing large samples of data and lead to inaccurate assessments of power output and turbine efficiency. It was informally noted that during months when data collection was more consistent, the Skystream power curve possessed much less noise. As this study did not take into consideration inverter, generator and battery efficiency and functioning, a large component to the Skystream's under-performance may be attributed to maintenance issues and power loss through faulty wires, worn-out parts or an inefficient inverter/generator.

As previously stated, the Bergey Excel 1kW power curve and coefficient of performance closely resembled those produced by other independent studies and thus the test site itself does present any apparent or serious siting issues when it comes to small wind turbine testing. When looking at how the Skystream performs at varying wind directions (Fig. 11), the south west sector (region where winds blow over the Archetype House) performs equal to that of the other sectors at lower wind speeds and is only limited by the sample size of high wind speed and not necessarily an obstacle interference.

4.9.3 Turbine Efficiency

Figs. 16 and 17 illustrate how the two turbines are performing with respect to their coefficient of performance (C_p) over various wind speed bins. The performance of the

Bergey Excel 1kW wind turbine is once again closely in line with that described by previous field testing reports (Seitzler, 2009; Summerville, 2005), whereas the C_p plot for the Skystream 2.4 kW wind turbine reiterates the under-performance seen in this turbine. The plot for the Bergey's C_p is slightly different from that produced by Seitzler (2009) with respect to the turbine performing better at lower wind speeds. However, this is not uncommon for varying test sites to produced C_p plots which peak at slightly different wind speeds. It was also found that many small wind turbine tests for coefficient of performance use the plot of C_p versus Tip Speed Ratio (TSR) for the turbine. The TSR is the ratio of rotor tip rotational speed to the speed of the rotor at the nacelle. This speed gives a more accurate description of how the rotor speed functions along the entire swept area of the rotor and thus can give a more precise account of the ratio of wind energy extraction. The TSR is established through the RPM measurement of the rotor tip versus that at the nacelle and is done with special sensors mounted on the rotor. Hence, this study could not present such findings.

4.9.4 Turbine Analysis

Through the turbine analysis, mainly with respect to power output, the two turbines are performing differently and once again, there is no indication of problematic site specific limitations. There is clearly much more noise in the Skystream data but the two turbines have similar patterns in performance. We see that variability in the wind leads to

variability in power output as expected and there appears to be no difference in turbine performance under accelerating winds versus decelerating winds. Deviations in power are quite substantial in the Skystream's power output and further investigation into possible causes should be undertaken.

4.10 Concluding Remarks

The Kortright Centre for Conservation test site presents data to suggest that the testing of small wind turbines is feasible in the near future. Distinct wind distribution patterns exist and the average wind speed is moderately below the annual Toronto average but nonetheless, the data collected from the Bergey Excel 1 kW wind turbine suggest that through certification, equipment investment and further site assessment, power curves much like those produced through certified testing can be produced. However, as testing was not done during the summer months where wind speeds tend to be below average, the temporality of testing still remains unclear. Having the turbines in a more centralized location to the meteorological tower will not only help in meeting SWCC certification standards as outlined in the IEC 61400-12-1, but will reduce discrepancies in wind measurements and data acquisition due to distance issues. The TRCA can also look into the acquisition of another Meteorological tower in the future to increase the potential number of turbines tested at the site. Much care needs to be taken in achieving sufficient sample sizes in wind data as to not hamper power curve analysis; particularly as the test

site have a lower frequency of higher wind speeds at the lower hub heights. Additionally, as the wind resource is more beneficial aloft at Kortright, the testing of small wind turbines of higher hub heights may prove more feasible. Further research is needed on terrain assessment of the site in order to determine the possible impacts of obstacles and the potential effects of turbulence on turbine performance. Results from this terrain analysis may provide information useful for site calibration and limitation assessment. If the TRCA is to continue using the Skystream for analysis purposes, technical enquires should be made as to why the turbine is under performing and the wind patterns do not seem to play a significant enough role to create the discrepancies noted from this study.

4.11 References

International Electrotechnical Commission (IEC) International Standard: Wind turbines – Part 12-1; Power performance measurements of electricity producing wind turbines. IEC 61400-12-1. 2005. 1st edition.

Intertek Wind Turbine Test Report. 2012. Power performance test report for the Fortis Wind Energy Montana tested at the Intertek Small Wind Regional Test Center (RTC).Intertek Test Report No. 100146060CRT-003.

Seitzler, M. 2009. The Electrical and Mechanical Performance Evaluation of a Roof-Mounted, One-Kilowatt Wind Turbine. California Wind Energy Collaborative.

Summerville, B. 2005.Small Wind Turbine Performance in Western North Carolina.Appalachian State University.

CHAPTER 5

CONCLUDING REMARKS

5.1 Conclusions

5.1.1 Wind energy potential across Ontario

Wind trends and wind speed means are greatest in the winter and fall seasons with similar patterns existing at the 10 and 30 m hub height although slightly weaker trends occur at 30 m. Not only are wind trends temporal in nature but they are localized throughout Ontario with much of the faster winds being located over the Great Lakes, lower Hudson Bay and James Bay. Studies have shown changes in lake/sea ice cover over the past decades have influence near surface atmospheric conditions of these water bodies and data from this study also suggest that changing ice patterns are leading to increased instability over the lakes, which subsequently drives the wind patterns experienced from surface forcing. Regions around Lake Superior for instance, are benefiting the most from these wind patterns and areas in southern Ontario are also seeing advantageous wind energy potential owing to the proximity to the surrounding Lakes. The wind industry in Ontario is spatially restricted presently and appears it will remain this way under current technologies. Higher wind energy potential exists over Ontario at the 30 m hub height and thus more cost will be needed in making small wind turbines of high rated power and higher hub heights to see optimal performance in Ontario. The province of Ontario may also benefit from offshore wind power productions with winds over the Laurentian Lakes and James Bay flowing more steadily. Ontario, most fortunately, is not experiencing any significant negative trends in wind speed nor power and thus the potential for wind

energy industry will only increase in the coming decades as long all driving forces promoting these wind regimes continue.

5.1.2 Feasibility of micro-wind turbines in Ontario

As seen from data analyzed in Chapter 2, wind trends are greatest in the winter and fall seasons and are spatially limited to regions around the Great Lakes, lower Hudson Bay and James Bay. It is purported through strong evidence that these wind patterns are driven by rapid changes in lake/sea ice which is causing stability changes of these water bodies and resulting in surface forcing of wind aloft. For Ontario, the winds at the 30 m hub height are more feasible for the small wind industry owing to greater yields seen at this height, but some regions will benefit more from raised hub heights of turbines than in other areas (Southern Ontario for instance). It was found that the annual savings from the Bergey Excel 1 kW wind turbines were not substantial in most regions of Ontario, with a majority of the province experiencing only 5 to 7% of household energy demands being met. However, these results in saving are based on general energy statistics for the province where true values are expected to vary geographically as populated areas are clustered to southern regions. Increasing turbine hub height, swept area and rated power will lead to much more savings across the province is expected to make the industry much more competitive with hydrocarbon sources.

5.1.3 Kortright Small Wind Test Site

Small wind turbine testing at the Kortright Centre for Conservation appears sufficiently viable in the near future. Although the site lacks SWCC certification and the full infrastructure and data capturing equipment needed to achieve IEC standards, drastic changes to the site are not necessary. The site's wind regime has distinct patterns of wind distribution and directionality and a slightly below average wind speed is present than that of most of Toronto. However, the tested Bergey Excel 1 kW wind turbine produced very good results which raise the confidence in the feasibility of turbine testing at Kortright even under current infrastructure. There are no existing data that suggest that the site presents any inherent issues to turbine testing and there appears to be no clear characteristics that lead to disturbance of wind patterns at the site. The Skystream 2.4 kW wind turbine has some obvious challenges to its performance but data analysis does not indicate siting issues but faults within the turbine itself. Nonetheless, a comprehensive site analysis and obstacle assessment of the Kortright site should be done to determine if wind regimes of any direction should be excluded from analysis, if turbulence is created in the wake of obstacles and if the site presents advantageous wind regimes year round. Testing of turbines should be done at higher hub heights where datasets can benefit from greater sample size of higher wind speeds at 1-minute averages.

6.1Complete Thesis References

Abe, K., Nishida, M., Sakurai, A., Ohya, Y., Kihara, H., Wada, E., Sato, K. (2004).Experimental and numerical investigations of flow fields behind a small wind turbine with a flanged diffuser. *Journal of Wind Energy and Industrial Aerodynamics,* ***92***, 315–330.

Abe, K., Nishidab, M., Sakuraia, A., Ohyac, Y., Kiharaa, H., Wadad, E., Satod, K. (2005).Experimental and numerical investigations of flow fields behind a small wind turbine with a flanged diffuser. *Journal of Wind Energy and Industrial Aerodynamics,* **93**, 951–970.

Akpinar, E. K., &Akpinar, S. (2005). An assessment on seasonal analysis of wind energy characteristics and wind turbine characteristics. *Energy Conservation and Management*, **46**, 1848-1867.

Archer, C. L., & Jacobson, M. Z. (2003). Spatial and temporal distributions of U.S. winds and wind power at 80 m derived from measurements. *Journal of Geophysics and Resources*, **108**, 4289.doi:10.1029/ 2002JD002076.

Archer, C. L., & Jacobson, M. Z. (2005).Evaluation of global wind power. *Journal of Geophysical Resources,***110**, 1-20.

Arifujjarnan, Md., Iqbal, M. T., Quaicoc, J. E., Khan, M. J. (2005).Modelling and control of a small wind-turbine.*18th annual Canadian conference on electrical and computer engineering, CCECE05, May 1–4, Saskatoon, Saskatchewan Canada*

Arifujjaman, Md. M., Iqbal, T., &Quaicoe, J.E. (2008).Energy capture by a small wind-energy conversion system. *Applied Energy*, **85**, 41-51.

Austin, J. A., & Colman, S. M. (2007). Lake Superior summer water temperatures are increasing more rapidly than regional air temperatures: A positive ice-albedo feedback. *Geophysical Research Letters,* **34**, *L06604.*

Austin, J. A., & Colman, S. M. (2008).A century of temperature variability in Lake Superior. *Limnology Oceanography,* **53**, 2724–2730.

Ayotte, K.W., Davy, R.J., Coppin, P.A. (2001).A simple temporal and spatial analysis of flow in complex terrain in the context of wind energy modeling. *Boundary-Layer Meteorology,* **98**, 275–295.

Baskut, O., Ozgener, O., &Ozgener, L. (2010). Effects of meteorological variables on exergetic efficiency of wind turbine power plants. *Renewable and Sustainable Energy Reviews*, **14**, 3237-3241.

Bechly, M. E., Clausen, P. D., Lindeyer, J., & Wood, D. H. (1997).The Fort Scratchley wind turbine. *Proceedings of the 35th ANZSES Conference, 1–3 December, Canberra, ACT.*

Bechrakis, D. A., Deane, J. P., McKeogh, E. J. (2004). Wind resource assessment of an area using short term data correlated to a long term data set. *Solar Energy,***76**, 725–732.

Becker, E. J., Ernesto, H. B., Higgins, W. (2009). Understanding the characteristics of daily precipitation over the United States Using the North American regional reanalysis. *Journal of Climate,***22**, 6268–6286.

Black, T. L. (1988), The step-mountain Eta coordinate regional model: A documentation, NOAA/NWS National Meteorological Center, 47 pp. *NCEP, 5200 Auth Road, Camp Springs, MD 20746.*

Bose, N. (1992). Icing on a small horizontal-axis wind turbine—Part 1: Glaze ice profiles. *Journal of wind engineering and industrial aerodynamics*, **45**, 75-85.

Bowen, A.J., Mortensen, N.G. (1996). Exploring the limits of WAsP the wind atlas analysis and application program. *Proceedings of European Union Wind Energy Conference, Goteburg, Sweden,* 584–587.

Boyle, G. (1996). *Renewable Energy: Power for a Sustainable Future.* Oxford, UK: Oxford University Press.

Breslow, P. B., Sailor, D. J. (2002). Vulnerability of wind power resources to climate change in the continental United States. *Renewable Energy,* **27**,585–98.

Bumby, J. R., & Martin, R. (2005).Axial-flux permanent-magnet air-cored generator for small-scale wind turbines. *Electric Power Applications, IEE Proceedings,* **152**, 1065-1075 IET.

Bukovsky, M. S., Karoly, D. J. (2007). A Brief Evaluation of Precipitation from the North American Regional Reanalysis. *Journal of Hydrometeorology,* **8**, 837–846.

Businger, J. A., Wyngaard, J. C., Izumi, Y., & Bradley, E. F. (1971). Flux profile relationships in the atmospheric surface layer. *Journal of Atmospheric Science,* **28**, 181–189.

Canadian Wind Energy Association [CanWEA].(2012) April.Canadian Wind Energy Market. Ottawa (ON): Canadian Wind Energy Association. Available from: http://www.canwea.ca/pdf/canweafactsheet-FedProInitiatives-final.pdf.

Celik, A. N. (2003). Energy output estimation for small-scale wind power generators usingWeibull-representative wind data. *Journal of Wind Energy and Industrial Aerodynamics,***91**, 693–707.

Chang, T. J., Wu, Y. T., Hsu, H. Y., Chu, C. R., & Liao, C. M. (2002).Assessment of wind characteristics and wind turbine characteristics in Taiwan.*Renewable Energy*, **28**, 851-871.

Chuang, H.Y., Manikin, G., &Treadon, R. E. (2001). The NCEP Eta Model Post Processor: A documentation, Off. Note XXX, 52 pp., Natl. Cent. *Environ. Predict, Camp Springs, Md.* Retrieved from http://www.emc.ncep.noaa.gov/officenotes/newernotes/on438.pdf.

Cohen, S., Agnew, T., Headley, A., Loute, P., Reycroft, J., & Skinner, W. (1994).Climate variability, climatic change, and implications for the future of the Hudson Bay bioregion. *The Hudson Bay Programme.*

Cole, J. J. et al. (2007). Plumbing the global carbon cycle: Integrating inland waters into the terrestrial carbon budget. *Ecosystems,***10**, 172–185.

Desai, A. R., Austin, J. A., Bennington1, V., & McKinley, G. A. (2009).Stronger winds over a large lake in response to weakening air-to-lake temperature gradient. *Nature Geoscience,***2**, 855-858.

Dominguez, F., Kumar, P., Vivoni, E. R. (2008). Precipitation recycling variability and ecoclimatological stability—A study using NARR data. Part II: North American monsoon region. *Journal of Climate,* **21**, 5187–5203.

Duguay, C.R., Terry, D., Prowse, B. R., Bonsal, R. D., Brown, M. P., La croix.,& Menard, P. (2006). Recent trends in Canadian lake ice cover. *Hydrological Processes,* **20**, 781–801.

Eggers, A. J. (2000).Modeling of yawing and furling behavior of small wind turbines.*2000 ASME Wind Energy Symposium, 19th, AIAA, Aerospace Sciences Meeting and Exhibit, 38th, Reno, NV,*1-11.

Elliott, D. L., Holladay, C. G., Barchet, W. R., Foote, H. P., Sandusky, W. F. (1986). Wind energy resource atlas of the United States. *Solar Technical Information Program, US Department of Energy, Washington, DC,* 210.Retrieved from http://rredc.nrel.gov/wind/pubs/atlas/.

Elliott, D. L., Wendell, L. L., & Gower, G. L. (1991) An Assessment of the Available Windy Land Area and Wind Energy Potential in the Contiguous United States, *Technical report*, Pacific Northwest Lab., Richland, WA (United States).

Fall, S., Niyogi, D., Gluhovsky, A., Pielke, R. A., Kalnay, E., &Rochon, G. (2010). Impacts of land use land cover on temperature trends over the continental United States: Assessment using the North American regional reanalysis. *International Journal of Climatology,* **30**, 1980–1993.

Felzer, B., Heard, P. (1999). Precipitation differences amongst GCMS used for the U.S. national assessment. *Journal of the American Water Resources Association,***35**, 1327–1339.

Frandsen, S., Christensen, C. J. (1992).Accuracy of estimation of energy production from wind power plants. *Wind Energy,* **16**, 257–267.

Fuller, J. D. (2012). Alpine wind speed and blowing snow trend identification and Analysis. *Doctoral dissertation, Colorado State University.*

Gagnon, A. S., Gough, W.A. (2005). Climate change scenarios for the Hudson Bay Region: An inter-model comparison. *Climatic Change,* **69**, 269–297.

Geng, Q., &Sugi, M. (2001). Variability of the North Atlantic cyclone activity in winter analyzed from NCEP-NCAR reanalysis data. *Journal of Climate*, **18**, 3863-3873.

Gough, W. A., Cornwell, A. R., & Tsuji, L. J. S. (2004). Trends in seasonal sea ice duration in Southwestern Hudson Bay. *Arctic,* **57**, 299-305.

Griffin, B. J., Kohfeld, K. E., Cooper, A. B., &Boenisch, G. (2010).Importance of location for describing typical and extreme wind speed behavior. *Geophysical Research Letters.,* **37**, *L22804.*doi:10.1029/2010GL045052.

Griggs, D. J., & Noguer, M. (2002). Climate change 2001: The scientific basis. Contribution of working group I to the third assessment report of the intergovernmental panel on climate change. *Weather*, **57**, 267-269.

Gripe, P. (2004). *Wind Power: Renewable Energy for Home, Farm, and Business. 2nd edition.* White River junction, UK: Chelsea Green Publishing.

Grogg, K. (2005). Harvesting the Wind: The Physics of Wind Turbines. *Carleton College,*1-41.

Guo, Z., Chang, L. (2005). Fem Study on permanent magnet synchronous generators for small wind turbines. Gustavson, M. R. (1979). Limits to wind power utilization. *Science*, **204**, 13-17.

Hicks, B. B. (1976). Wind profile relationships from the 'Wangara' experiment. *Quarterly Journal of Royal Meteorological Society,* **102**, 535-551.

Higgins, R.W., Yao, Y., & Wang, X. L. (1997). Influence of the North American monsoon system on the U.S. summer precipitation regime. *Journal of Climate,* **10**, 2600–2622.

Hirahara, H., Hossain, M. Z., Kawahashi, M., & Nonomura, Y. (2005). Testing basic performance of a very small wind turbine designed for multi-purposes. *Renewable Energy*, **30**, 1279-1297.

Högström, U. (1988). Non-dimensional wind and temperature profiles in the atmospheric surface layer: a re-evaluation. *Boundary Layer Meteorology,* **42**, 55–78.

Holt, E., Wang, J. (2012). Trends in wind speed at wind turbine height of 80 m over the contiguous United States using the North American Regional Reanalysis (NARR).*Journal of Applied Meteorological and Climatology,* **51**, 2188- 2202.

Houghton, J. T., Ding, Y., Griggs, D. J., Noguer, M., Van der Linden, P. J., Dai, X., & Johnson, C. A. (2001). Climate change 2001: The scientific basis. Contribution of working group I to the third assessment report of the intergovernmental panel on climate change. *Cambridge, United Kingdom, New York, USA, Cambridge University Press*, **881**.

Hundecha, Y., St-Hilaire, A., Ouarda, T. B. M. J., El Adlouni, S., &Gachon, P. (2008).A nonstationary extreme value analysis for the assessment of changes extreme annual wind speed over the Gulf of St. Lawrence. *Journal of Applied Meteorology and Climatology,* **47**, 2745–2759.

Independent Electricity System Operator, IESO (2012). Supply Overview. Retrieved from http://www.ieso.ca/imoweb/media/md_supply.asp, December 18, 2012.

International Electrotechnical Commission (IEC) (2005). Wind turbines part 12e1: Power performance measurements of electricity producing wind turbines, Ed.1.0. Geneva, Switzerland: International Standard, IEC 61400-12-1.

Intertek Wind Turbine Test Report.(2012). Power performance test report for the Fortis Wind Energy Montana tested at the Intertek Small Wind Regional Test Center (RTC). Intertek Test Report No. 100146060CRT-003.

Janjić, Z. I. (1994). The step-mountain Eta coordinate model: Further developments of the convection, viscous sublayer, and turbulence closure schemes. *Monthly Weather Review,* **122**, 927–945.

Klink, K. (1999). Trends in mean monthly maximum and minimum surface wind speeds in the coterminous United States, 1961 to 1990. *Climate Research,* **13**, 193–205.

Lambert, S. J. (1995).The effect of enhanced greenhouse warming on winter cyclone frequencies and strengths. *Journal of Climate,* **8**, 1447–1452.

Li, M. (2005). Investigation of wind characteristics and assessment of wind energy potential for Waterloo region, Canada.

Li, M., & Li, X. (2005).Investigation of wind characteristics and assessment of wind energy potential for Waterloo region, Canada. *Energy Conversion and Management,* **46**,3014-3033.

Li, X., Zhong, S., Bian, X., &Heilman, W. E. (2010). Climate and climate variability of the wind power resources in the Great Lakes region of the United States. *Journal of Geophysical Research,* **115**, D18107.doi:10.1029/2009JD013415.

Li, X., Zhong, S., Bian, X., Heilman, W. E., Luo, Y., & Dong, W. (2010).Hydroclimate and variability in the Great Lakes region as derived from the North American regional reanalysis. *Journal of Geophysical Research,* **115**, 1-14.

Lobocki, L. (1993). A procedure for the derivation of surface-layer bulk relationships from simplified 2nd-order closure models. *Journal of Applied Meteorology,* **32**, 126 – 138.

Lorenz, D. J., & De Weaver, E. T. (2007). Tropopause height and zonal wind response to global warming in the IPCC scenario integrations. *Journal of Geophysical Research,* **112**, D10119.doi:10.1029/2006JD008087.

Lu, L., Yang, H., Burnett, J. (2002). Investigation on wind power potential on Hong Kong islands—an analysis of wind power and wind turbine characteristics. *Renewable Energy***27**,1–12.

Lu, X., McElroy, M. B., Kiviluoma, J. (2011).Global potential for wind-generated electricity. *Proceedings of the National Academy of Sciences of the United States of America.*

Lubitz, D.W. (2012). Impact of ambient turbulence on performance of a small wind turbine. *Renewable Energy*. Retrieved from http://dx.doi.org/10.1016/j.renene.2012.08.015

Lucena, A., Szkloa, A. S., Schaeffer, R., Rodrigues de Souza, R., Cesar, B., Costa, I. V., Pereira, A. O., Cunha, S. (2009).The vulnerability of renewable energy to climate change in Brazil. *Energy Policy,* **37**, 879-889.

Luo, Y., Berbery, E. H., Mitchell, K. E., Betts, A. K. (2007). Relationships between land surface and near-surface atmospheric variables in the NCEP North American regional reanalysis. *Journal of Hydrometeorology,* **8**, 1184–1203.

Magnuson, J. J., Robertson, D. M., Benson, D. J., Wyne, R.H., Livingstone, D. M., Arai, T.,Assel, R. A., Barry, R. G., Card, V., Kuusisto, E., Granin, N. G., Prowse, T. D., Stewart, K. M., &Vuglinski, V. S. (2000). Historical trends in lake and river ice cover in the Northern Hemisphere. *Science,* **289**,1743–1746.

Manwell, J. F., McGowan, J. G., Rogers, A. L. (2009). *Wind turbine design and testing .Wind Energy Explained.* New Jersey, United States: John Wiley & Sons, Ltd, Hoboken.

Markovic, M., Jones, C. G., Winger, K., &Paquin, D. (2009). The surface radiation budget over North America: Gridded data assessment and evaluation of regional climate models. *International Journal of Climatology,* **29**, 2226–2240.

McGowan, J. G., Manwell, J. F., & Rogers, A. L. (2002).*Wind energy explained: Theory, design and application.* West Sussex: John Wiley and Sons.

Maslanik, J. A., Serreze, M.C., & Barry, R.G. (1996). Recent decreases in Arctic summer ice cover and linkages to atmospheric circulation anomalies. *Geophysical Research Letters,* **23**, 1677–1680.

Matsushima, T., Takagi, S., &Muroyama, S. (2006). Characteristics of a highly efficient propeller type small wind turbine with a diffuser. *Renewable Energy*, **31**, 1343-1354.

Mesinger, F., Janjić, Z. I., Nickovič, S., Gavrilov, D., &Deaven, D. G. (1988). The step-mountain coordinate: Model description and performance for cases of Alpine lee cyclogenesis and for a case of an Appalachian redevelopment. *Monthly Weather Review,* **116**, 1493–1518.

Mesinger, F., Di Mego, D., Kalnay, E., Shafran, P., Ebisuzaki, W., Jovic, D., Woollen, J., Mitchell, K., Rogers, E., Ek, M. B., Fan, Y., Grumbine, R., Higgins, W., Li, H., Lin, Y., Manikin, G., & Parrish, D., Shi, W. (2004). North American regional reanalysis.*15th Symposium on Global Change and Climate Variations*, paper P1.1, Combined Preprints CD-ROM, 84th AMS Annual Meeting, Seattle, WA.

Mesinger, F., Di Mego, G., Kalnay, E., Mitchell, K., Shafran, P. C., Ebisuzaki, W., Jovic, D.,Woollen, J., Rogers, E., Berbery, E. H., Ek, M. B., Fan, Y., Grumbine, R., Higgins, W., Li, H., Lin, Y., Manikin, G., Parrish, D., & Shi, W. (2006). North American regional reanalysis: A long-term, consistent, high-resolution climate dataset for the North American domain, as a major improvement upon the earlier global reanalysis datasets in both resolution and accuracy. *Bulletin of American Meteorology Society,***87**, 343–360.

Mirecki, A., Roboam, X., &Richardeau, F. (2007).Architecture complexity and energy efficiency of small wind turbines. *Industrial Electronics,* **54**, 660-670.

Nfaoui, H., Buret, J., & Sayigh, A.A.M. (1998). Wind characteristics and wind energy potential in Morocco. *Solar Energy,* **63**, 51–60.

Oort, A. H. (1978). Adequacy of the rawinsonde network for global circulation studies tested through numerical model output. *Monthly Weather Review*,**106**, 174-195.

Orlando, N. A., Liserre, M., Monopoli, V. G., Mastromauro, R. A., &Dell'Aquila, A. (2008).Comparison of power converter topologies for permanent magnet small wind turbine system. *Industrial Electronics*, 2359-2364.

Palecki, M. A., & Barry, R.G. (1986). Freeze-up and break-up of lakes as an index of temperature changes during the transition seasons: A case study for Finland. *Journal of Climate and Applied Meteorology,* **25,** 893–902.

Pennell, W. T., Barchet, W. R., Elliott, D. L., Wendell, L. L., &Hiester, T. R. (1980). Meteorological aspects of wind energy: Assessing the resource and selecting the sites. *Journal of Wind Engineering and Industrial Aerodynamic,* **5**, 223-246.

Pryor, S. C., Barthelmie, R. J., Kjellstro, M. E. (2005). Potential climate change impact on wind energy resources in Northern Europe: Analyses using a regional climate model. *Climate Dynamics,* **25**, 815–35.

Pryor, S. C., Barthelmie, R. J., Young, D. T., Takle, E. S., Arritt, R. W., Flory, D., Gutowski, JrW. J., Nunes, A., & Roads, J. (2009). Wind speed trends over the contiguous United States. *Journal of Geophysical Research,***114**, 1-18.

Pryor, S. C., Barthelmie, R. J. (2010). Climate change impacts on wind energy: A review. *Renew Sustainable Energy Review,* **14**, 430–437.

Pryor, S. C., &Ledolter, J. (2010).Addendum to "Wind speed trends over the contiguous United States." *Journal of Geophysical Research, **115***, D10103.doi:10.1029/2009JD013281.

Richard, T. L., Dragert, H., & McIntyre, D. R. (1966). Influence of atmospheric stability and over-water fetch winds over the lower Great Lakes. *Monthly Weather Review,* **7**,448-453.

Robertson, D. M., Ragotzkie, R. A., & Magnuson, J. J. (1992).Lake ice records used to detect historical and future climatic changes. *Climatic Change,* **21**,407–427.

Ruiz-Barradas, A., & Nigam, S. (2006). Great Plains hydro-climate variability: The view from North American regional reanalysis. *Journal of Climate,* **19**, 3004–3010.

Seitzler, M. (2009). The electrical and mechanical performance evaluation of a roof mounted, one-Kilowatt wind turbine. *Report CWEC-2009-003*. Davis CA, USA: California Wind Energy Collaborative, University of California, Davis

Serreze, M. C., Walsh, J. E., Chapin, F. S., Osterkamp, T.,Dyurgerov, M., Romanovsky, V.,Oechel, W. C., Morison, J., Zhang, T., & Barry, R. G. (2000).Observational evidence of recent change in the northern high-latitude environment. *Climatic Change,* **46**, 159–207.

Shikha, T. S., Bhatti, D. P., Kothari, A. (2003). Aspects of technological development of wind turbines. *Journal of Energy Engineering*, **81**,129-144.

Suarez, J. C., Gardiner, B. A., Quine, C. P. (1999). A comparison of three methods for predicting wind speeds in complex forested terrain. *Applied Meteorology,* **6**, 329–342.

Summerville, B. (2005). Small wind turbine performance in Western North Carolina, report. Boone, NC: Appalachian State University. Retrieved from http:// www.wind.appstate.edu/reports/researcharticlesmallwindperformanceBJS.

Trapp, R. J., Diffenbaugh, N. S., Brooks, H. E., Baldwin, M. E., Robinson, E. D., & Pal, J. S. (2007). Changes in Severe Thunderstorm Environment Frequency During the 21st Century Caused by Anthropogenically Enhanced Global Radiative Forcing. *Proceedings of the National Academy of Sciences,* **104**, 19719–19723.

Wang, F., Bai, L., Fletcher, J., Whiteford, J., & Cullen, D. (2008).Development of small domestic wind turbine with scoop and prediction of its annual power output. *Renewable Energy*, **33**, 1637-1651.

West, G. L., Steenburgh. W. J., & Cheng, W. Y. Y. (2007). Spurious grid-scale precipitation in the North American regional reanalysis. *Monthly Weather Review,* **135**, 2168–2184.

Wood, D. (2011). *Small Wind Turbines. Advances in Wind Energy Conversion Technology*. Springer Berlin Heidelberg, 195-211.

Wright, A. K., & Wood, D. H. (2004). The starting and low wind speed behaviour of a small horizontal axis wind turbine. *Journal of Wind Energy and Industrial Aerodynamics,* **92**, 1265–1279.

Yao, Y., Huang, H. G., Lin, Q. (2012). Climate change impacts on Ontario wind power resource. *Environmental Systems Research* , **1**, 1-11.

Yoshimura, K., &Kanamitsu, M. (2008). Dynamical global downscaling of global reanalysis. *Monthly Weather Review,* **136**, 2983–2998

A.1 APPENDIX

NARR grid cells with coding error for 30 m winds

Table A1: Omitted NARR grid cells affected by coding error in 30 m wind estimates with corresponding latitude and longitude coordinate. Row and column values correspond to cells numbers as seen in diagrams.

Row	Column	*i*-coordinate	*j*-coordinate	Latitude North	Longitude West
39	36	231	158	51.34711	80.02112
40	36	231	159	51.62005	79.85522
40	38	233	159	51.40965	78.98035
40	39	234	159	51.30206	78.5459
41	31	226	160	52.39329	81.92004
41	32	227	160	52.29648	81.4696
41	33	228	160	52.19801	81.02112
42	30	225	161	52.76431	82.21655
43	30	225	162	53.03991	82.05878
43	38	233	162	52.22319	78.45758
43	39	234	162	52.11375	78.01672
44	28	223	163	53.50377	82.82428
44	29	224	163	53.41036	82.36072
44	37	232	163	52.60223	78.72437
46	36	231	165	53.25172	78.8175
47	27	222	166	54.42469	82.8219
47	36	231	166	53.52258	78.63721
49	21	216	168	55.50493	85.41516
49	24	219	168	55.24862	83.94861
49	25	220	168	55.15954	83.46368
49	34	229	168	54.2781	79.1944
50	15	210	169	56.24873	88.27087
50	17	212	169	56.10113	87.26257
50	18	213	169	56.02449	86.76117
50	26	221	169	55.34439	82.81946

Row	Column	*i* -coordinate	*j*-coordinate	Latitude North	Longitude West
50	33	228	169	54.65464	79.48029
52	6	201	171	57.38601	92.68872
52	11	206	171	57.08589	90.07214
52	12	207	171	57.01992	89.55365
52	13	208	171	56.952	89.03687
52	14	209	171	56.88211	88.52179
53	10	205	172	57.43234	90.47534
53	34	229	172	55.35999	78.45154
53	35	230	172	55.25088	77.97827
54	6	201	173	57.95364	92.48163
54	36	231	173	55.40825	77.31079
55	5	200	174	58.29209	92.91467
55	36	231	174	55.67603	77.11163
56	36	231	175	55.94337	76.90997
57	1	196	176	59.06091	94.90643
57	2	197	176	59.01349	94.35413
57	3	198	176	58.96396	93.80334
57	36	231	176	56.21027	76.70569